Marine Pollution Bulletin
September 2023, Volume 194 Issue Part B Pages 115386 (15p.)
https://doi.org/10.1016/j.marpolbul.2023.115386
https://archimer.ifremer.fr/doc/00849/96130/

Hydrocarbons in size-fractionated plankton of the Mediterranean Sea (MERITE-HIPPOCAMPE campaign)

Guigue Catherine [1, *], Tesán-Onrubia Javier Angel [1], Guyomarc'h Léa [1], Bănaru Daniela [1], Carlotti François [1], Pagano Marc [1], Chifflet Sandrine [1], Malengros Deny [1], Chouba Lassaad [2], Tronczynski Jacek [3], Tedetti Marc [1]

[1] Aix Marseille Univ., Université de Toulon, CNRS, IRD, MIO, Marseille, France
[2] Institut National des Sciences et Technologies de la Mer (INSTM), 28, rue 2 mars 1934, Salammbô 2025, Tunisia
[3] Ifremer, CCEM Contamination Chimique des Ecosystèmes Marins, F-44311 Nantes, France

* Corresponding author : Catherine Guigue, email address : catherine.guigue@mio.osupytheas.fr

Abstract :

Aliphatic and polycyclic aromatic hydrocarbons (AHs and PAHs, respectively) were analyzed in the dissolved fraction (<0.7 μm) of surface water and in various particulate/planktonic size fractions (0.7–60, 60–200, 200–500 and 500–1000 μm) collected at the deep chlorophyll maximum, along a North-South transect in the Mediterranean Sea in spring 2019 (MERITE-HIPPOCAMPE campaign). Suspended particulate matter, biomass, total chlorophyll a, particulate organic carbon, C and N isotopic ratios, and lipid biomarkers were also determined to help characterizing the size-fractionated plankton and highlight the potential link with the content in AHs and PAHs in these size fractions. Σ28AH concentrations ranged 18–489 ng L−1 for water, 3.9–72 μg g−1 dry weight (dw) for the size fraction 0.7–60 μm, and 3.4–55 μg g−1 dw for the fractions 60–200, 200–500 and 500–1000 μm. AH molecular profiles revealed that they were mainly of biogenic origin. Σ14PAH concentrations were 0.9–16 ng L−1 for water, and Σ27PAH concentrations were 53–220 ng g−1 dw for the fraction 0.7–60 μm and 35–255 ng g−1 dw for the three higher fractions, phenanthrene being the most abundant compound in planktonic compartment. Two processes were evidenced concerning the PAH patterns, the bioreduction, i.e., the decrease in concentrations from the small size fractions (0.7–60 and 60–200 μm) to the higher ones (200–500 μm and 500–1000 μm), and the biodilution, i.e., the decrease in concentrations in plankton at higher suspended matter or biomass, especially for the 0.7–60 and 60–200-μm size fractions. We estimated the biological pump fluxes of Σ27PAHs below 100-m depth in the Western Mediterranean Sea at 15 ± 10 ng m−2 day−1, which is comparable to those previously reported in the South Pacific and Indian Ocean.

Keywords : Hydrocarbons, PAHs, Plankton, Size fractions, Bioaccumulation, Mediterranean Sea

Highlights

- Analysis of hydrocarbons (AHs, PAHs) in water and plankton from the Mediterranean
- Differences in AHs and PAHs between 0.7-60 and 60-1000-µm plankton size fractions
- AHs showed an anthropogenic origin in water but a biogenic signature in plankton
- Decrease in PAH concentrations with increase in plankton size and biomass
- Estimate of vertical flux of PAHs related to biological pump: 15 ± 10 ng m^{-2} day^{-1}

1. Introduction

Hydrocarbons, in particular polycyclic aromatic hydrocarbons (PAHs), are among the most widespread organic pollutants in the marine environment (Hylland, 2006; Duran and Cravo-Laureau, 2016; Ben Othman et al., 2023). PAHs are considered to be almost exclusively of anthropogenic origin, possibly coming from crude oil or its derivatives (petrogenic PAHs) or from the combustion of fossil fuels and biomass (pyrogenic PAHs) (Wang et al., 1999; Yunker et al., 2002; Stogiannidis and Laane, 2015). Aliphatic hydrocarbons (AHs), which also represent an important class of hydrocarbons in the marine environment, can be of anthropogenic (petroleum) and biogenic (terrestrial or marine) origin (Volkman et al., 1992; Bouloubassi and Saliot, 1993; Love et al., 2021). PAHs are listed as priority pollutants by various international organizations (US-EPA, 2012; EU-Directive, 2013) due to their deleterious effects on living organisms (Honda and Suzuki, 2020). Thus, for many years, PAHs, and to a lesser extent AHs, have been studied in different matrices of the marine ecosystem, such as surface sediments (Mille et al., 2007; Zaghden et al., 2017; Mandić et al., 2018), the dissolved phase of water (Guigue et al., 2014; Adhikari et al., 2015; Tong et al., 2019), suspended particles (Bouloubassi et al., 2006; Mzoughi and Chouba, 2011; Rocha and Rocha, 2021), surface microlayer (Stortini et al., 2009; Guitart et al., 2010; Guigue et al., 2011), and biota, especially macro-organisms (fish, crustaceans, mollusks…) (Baumard et al., 1998; Tolosa et al., 2005; Pirsaheb et al., 2018).

The incorporation and accumulation of PAHs in marine food webs is known to induce major disturbances of ecosystems, and to have negative impacts on the exploitation of marine resources and habitats, socio-economic activities, and human health (Islam and Tanaka, 2004; Balcıoğlu, 2016; Romero et al., 2018). However, even though the accumulation of PAHs in upper food webs has been quite well documented so far, these processes have been much less

investigated in plankton, i.e., the first trophic levels of pelagic marine ecosystems. Yet, plankton, which includes phytoplankton (mostly unicellular photosynthetic autotrophic organisms), zooplankton (heterotrophic eukaryotes), and bacterioplankton (heterotrophic prokaryotes), is recognized as a key gateway and playing a major role in the transfer of contaminants from water to upper food webs (Berrojalbiz et al., 2011; Tiano et al., 2014; Tao et al., 2018; Chouvelon et al., 2019; Tedetti et al., 2023).

Given their high surface area/volume ratio and the subsequent large areas of exchanges, phytoplankton cells display high adsorption and absorption – and thus bioconcentration – capacities of contaminants present at the dissolved state in water (Martin and Knauer, 1973; Fan and Reinfelder, 2003; Heimbürger et al., 2010; Chouvelon et al., 2019). Assuming partition equilibrium processes between the cells and the surrounding water (Frouin et al., 2013), the bioconcentration of organic contaminants in phytoplankton may be directly related to their octanol-water partitioning coefficient (Log K_{OW}), i.e., their degree of hydrophobicity (the higher the Log K_{OW}, the greater the contaminant bioconcentration) (Swackhamer and Skoglund, 1993; Nizzetto et al., 2012; Li et al., 2020), and to the size of the phytoplankton species (the smaller the cell size, the greater the contaminant bioconcentration) (Fan and Reinfelder, 2003). On the other side, the bioaccumulation processes in zooplankton by both the water aqueous phase and the diet are made complex by 1) the influence of trophic interactions and transfers between phytoplankton and zooplankton and within zooplanktonic compartment, and 2) the removal processes of contaminants implemented by these organisms, including metabolization, passive release and excretion (Berrojalbiz et al., 2009; Tiano et al., 2014; Alekseenko et al., 2018; Tao et al., 2018; Li et al., 2020). Ultimately, all these processes, which can act concurrently in the same or opposite directions, makes it difficult to understand and predict the pattern of contaminant concentrations within the planktonic food

web (Nizzetto et al., 2012; Strady et al., 2015; Alekseenko et al., 2018; Castro-Jiménez et al., 2021; Li et al., 2021).

Recently, some works have focused on the accumulation of PAHs in the planktonic compartment (Berrojalbiz et al., 2009, 2011; Tao et al., 2017a, b, 2018; González-Gaya et al., 2019). These have provided a very interesting insight of the PAH accumulation pattern within the plankton and showed a link between this accumulation and the surrounding biogeochemical parameters. Nevertheless, in these studies, plankton has been generally taken as an entire compartment, without any separation into size fractions. Furthermore, the lipid content was not taken into account, even though, due to their hydrophobic nature, lipids represent a major matrix contributing to the accumulation of the organic contaminants within marine and planktonic organisms (Mackay and Fraser, 2000; Arnot and Gobas, 2006; Lee et al., 2006; Tesán-Onrubia et al., 2023).

In this context, the objectives of the present work were to **1)** determine the contents in hydrocarbons (AHs and PAHs) in the dissolved fraction (< 0.7 µm) of surface water and in various particulate/planktonic size fractions (0.7-60, 60-200, 200-500 and 500-1000 µm) from sampling in the deep chlorophyll maximum (DCM), along a North-South transect in the Mediterranean Sea during the MERITE-HIPPOCAMPE campaign. For the different size fractions, suspended particulate matter (SPM), biomass, total chlorophyll *a* (TChl*a*), particulate organic carbon (POC), C and N isotopic ratios ($\delta^{13}C$, $\delta^{15}N$) and lipid biomarkers were also determined. **2)** Evaluate the spatial variations (between stations) and the distributions within the planktonic size fractions of these different parameters (mainly AHs, PAHs, POC, lipids), as well as the correlations between them. **3)** Investigate the accumulation patterns of PAHs within plankton according to the size fraction, trophic level, organic carbon partitioning and biomass. **4)** Assess, *via* the estimation of hydrocarbon vertical fluxes, the role of Mediterranean plankton as biological pump for hydrocarbons.

2. Material and Methods

2.1. Study area

The MERITE-HIPPOCAMPE cruise took place in spring 2019 (from April 13 to May 14), aboard the R/V *Antea*, along a North-South transect in the Mediterranean Sea, from the French coast (La Seyne-sur-Mer, Northwestern Mediterranean) to the Gulf of Gabès in Tunisia (Southeastern Mediterranean). Leg 1 (13-28 April) covered the southward transect, between La Seyne-sur-Mer and Tunis, with sampling of stations St2, St4, St3, St10 and St11. Leg 2 (30 April-14 May) included the end of the southward transect (from Tunis to the Gulf of Gabès), and the return trip back northward to La Seyne-sur-Mer, with sampling of stations St15, St17, St19, St9 and St1 (Fig. 1a, b) (Tedetti and Tronczynski, 2019; Tedetti et al., 2023). The ten stations were chosen according to criteria of physical, biological and biogeochemical conditions and level of anthropogenic pressures, as well as the location of bloom areas and ecoregions of the Mediterranean (see full description in Tedetti et al., 2023).

2.2. Sampling, filtration, sieving and conditioning

At each station, a conductivity-temperature-depth probe (CTD; Seabird SBE 911*plus*) equipped with a TChl*a* fluorescence sensor (Chelsea ctg) was deployed over the depth range 0-250 m (or 0-bottom when depth was < 250 m) to identify the DCM. The CTD deployments were carried out 2-3 times during the time spent in station to assess the depth range of the DCM before the deployments of the McLane pumps and the MultiNet (see sections 2.2.1. and 2.2.2.). For each station, the sampling depth ranges in the DCM are reported Table S1.

2.2.1. In situ filtration with McLane pumps. Two McLane *in situ* pumps (WTS6-142LV, 4-8 L min^{-1}) were used to collect high amounts of particles/plankton in the DCM. Each pump was mounted with a regular 142-mm filter holder for hosting a pre-combusted

(450 °C, 6 h), pre-weighted 142-mm diameter glass fiber (GF/F) filter (Whatman). The holder was covered with a sock-type pre-filter of 60-µm pore size, so as to collect on the filters the size fraction 0.7-60 µm, which is mainly dominated by phytoplankton (Tesán-Onrubia et al., 2023). Just prior to deployment of the pumps, all the filter holder and filter systems were rinsed with ultra-pure water. Both pumps were deployed at the same time by the ship's Moon-Pool on the hydrographic cable to reach the DCM. At the DCM, the pumping lasted 40-60 min, so that ~ 250 L of seawater was passed over each GF/F filter. Back on board, the filters were recovered and dried. One filter was used for the analysis of SPM and hydrocarbons (AHs and PAHs), while the other filter was dedicated to SPM, TChl*a*, POC, and C and N isotopic ratios ($\delta^{13}C$, $\delta^{15}N$). Before drying, this second filter was also rinsed with ultra-pure water to remove residues of the seawater salts. Finally, the GF/F filters were placed in glass boxes and stored at -18 °C on board and then in the laboratory before analysis. It should be noted that molecular lipid analyzes were not conducted on these filters/size fraction 0.7-60 µm.

2.2.2. Plankton sampling with MultiNet followed by sieving. Multiple Plankton Sampler (Midi type, Hydro-Bios), here referred to as "MultiNet", was used to collect plankton (mainly zooplankton) in the DCM. The MultiNet was made of 5 individual opening and closing nets with 0.25-m^2 aperture, 60-µm mesh size, and cod ends of 60-µm mesh size, as well as two flowing meters to measure the volume of water filtered by the nets, a CTD sensor and a TChl*a* fluorometer (Chelsea ctg). The MultiNet was deployed horizontally in the DCM from the rear of the ship *via* the electromechanical cable. The Multinet position was maintained stable at the defined depth by means of a V-fin deflector, a helicoidal bucket connector gathering the cod ends, a controlled vessel speed (2 knots), and real-time control of its position from the on board desk unit. Once the five nets were filled (30-100 min), the MultiNet was brought on board, the cod ends rinsed out with local seawater, and their content

transferred into pre-cleaned 10-L HDPE bottles. The device was then returned to the water as many times as necessary until sufficient quantities of plankton were obtained.

In the on board clean lab container (IFREMER, 435 CNXU 300022/1), plankton was then fractionated on a column of five stainless steel sieves (60, 200, 500, 1000 and 2000-µm mesh size) by wet-sieving with GF/F filtered seawater previously retrieved from ASTI pump/in-line filtration system and stored in a stainless steel jerry can (see section 2.2.3). The planktonic size fractions recovered on the stainless-steel sieves (i.e., 60-200, 200-500, 500-1000, 1000-2000 and > 2000 µm) were shared out for the different analyzes. For the analyzes of hydrocarbons and lipids, each size fraction was transferred into a pre-combusted 150-mL amber glass flask. For the analyzes of POC and $\delta^{13}C/\delta^{15}N$, each size fraction was transferred into another pre-combusted 150-mL amber glass flask. It is worth noting that the quantities obtained for the size fractions 1000-2000 and > 2000 µm were not sufficient enough for PAH analyzes. Hence, for hydrocarbons, lipid biomarkers, POC, and $\delta^{13}C/\delta^{15}N$, only the size fractions 60-200, 200-500 and 500-1000 µm are exploited in the present work. The glass flasks were stored at -18 °C on board and then in the laboratory before analysis.

2.2.3. Water sampling and in-line filtration with ASTI pump. Seawater was sampled at ~ 5-20-m depth, depending on the stations, with a pneumatically-operated Teflon ASTI pump (model PFD2) set up on board, connected to Teflon tubing, which was weighted down and immersed from port side with the hydrology gallows. The pump was connected to a clean dry air supply. The seawater brought on board in the Teflon tubing by means of the pump was then filtered in-line onto a pre-combusted GF/F 142-mm filter using a Teflon filtration holder. The seawater filtered through GF/F was stored in two stainless steel jerry cans of 20 L each. The seawater of the first jerry can was used exclusively for sieving the plankton collected with the MultiNet. The seawater of the second jerry can was amended with 50 mL of dichloromethane (CH_2Cl_2) for subsequent analyzes of dissolved (< 0.7 µm) AHs and PAHs.

This jerry can was stored at ~ 20 °C on board and then in the laboratory before analysis. Before filling the jerry cans, several liters of filtered seawater were thrown away.

2.3. Analysis

2.3.1. SPM, Biomass. SPM was measured on the size fraction 0.7-60 µm by weighing, with a precision balance, the tare, the entire (142-mm GF/F) filters before filtration, and the entire filters, wet and dry (freeze dried), after filtration, taking into account the volumes of water filtered with the McLane pumps (Tesán-Onrubia et al., 2023). Dry-weight biomasses of size fractions 60-200, 200-500 and 500-1000 µm were determined after drying samples on pre-weighed GF/F filters (60 °C, 24 h) and then re-weighed with a microbalance, taking into consideration the volumes of water filtered by the MultiNet (Fierro-González et al., 2023). The contributions of zooplankton, phytoplankton and detritus components to the total weighted biomass were estimated according to Fierro-González et al. (2023). SPM is expressed in mg L^{-1}, and biomass concentrations in µg (or mg) dry weight (dw) L^{-1}.

2.3.2. TChla, POC, $\delta^{13}C$, $\delta^{15}N$. For the determination of TChl*a* concentration on the size fraction 0.7-60 µm, a 22-mm diameter aliquot of the 142-mm GF/F filter was placed in a tube in which 5 mL of pure methanol was added. Following 20-30 min of extraction, the fluorescence of the extract was measured on a Turner Fluorometer 110 equipped with the Welschmeyer kit to avoid chlorophyll *b* interference (Welschmeyer, 1994). Calibrations were made using a pure Sigma Chl*a* standard (Raimbault et al., 2004). The volume of water passed over the TChl*a* aliquot was calculated as a function of the volume of water passed over the filter, its impacted surface and the surface of the aliquot. TChl*a* concentration is expressed in µg L^{-1}. POC concentration and $\delta^{13}C/\delta^{15}N$ were determined on size fractions 0.7-60, 60-200, 200-500 and 500-1000 µm. The samples for POC, i.e., 22-mm diameter aliquots of the freeze dried 142-mm GF/F filters (0.7-60 µm) and ~ 1 mg of the freeze dried plankton material (60-

200, 200-500 and 500-1000 µm) were washed with 100 µL of sulfuric acid (H_2SO_4 0.5 N) to remove any inorganic carbon, and stored in 25-mL Schott® glass bottles before being analyzed using the persulfate wet-oxidation procedure according to Raimbault et al. (1999). Blanks were prepared for each set of samples. The volume of water passed over the POC aliquot (0.7-60 µm) was calculated as a function of the volume of water passed over the filter, its impacted surface and the surface of the aliquot. For the size fraction 0.7-60 µm, POC concentration is expressed either in mg L^{-1} or in mg g^{-1} dw (when normalizing by SPM). For the size fractions 60-200, 200-500 and 500-1000 µm, POC concentration is expressed in mg g^{-1} dw. Concerning $\delta^{13}C/\delta^{15}N$ samples, the SPM collected on the GF/F filters were scraped off with a scalpel (0.7-60 µm), whereas plankton fractions (60-200, 200-500 and 500-1000 µm) were ground to fine powder with an agate mortar and pestle. Samples were then acidified (for $\delta^{13}C$) or not (for $\delta^{15}N$) and analyzed using an elemental analyzer (Flash EA 2000, Thermo Scientific®) coupled with a continuous flow isotope ratio mass spectrometer (Delta V Plus, Thermo Scientific®) (see details in Tesán-Onrubia et al., 2023). Isotope compositions in all size fractions are expressed in ‰ as deviations from the standard reference materials (N_2 in air for $\delta^{15}N$ and Vienna Pee Dee Belemnite for $\delta^{13}C$).

2.3.3. Lipid biomarkers. Lipid biomarkers were determined on the size fractions 60-200, 200-500 and 500-1000 µm. For each size fraction, ~ 10 mg of freeze dried plankton were mixed with 15 mL methanol (MeOH) and reduced with excess sodium borohydride ($NaBH_4$) (70 mg, 30 min at 20 °C). This process was conducted to reduce any hydroperoxides in samples (Galeron et al., 2015), which are known to induce autoxidative damage of some lipids during the hot saponification step. Saponification was carried out on each reduced sample. After $NaBH_4$ reduction, water (15 mL) and potassium hydroxide (KOH) (2 g) were added and the mixture directly saponified by refluxing (2 h). After cooling, the contents of the flask were acidified with hydrochloric acid (HCl) to pH 1, and extracted 3 times with 30-mL

CH_2Cl_2. The combined CH_2Cl_2 extracts were dried over anhydrous sodium sulfate (Na_2SO_4), filtered and concentrated to give the total lipid extract. These latter were derivatized by dissolution in 300 µL pyridine/bis(trimethylsilyl)trifluoroacetamide (BSTFA, Supelco) (2:1, v/v) and silylated (50 °C, 1 h). After evaporation to dryness under a stream of N_2, the derivatized residue was dissolved in hexane/BSTFA (2:1, v/v) to avoid desilylation and analyzed using gas chromatography-electron ionization quadrupole time of flight mass spectrometry (GC-QTOF). Individual fatty acids, fatty alcohols and sterols were identified and quantified using an Agilent 7890B/7200 GC-QTOF System (Agilent Technologies, France) according to Rontani et al. (2017). It should be noticed that the polyunsaturated fatty acid concentrations must be regarded as minimal values because they might have been affected by oxidative losses occurring during the 2-year storage of samples at -18 °C before analysis. Concentrations of individual and total lipid biomarkers (fatty acids, fatty alcohols and sterols) are expressed in mg g^{-1} dw.

2.3.4. Hydrocarbons. Twenty-eight AHs, i.e., a series of *n*-alkanes from *n*-C_{15} to *n*-C_{40} and two isoprenoids, pristane (Pr) and phytane (Phy), were determined in this study. Unresolved complex mixture (UCM) was not detected in our samples. For PAHs, we determined the concentrations of 17 parent PAHs, namely naphthalene (Nap), acenaphthylene (Acy), acenaphtene (Ace), fluorene (Flu), dibenzothiophene (DBT), phenanthrene (Phe), anthracene (Ant), fluoranthene (Flt), pyrene (Pyr), benz[*a*]anthracene (BaA), chrysene (Chr), benzo[*b*]fluoranthene (BbF), benzo[*k*]fluoranthene (BkF), benzo[*a*]pyrene (BaP), dibenz[*a,h*]anthracene (DahA), benzo[*g,h,i*]perylene (BP), indeno[1,2,3-*cd*]pyrene (IndP), as well as the concentrations of methylated derivatives (methyl- = C1-, dimethyl- = C2-, trimethyl- = C3-) of the five compounds Nap (C1, C2, C3), Flu (C1, C2), DBT (C1, C2), Phe/Ant (C1, C2) and Flt/Pyr (C1), which lead to a total of 27 PAHs (or groups of PAHs). AHs and PAHs were determined on the dissolved fraction (< 0.7 µm) of seawater, as well as

on the size fractions 0.7-60, 60-200, 200-500 and 500-1000 µm. For the fractions > 0.7 µm, samples (entire GF/F filters and plankton) were freeze dried for 24-96 h, then spiked with a multi-standard mixture containing surrogate standards for AHs (C_{16}-d_{34}, C_{24}-d_{50} and C_{36}-d_{74}) and PAHs (Nap-d_8, Flu-d_{10}, Phe-d_{10}, Flt-d_{10} and BaP-d_{12}), and extracted with CH_2Cl_2 using accelerated solvent extraction (ASE 350, Dionex, Thermo Scientific) with the following procedure: 150 °C, 110 bars, 3 cycles of 10 min, 100% of rinsing and purging for 60 s (Guigue et al., 2017; Fourati et al., 2018a). For the fraction < 0.7 µm, samples, i.e., 20 L of filtered seawater with 50 mL of CH_2Cl_2, were spiked with the multi-standard mixture and extracted by liquid-liquid extraction with CH_2Cl_2 (3 × 60 mL per liter) according to Guigue et al. (2014) and Fourati et al. (2018b). All CH_2Cl_2 extracts were concentrated using a rotary evaporator and solvent was exchanged by *n*-hexane. Extracts were reduced to ~ 1 mL, and cleaned with a silica-alumina column (10 mm i.d., made of glass) packed from bottom to top with 1-3 g deactivated alumina (by 3% ultra-pure water w/w), 1-3 g activated silica, and 1 g dehydrated Na_2SO_4, depending on the quantity of extracted matter. First, the sorbents were conditioned with 20 mL *n*-hexane, then the extract was deposited on the top of the column and both AHs and PAHs were eluted with 50-mL *n*-hexane:CH_2Cl_2 (9:1 v/v). This was followed by solvent reduction to 200-500 µL and deuterated mixtures for AHs (C_{19}-d_{40} and C_{30}-d_{62}) and PAHs (Ace-d_{10}, Ant-d_{10}, Pyr-d_{10}, Chr-d_{12} and Per-d_{12}) were spiked as internal standards before analysis.

AHs and PAHs were analyzed separately by gas chromatography (Trace ISQ, Thermo Electron) equipped with a mass spectrometry (MS) detector operating at an ionization energy of 70 eV, with hydrogen (1.2 mL min^{-1}) as carry gas. The capillary column (HP-5MS, Agilent Technologies, USA) was 30 m in length with an internal diameter of 0.25 mm and a film thickness of 0.25 µm. The injector (used in splitless mode) and detector temperatures were 250 and 320 °C, respectively. The column temperature was initially held at 70 °C for 3 min,

increased to 150 °C at 15 °C min^{-1}, then increased to 320 °C at 7 °C min^{-1} and finally held for 10 min. AHs and PAHs were identified and quantified in full scan and selected ion monitoring (SIM) modes simultaneously using two distinct methods (Guigue et al., 2011, 2014, 2017). All solvents and chemicals used were of high purity grade. Σ AHs and Σ PAHs represented the sum of the targeted AH and PAH compounds, respectively. Concentrations of dissolved AHs and PAHs are expressed in ng L^{-1}. Concentrations of AHs and PAHs for the fractions > 0.7 µm are expressed in µg g^{-1} dw and ng g^{-1} dw, respectively.

The quality control procedures were strictly followed throughout the whole sampling and laboratory treatments. They included control/validation of GC-MS calibration and tuning, laboratory and field blanks, method limit of detection/quantification (LODs/LOQs), as well as surrogate recoveries. Field and laboratory blanks were prepared, processed and analyzed in the same manner as the real samples. LOQs ranged from 30 to 100 pg L^{-1} and from 10 to 50 pg L^{-1} in water for AHs and PAHs, respectively. They ranged from 0.3 to 1 ng g^{-1} and from 0.1 to 0.5 ng g^{-1} in plankton for AHs and PAHs, respectively. Blank values were below LODs or LOQs and surrogate recoveries were > 75 and > 70% for AHs and PAHs, respectively. All the concentrations reported here were not neither blank- nor recovery-corrected.

2.4. Data handling

To fully compare our PAH concentrations in the planktonic size fractions with those in literature, we estimated the concentrations of individual PAHs (and of POC) in the entire size fraction 60-1000 µm by summing the concentrations of individual PAHs (and of POC) in the fractions 60-200, 200-500 and 500-1000 µm, each of these concentrations being weighted (multiplied) by the contribution of the biomass of the given fraction to the total biomass of the fraction 60-1000 µm ($f_{Biomass}$ = biomass of the given fraction / biomass 60-1000 µm).

According to González-Gaya et al. (2019), we estimated the biological pump fluxes of PAHs, i.e., the vertical fluxes of PAHs exported in depth through the biological pump process (in ng m^{-2} day^{-1}), for the Western basin of the Mediterranean Sea. For this, we normalized the PAH concentrations in the size fraction 60-1000 µm at each station (in ng g^{-1} dw) by the corresponding organic carbon (OC) content (in g C g^{-1} dw). Then, we averaged these OC-normalized PAH concentrations (in ng g^{-1} C dw), and multiplied this obtained mean concentration by the vertical settling flux of POC (in g C m^{-2} day^{-1}) below 100-m depth for the Western Mediterranean Sea estimated by Guyennon et al. (2015), where POC is defined as being fueled by the natural mortality of the largest organisms (mesozooplankton, diatoms and ciliates) and by the excretion of fecal pellets and sloppy feeding by mesozooplankton. This calculation was performed for total PAHs (sum of our 27 parent and alkylated compounds; Σ_{27}PAHs) but also for Phe alone, which was the dominant PAH in the planktonic fractions.

The partition coefficient between particulate matter and water (K_D in L kg^{-1}) was calculated for seven individual PAHs (the ones present both in water and particulate/planktonic phases, namely Nap, Flu, Phe, Flt, Pyr, BaA and Chr) in each size fraction (0.7-60, 60-200, 200-500, 500-1000 and 60-1000 µm) as (C_P / C_W) × 1000 where C_P is the concentration of the given PAH in the given size fraction in ng g^{-1} dw, and C_W is the concentration of the PAH in the dissolved phase (size fraction < 0.7 µm) in ng L^{-1}. The partition coefficient between organic carbon and water (K_{OC} in L kg^{-1}) was then determined for the seven individual PAHs in each size fraction as K_D / f_{OC} where f_{OC} is the contribution of the OC mass (in g) to the total matter mass (in g) for a given size fraction (f_{OC} = POC in mg g^{-1} dw / 1000).

According to the previous works by Berrojalbiz et al. (2011) and González-Gaya et al. (2019), we assume that the relationships between SPM or biomass concentration in a given

size fraction and the concentration of individual PAHs in this size fraction can be approximated by a power function of the form: $C_P = aSPM^{-m}$ or $aBiomass^{-m}$ where a is the constant and m the slope of the regression. In the present study, the Log K_{OC} and slope (m) values were exploited to highlight the influence of plankton on the bioaccumulation of PAHs.

2.5. Statistics

Statistical analyzes were performed using XLSTAT software (version 2021.1.1). Student's parametric test (t-test) was used to determine significant differences between the means of two groups, i.e., the mean concentrations in two size fractions over the 10 stations.

3. Results and Discussion

3.1. TChl*a*, POC and SPM/biomass

In the size fraction 0.7-60 µm sampled from the DCM, TChl*a*, POC and SPM concentrations followed substantially the same spatial distribution (Fig. 2a; Table S1), and were thus significantly positively correlated with each other ($r = 0.70\text{-}0.93$, $n = 10$, $p < 0.05$). The lowest concentrations were found at two southern coastal stations, St17 and St15. Low values were also recorded at St3 and St11. The highest concentrations were observed at the offshore station St9. High values were also found at two coastal stations, St19 and St1 (Fig. 2a; Table S1).

These results are in accordance with the observations by Tedetti et al. (2023) who highlighted that St9 displayed the highest contents in silicates [$Si(OH)_4$] and nitrates (NO_3^-), and the highest concentrations in POC and TChl*a* in the size fraction > 0.7 µm in the DCM compared to the other stations. The high levels of TChl*a* in St9 during the sampling period

were also confirmed from satellite data (Tedetti et al., 2023). Indeed, St9, situated at the boundary of the Ligurian consensus region (Ayata et al., 2018) in the deep convection area, benefited from a relatively intense phytoplankton bloom in late March 2019 (still visible in May), consecutive to a pronounced winter convection process (Margirier et al., 2020; Bosse et al., 2022). In line with our results, Tedetti et al. (2023) also reported high concentrations in $Si(OH)_4$, phosphates (PO_4^{3-}), and TChl*a* and POC in the fraction > 0.7 µm at St19. This enrichment could be related to nutrient inputs and the subsequent stimulation of phytoplankton activity from Saharan dust deposition event that occurred in the south of the Gulf of Gabès during sampling. Such Saharan dust deposition events have been already reported and recognized to provide nutrients in this area (Béjaoui et al., 2019). Apart from St9 and St19, the fraction 0.7-60 µm exhibited higher TChl*a*, POC and SPM contents for the northern stations (St1-St4) than for the offshore and southern stations (St10-St17) (Fig. 2a), which is consistent with their positioning in terms of bloom-condition areas and consensus regions defined by D'Ortenzio and d'Alcalà (2009) and Ayata et al. (2018).

The highest biomasses of the size fractions 60-200, 200-500 and 500-1000 µm recovered from the DCM sampling were determined at the southern (St17, St19) and northern (St4, St1) coastal stations. The lowest ones were recorded at St3 and St10 (Fig. 2b; Table S1). The size fractions 60-200 and 200-500 µm contributed the most to the total biomass (37 and 41% on average, respectively), while the contribution of the fraction 500-1000 µm was smaller (22% on average) (Fig. 2b; Table S1).

The spatial distribution pattern of the biomasses of the size fractions 60-200, 200-500 and 500-1000 µm (Fig. 2b) did not really correspond to that of the SPM of the fraction 0.7-60 µm (Fig. 2a). According to Fierro-González et al. (2023) and Tesán-Onrubia et al. (2023), the biomass of the fractions 60-200 and 200-500 µm was dominated by detritus and phytoplankton, which represented on average 68.8% (fraction 60-200 µm) and 59.2%

(fraction 200-500 µm) of the total biomass (against 31.2 and 40.8% for zooplankton, respectively). An inverse pattern was found for the fraction 500-1000 µm whose biomass was dominated by zooplankton (69.8% on average). Zooplankton was mainly composed of copepods, which accounted for 48.9, 91.9 and 69.7% of total zooplankton in the fractions 60-200, 200-500 and 500-1000 µm, respectively (Fierro-González et al., 2023; Tesán-Onrubia et al., 2023). Compared to the other stations, the fraction 60-200 µm at St4 was enriched in phytoplankton, while the fractions 60-200 and 200-500 µm at St17 were enriched in detritus.

The POC concentrations in the fractions 60-200, 200-500 and 500-1000 µm were the highest in the three offshore stations, i.e., St9-St11, and at the coastal station St1. They were the lowest at the coastal stations St17, St4 and St3 (Fig. 2c; Table S1). The low POC levels at St17 could be related to the high proportion of detritus within the biomass at this site. The POC concentrations were generally the highest for the fraction 200-500 µm, and the lowest for the 60-200 µm. The POC concentrations of the three size fractions were quite well correlated with each other ($r = 0.87\text{-}0.91$, $n = 9\text{-}10$, $p < 0.05$). However, the latter were not at all correlated with the those of the 0.7-60-µm fraction, as seen from Fig. 2a, c.

3.2. Lipids

Concentrations of total lipid biomarkers in the planktonic fractions 60-200, 200-500 and 500-1000 µm from the DCM are shown in Fig. 3. Concentrations of individual compounds are also presented in Table S2. Concentration of total (Σ_{39}) lipids (= concentrations of Σ_{25}fatty acids + Σ_{8}fatty alcohols + Σ_{6}sterols) ranged from 3.5 mg g^{-1} dw (equivalent to 0.35%) at St2, fraction 500-1000 µm to 35.6 mg g^{-1} dw (equivalent to 3.6%) at St9, fraction 200-500 µm (Fig. 3a). The highest Σ_{39}lipid concentrations were recorded in the three offshore stations St9-St11, as well as in the southern coastal stations St15 and St19, while the lowest ones were found at St17 and St3 (Fig. 3a). Σ_{39}lipid concentrations in the three fractions were

significantly positively correlated with each other ($r = 0.79$-0.86, $n = 9$-10, $p < 0.05$) and no significant difference was detected between the mean concentrations of the three fractions over the 10 stations (t-test, $p > 0.05$). The distribution of Σ_{39}lipid concentrations throughout stations and fractions was very close to that of POC (Fig. 2c). Logically, a significant positive relationship appeared between Σ_{39}lipid and POC concentrations when considering the fractions 60-200, 200-500 and 500-1000 µm ($r = 0.69$, $n = 29$, $p < 0.05$) (Fig. S1a). This underlines the strong link between the lipid and POC contents in the planktonic compartment. Interestingly, our Σ_{39}lipid concentrations (determined by GC-MS) were compared to those obtained by colorimetric method by Tesán-Onrubia et al. (2023) on the same samples. Both were rather well correlated ($r = 0.75$, $n = 29$, $p < 0.05$) albeit the colorimetric method gave slightly higher concentrations (Fig. S1b).

The Σ_{39}lipid concentrations we measured here in the three fractions (0.35-3.6%) were quite low compared to works by Båmstedt (1986) who found up to 61% lipid in some copepod species from temperate areas. However, they were of the same order of magnitude as a previous study conducted in the Mediterranean waters (3.0 ± 2.8%; Tiano et al., 2014). According to Lee et al. (2006), the plankton that has a year-round low-level supply of food available do not accumulate lipid reserves. This is in agreement with the oligotrophic character of the Mediterranean waters along with poor seasonality of food supply for plankton. In addition, even though zooplankton is known to have a higher content in lipids than phytoplankton, the occurrence of phytoplankton and detritus in addition to zooplankton species (mainly copepods) in each of our size fractions tended to lower their lipid content (Tesán-Onrubia et al., 2023), as for St17 where the high proportion of detritus was accompanied by a very low lipid content.

Concentrations of Σ_{25}fatty acids, Σ_{8}fatty alcohols and Σ_{6}sterols represented 80 ± 7.9%, 15 ± 8.6% and 5.0 ± 2.5% of the Σ_{39}lipid concentration, respectively (Fig. 3b-d). The

distribution of Σ_{25}fatty acid concentrations throughout stations and fractions (Fig. 3b) was very similar to that of Σ_{39}lipid concentrations (Fig. 3a). While the distribution of Σ_{6}sterol concentrations (Fig. 3d) followed also quite well those of Σ_{39}lipids and Σ_{25}fatty acids, the distribution of Σ_{8}fatty alcohol concentrations (Fig. 3c) was rather different from the three others. Overall, as for Σ_{39}lipids and Σ_{25}fatty acids, the highest Σ_{8}fatty alcohol and Σ_{6}sterol concentrations were measured in St9-St11, followed by St15, St19 and St1 (Fig. 3c, d).

The prevalence of 16:0, 14:0, 18:1w9, 18:0 and 16:1w7 compounds for fatty acids, and of 16:0 and 14:0 compounds for fatty alcohols (Table S2) reflected the overall dominance of the carnivorous/omnivorous zooplankton (Lee et al., 2006). Nevertheless, some indicators allowed us to point out substantial differences between stations. Indeed, some phytoplankton (organisms or detrital matter) biomarkers, such as 16:1w7/18:1w9 and 16:1w7/16:0 fatty acid ratios and the relative abundance of phytol among the fatty alcohols, were abundant at St4 and St17 (Fig. S2a-c). This could be related to the much higher contributions of phytoplankton and detritus found within the total biomass for the fractions 60-200 to 500-1000 µm at these two stations (Fierro-González et al., 2023; Tesán-Onrubia et al., 2023). These phytoplankton biomarkers revealed more pronounced signatures of diatoms and/or organisms feeding on phytoplankton residues (Falk-Petersen et al., 1981, 1982; Sargent and Falk-Petersen, 1981; Tolosa et al., 2004). Zooplankton biomarkers were also used: the relative abundance of 22:1, 20:5 and 22:6 fatty acids. The latter were higher in offshore stations, especially at St11 in the fraction 500-1000 µm, and St15 (Fig. S3a-c). They could highlight together the presence of herbivorous zooplankton feeding on diatoms (Kates and Volcani, 1966; Harrington et al., 1970; Graeve 1993; Lee et al., 2006). Indeed, according to Fierro-González et al. (2023), there was a high % (in biomass) of large crustaceans which could be euphausiids, actually potential consumers of diatoms, in the fractions 500-100 and 1000-2000 µm at St11 and St15. Moreover, according to the taxonomy results (M. Pagano personal communication), the % (in

number) of herbivorous filter feeders (large calanides of the Calanus type) over the entire water column was the highest at these two stations, especially St11.

Among sterols, cholesterol (Cholest-5-en-3ß-ol) was the dominant compound (63.5 ± 6.5%) followed by Cholesta-5,22*E*-dien-3ß-ol (14.4 ± 6.5%) (Table S2). These % are in agreement with previous values found in crustaceans from the Northern Adriatic Sea (Serrazanetti et al., 1989). The concentrations of cholesterol were low, in accordance with the overall low lipid content. This may be due not only to the composition of the zooplankton diet, but also to the absence in these organisms of biochemical mechanisms capable of converting into cholesterol some of the most diffused sterols in the marine environment (Serrazanetti et al., 1989).

3.3. Hydrocarbons

3.3.1. AH distribution

In seawater, dissolved Σ_{28}AH concentrations varied from 18 ng L^{-1} (St10) to 489 ng L^{-1} (St1) (Fig. S4a; Table S3). The highest values were recorded at St1, St9, St11, and at the Tunisian coasts (St15-St19), and were associated with monomodal molecular profiles in the range *n*-C_{22}-*n*-C_{36} without predominance of odd over even carbon numbered *n*-alkanes, which reflected anthropogenic inputs from uncombusted oil-derived products (Fig. S4b) (Bouloubassi and Saliot, 1993; Wang et al., 1997). The lower concentrations recorded at St2-St4 and St10 were associated with bimodal molecular profiles exhibiting, in the range *n*-C_{24}-*n*-C_{36}, anthropogenic input residues, and in the range *n*-C_{15}-*n*-C_{24}, the peculiar abundance of *n*-C_{16} and *n*-C_{18} linked to microorganism contribution (bacteria, fungi, yeast) and their action on algal detritus (Fig. S4c) (Elias et al., 1997). These molecular profiles have been already observed in the dissolved phase of variably anthropogenic-stressed marine coastal areas (Guigue et al., 2014).

In the fraction 0.7-60 µm, Σ_{28}AH concentrations varied from 3.9 µg g^{-1} dw (St9) to 104 µg g^{-1} dw (St11) (Fig. 4a; Table S4). The molecular profiles were dominated by *n*-C_{15} and *n*-C_{17} (Fig. 4b), indicative of phytoplanktonic contribution linked to high primary production (Blumer et al., 1971; Goutx and Saliot, 1980). Despite these predominant biological fingerprints, no correlation was found between *n*-C_{15} or *n*-C_{17} and TChl*a* concentrations (r = -0.12 to 0.23, n = 19, p > 0.05). For instance, *n*-pentadecane (*n*-C_{15}) has been shown to be produced by cyanobacteria, mainly in the lower euphotic zone, and rapidly consume by heterotrophic prokaryotes in the ocean (Love et al., 2021). This could explain the absence of correlation between *n*-C_{15} and TChl*a* concentrations.

In the fractions 60-200, 200-500 and 500-1000 µm, Σ_{28}AH concentrations ranged from 3.4 µg g^{-1} dw (St17, 60-200 µm) to 55 µg g^{-1} dw (St11, 500-1000 µm) (Fig. 4c; Table S4). While Σ_{28}AH concentrations in these three fractions were significantly positively correlated with each other (r = 0.62-0.88, n = 9-10, p < 0.05), they were all weakly correlated with that of the fraction 0.7-60 µm (r = 0.24-0.64, n = 9-10, p < 0.05 or > 0.05). No significant difference was detected between the mean concentrations of the four fractions over the 10 stations (t-test, p > 0.05). Interestingly, Σ_{28}AH concentration was significantly positively correlated to Σ_{39}lipid and POC concentrations only in the fraction 60-200 µm (r = 0.62-0.65, n = 10, p < 0.05).

Pristane was one of the main compounds within the low molecular weight range (< *n*-C_{22}) (Fig. 4d; Table S4), which is in line with the presence of zooplankton, especially the dominance of copepods (Blumer et al., 1963). Indeed, the high values of pristane in the fractions 200-500 and 500-1000 µm at St11 (Table S4) coincided with very high proportions of zooplankton (Fierro-González et al., 2023). Also, the abundance of *n*-C_{15} and *n*-C_{17} revealed the presence of phytoplanktonic residues (Fig. 4d), although no significant correlation was observed with these two latter biomarkers and the 16:1w7 diatom biomarker

(r = -0.28 to 0.16, n = 29, p > 0.05) (Blumer at al., 1971). The high molecular weight compounds (> *n*-C_{22}) displayed the predominance of odd over even carbon numbered compounds (*n*-C_{27}, *n*-C_{29}, *n*-C_{31}, *n*-C_{33}) (Fig. 4d; Table S4), illustrating the presence of terrigenous higher plant debris in the samples (Douglas and Eglinton, 1966). It is unlikely that these debris were ingested by the organisms. It seems more likely that they were part of some allochthonous detritus collected along with zooplankton as observed by imagery analyzes (Fierro-González et al., 2023). Moreover, a background series of *n*-alkanes with no predominance of odd over even compounds was visible and may originate from anthropogenic inputs with minor occurrence. These results (AH concentrations and their molecular profiles in plankton) are in good agreement with previous studies from neighboring areas (Serrazanetti et al., 1989, 1991; Salas et al., 2006).

This class of compounds is very useful to better assess the sources of hydrocarbons in planktonic organisms. Nevertheless, the dominance of biogenic signatures observed here makes AH biomarkers not very explanatory in the study of the bioaccumulation of anthropogenic hydrocarbons.

3.3.2 PAH distribution

In seawater, the dissolved Σ_{14}PAH concentrations ranged from 0.9 ng L^{-1} (St11) to 16 ng L^{-1} (St4) (Fig. S5a; Table S5). The concentrations were quite low (< 5 ng L^{-1}) and the methylated derivatives were not really identifiable, except at St4 (Fig. S5b, c). At this station, the concentration reached 16 ng L^{-1} due to significant inputs of C1-, C2- and C3-Nap (Fig. S5c). The 2-3 ring PAHs were the major compounds representing 71 ± 16% of the total PAHs, which is in accordance with their lower hydrophobicity (Fig. S5b, c; Table S5). The quite low levels of concentrations along with the highly altered methylated derivatives at almost all sites reflected remote or aged (weathered/photo-degraded) inputs, except at St4,

where local and recent moderate petrogenic inputs were suspected (Wang and Fingas, 1995; Chifflet et al., 2023).

In the fraction 0.7-60 µm, the Σ_{27}PAH concentrations ranged from 53 ng g^{-1} dw (St9) to ~ 220 ng g^{-1} dw (St3 and St11) (Fig. 5a; Table S6). The PAH profiles in the fraction 0.7-60 µm (Fig. 5b) were different from those found in water (Fig. S5b, c), the 2-3 ring PAHs being less abundant (49 ± 9% of total PAHs) and the 4-6 ring PAHs more abundant (Fig. 5b), which is consistent with previous studies on particles in the Mediterranean Sea (Dachs et al., 1997; Marti et al., 2001). However, as for PAHs in water (Fig. S5b, c), the methylated derivatives were not well visible in this fraction and suspected to be highly degraded. Hence, the PAH profiles in the fraction 0.7-60 µm might be explained by a high microbial degradation which rather affected LMW PAHs, especially methylated derivatives (Lipiatou et al., 1993; Dachs et al., 1997). Another explanation could be inputs of atmospheric aerosols or from sediments (Chifflet et al., 2023), which are important sources of pyrogenic PAHs (HMW PAHs with a low proportion of methylated derivatives) (Lipiatou et al., 1997), but the lack of 5-6 ring compounds suggests that these inputs were minor.

In the fractions 60-200, 200-500 and 500-1000 µm, the Σ_{27}PAH concentrations ranged from 35 ng g^{-1} dw (St19, 200-500 µm) to 255 ng g^{-1} dw (St1, 60-200 µm) (Fig. 5c; Table S6). The lowest Σ_{27}PAH concentrations were overall found at St9, St17 and St19 (Fig. 5c). Two of them, St9 and St19, showed the highest TChl*a* concentrations. These two stations displayed a particular biogeochemical context with regard to the other stations, as explained in section 3.1. Σ_{27}PAH concentrations in these three fractions were rather well positively correlated with each other ($r = 0.50\text{-}0.73$, $n = 9\text{-}10$, $p < 0.05$ or > 0.05), but not significantly correlated with that in the fraction 0.7-60 µm ($r = 0.14\text{-}0.55$, $n = 9\text{-}10$, $p > 0.05$). The mean Σ_{27}PAH concentration of the fraction 60-200 µm was significantly higher than those of the fractions 200-500 and 500-1000 µm (Fig. 5c) (t-test, $p < 0.05$). Σ_{27}PAH concentration was significantly

positively correlated to Σ_{28}AH concentration only in the fraction 0.7-60 µm ($r = 0.84$, $n = 10$, $p < 0.05$), while Σ_{27}PAH concentrations were not correlated with Σ_{39}lipid and POC concentrations whatever the size fraction. The PAH molecular profiles in the three fractions, i.e., dominance (80 ± 12%) of the 2-3 ring compounds (parents and methylated), especially Phe, and very low abundance of the 4-6 ring compounds (Fig. 5d), were in agreement with those reported by Salas et al. (2006) and Berrojalbiz et al. (2011).

3.4. Comparison of plankton PAH concentrations and biological pump fluxes of PAHs

It is important to note that comparisons of our concentrations/fluxes of PAHs and individual Phe (the dominant PAH in our study and also in most of previously works) with those reported in the literature should be taken with caution since the methodologies for sampling/separations of planktonic fractions, the planktonic size fractions, analyzes of PAHs and the number of PAHs analyzed are not the same. Despite these limitations, these comparisons still allow us to situate our data in relation to those obtained formerly.

The Σ_{27}PAH and Phe concentrations in plankton we determined here in the Western Mediterranean Sea were globally lower than those measured in the Western and Eastern Mediterranean Sea (Berrojalbiz et al., 2011), and in the Atlantic, Pacific and Indian Oceans (González-Gaya et al., 2019), when taking into account maximal and mean values (see data in Table 1). Salas et al. (2006) also found higher concentrations in the Galician coast (NW Spain) after the Prestige oil spill (353-2035 ng g^{-1} dw; not reported in Table 1). However, when considering minimal and median values, our Σ_{27}PAH concentrations were very close to those of other oceanic areas, and our Phe concentrations were even slightly higher (Table 1).

From the vertical settling flux of POC (reported in Table 1) and OC-normalized PAH concentrations (not presented in Table 1), we estimated the biological pump fluxes of

Σ_{27}PAHs and Phe below 100-m depth in the Western Mediterranean Sea at 15 ± 10 and 4 ± 2 ng m^{-2} day^{-1}, respectively (Table 1). González-Gaya et al. (2019) found mean biological pump fluxes of Σ_{64}PAHs and Phe below the surface mixed layer depth of 172 and 23 ng m^{-2} day^{-1} in the North Atlantic, 91 and 6 ng m^{-2} day^{-1} in the South Atlantic, 55 and 7 ng m^{-2} day^{-1} in the North Pacific, 14 and 1 ng m^{-2} day^{-1} in the South Pacific, and 22 and 2 ng m^{-2} day^{-1} in the Indian Ocean (Table 1). Therefore, our biological pump fluxes were lower than those in the Atlantic and North Pacific but comparable to those in the South Pacific and Indian Ocean. The annual biological pump flux of Σ_{27}PAHs for the whole Western Mediterranean Sea would be of 5274 ± 3467 kg yr^{-1}.

3.5. Accumulation patterns of PAHs within plankton

It is important to note that only seven parent PAHs (Nap, Flu, Phe, Flt, Pyr, BaA and Chr) were found both in water and all particulate/planktonic size fractions (Table S7). They were thus selected to investigate the accumulation patterns of PAHs within plankton (see below).

3.5.1. Concentration pattern with the size fraction and trophic level

The concentrations of Σ_7PAHs and Σ_6PAHs (without Phe) significantly decreased from the fractions 0.7-60 or 60-200 µm to the fractions 200-500 or 500-1000 µm (t-test, $p < 0.05$) (Fig. 6a, b), highlighting the bioreduction process of PAHs within the planktonic food web, i.e., decreasing concentration with increasing organism size/trophic level. The fact that the highest concentrations were found in the smallest fraction (0.7-60 µm) is in agreement with recent observations (Berroralbiz et al., 2011; Tao et al., 2018; González-Gaya et al., 2019) and related to the strong capacity of small cells to accumulate contaminants due to their high surface/volume ratio (Fan and Reinfelder, 2003; Heimbürger et al., 2010; Chouvelon et al., 2019). Fig. 7 shows the concentration levels in relation with the trophic levels, given by $\delta^{13}C$

and $\delta^{15}N$. It appears that the fraction 0.7-60 µm was trophically decoupled from the three other ones. In other words, the bioaccumulation of PAHs in the upper 60-200-µm fraction would not take place by trophic transfer from the 0.7-60-µm fraction but rather by water (bioconcentration). Then, considering the trophic proximity between the fractions 60-200, 200-500 and 500-1000 µm, it is possible that besides transfer from water, the PAHs were also transferred by ingestion/diet between these three fractions (Fig. 7a, b). The overall bioreduction observed would be due to the fact that when going up in the trophic levels, even if there was trophic transfer of PAHs, the processes of absorption directly by the water would have been less and less effective and the removal processes of PAHs (such as depuration or metabolization) likely more effective, which ultimately would have led to this decrease of PAH concentrations within the planktonic food web.

Phe presented a different pattern from the other compounds, with the highest concentrations mainly found in the fraction 60-200 µm (Fig. 6c; Fig. 7c). Phe was the most abundant compound representing for all sites 14, 51, 48 and 41% of Σ_7PAHs in the fractions 0.7-60, 60-200, 200-500 and 500-1000 µm, respectively. Berrojalbiz et al. (2011) also reported Phe (and alkylated homologues) as dominant compound in particles and plankton along a West-East transect in the Mediterranean Sea. In the present work, the peculiar Phe bioaccumulation in the fraction 60-200 µm, systematically observed at all stations (see Table S6), is intriguing. It could originate from a biogenic production within the collected plankton, as already suggested by Nizzetto et al. (2008). However, since there were no correlations between Phe concentrations, neither with POC, TChl*a*, nor lipids (in both fractions 0.7-60 and 60-200 µm) ($r = -0.33$ to -0.04, $n = 20$, $p > 0.05$), this suggests that even if this process had occurred, it would have been minor and hidden within the complex dynamics of Phe in plankton. Another explanation for the Phe bioaccumulation in the 60-200-µm fraction could

be that this compound was less subjected to depuration/metabolization processes than the other compounds and than in the other fractions.

3.5.2. Water-OC partitioning and influence of biomass

For each fraction at each station, the water-particulate matter coefficients (K_D in L kg^{-1}), then the water-organic carbon partition coefficients (K_{OC} in L kg^{-1}) were calculated for the 7 targeted PAHs (Tables S7-S9). It should be noticed that K_D and K_{OC} values were determined using dissolved PAH concentrations measured in surface waters (at ~ 5-20-m depth depending on stations) and particulate/plankton PAH concentrations measured in the DCM (at ~ 20-60 depth depending on the stations). Despite these depth discrepancies, and the possible differences in the dissolved PAH concentrations between surface waters and the DCM, we believe that the use of K_{OC} is more suitable and reflects the PAH biogeochemistry much better than the use of K_{OW} that are theoretical values provided under partition equilibrium conditions (these equilibrium conditions certainly did not prevail in the water at the time of sampling). Consistent with the concentration patterns, Log K_{OC} values clearly decreased with the size fractions, which confirms the higher PAH bioaccumulation in the smaller size fractions (Fig. 8a). Moreover, for each individual compound and each station, the PAH concentrations in size fractions (ng g^{-1} dw) were plotted against the plankton biomass concentrations (mg dw L^{-1}). For most of PAHs and size fractions (except 500-1000 µm), the concentrations decreased with biomass, following a power function equation $[PAH] = a[Biomass]^{-m}$ (Fig. 8b; Table S10), reinforcing the results presented above (Fig. 6, 7). This highlights the biodilution process, which reflects the decrease in PAH concentrations with plankton biomass (Berrojalbiz et al., 2011; Nizzetto et al., 2012; Everaert et al., 2015; Morales et al., 2015; Ding et al., 2021).

The -m slope values originating from the power function equations were further examined because they are indicative of the influence level of the SPM or biomass load on the PAH concentration (Berrojalbiz et al., 2011). As for Log K_{OC}, the -m values noticeably decreased with the size fraction (Fig. 8b), which illustrates once again the more important role of the smaller fractions in the bioaccumulation of PAH, as well as the biodilution process. These m values were then plotted against Log K_{OC}. Finally, a positive significant relationship was found between "-m" and the Log K_{OC} for the 7 PAHs and the different size fractions (0.7-60, 60-200, 200-500, 500-1000 µm, as well as 60-1000 µm) (Fig. S6; Table S11). Such a linear relationship highlighted the strong link between the PAH bioaccumulation (from water) and the impact of the planktonic biomass on the PAH concentrations in plankton, implying also the biological pump process for the PAHs. González-Gaya et al. (2019) observed the same type of relationship between -m slope and Log K_{OW}. Tao et al. (2018) also reported a decrease in the PAH concentration along with phyto- and zooplankton biomass, but without any obvious linear relationship between Log K_{OW} et -m. The present results show that through the bioaccumulation process, the plankton, and in particular its smallest fractions, plays a key role in the PAH cycling in the Mediterranean Sea. Besides, biotransformation/degradation is another essential fate for PAHs in the ocean. This biological reworking has already been reported by González-Gaya et al. (2019), who observed a linear negative relationship between Log K_{ow} and -m for some LMW PAHs. In our study, the biological removal was very likely present, especially in the fraction 60-200 µm, for which we also found a negative linear relationship between Log K_{OC} et -m for the LMW HAPs, as well as the low abundance of methylated derivatives.

4. Conclusion

In this study, we determined the hydrocarbon (AH and PAH) content in water and size-fractionated plankton to help characterizing the bioaccumulation of these compounds at the water-plankton interface in the Western Mediterranean Sea. Zooplankton was mainly composed of copepods and its low lipid content was in accordance with the oligotrophic character of the Mediterranean waters, along with poor seasonality of food supply for plankton. Concerning AHs, anthropogenic inputs were recorded in water at all sites, even though these inputs were masked in plankton by major biogenic signatures. Regarding PAHs, profiles in water and in the 0.7-60-µm size fraction were quite similar but distinct from those in zooplankton, highlighting difference in the processes driving the bioconcentration (passive transfer from water to phytoplankton) and bioaccumulation (passive transfer from water and active transfer from ingestion). The peculiar bioaccumulation of Phe in the 60-200 µm is intriguing and could be related to reduced metabolization/depuration processes. We also demonstrate the strong PAH bioconcentration in the 0.7-60-µm fraction, followed by a limited transfer to higher size fractions through bioaccumulation, ultimately underscoring a bioreduction process. Furthermore, the biodilution process (the decrease in concentration at higher SPM/biomass) was evidenced for the fractions 0.7-60 and 60-200 µm. Finally, our results point out the key role of the smallest size fractions of plankton in the PAH cycling in the Mediterranean Sea.

Data availability

All data from this paper is stored in the MISTRALS-SEDOO database (https://mistrals.sedoo.fr/MERITE/) and will be made publicly accessible once all the articles related to the MERITE-HIPPOCAMPE cruise are published. In the meantime, data can be obtained upon request from the corresponding author.

Author contribution statement

All the authors participated in the MERITE-HIPPOCAMPE project and design of the manuscript.

Conception and design of study: C.G., J.A.T.-O., D.B., F.C., M.P., S.C., J.T., M.T.

Acquisition of data: C.G., J.A.T.-O., L.G., D.B., F.C., M.P., S.C., D.M., L.C., M.T.

Analysis and/or interpretation of data: C.G., J.A.T.-O., L.G., D.B., F.C., M.P., S.C., D.M., L.C., J.T., M.T.

Drafting the manuscript: C.G., M.T.

Revising/editing the manuscript: C.G., J.A.T.-O., L.G., D.B., F.C., M.P., S.C., D.M., L.C., J.T., M.T.

Project administration and funding acquisition: F.C., M.P., J.T., M.T.

Acknowledgments

The MERITE-HIPPOCAMPE project was initiated and funded by the cross-disciplinary *Pollution & Contaminants* axis of the CNRS-INSU MISTRALS program (joint action of the MERMEX-MERITE and CHARMEX subprograms). The project also received financial support from the IRD French-Tunisian International Joint Laboratory (LMI) COSYS-Med. The MERITE-HIPPOCAMPE cruise was organized and supported by the French Oceanographic Fleet (FOF), CNRS/INSU, IFREMER, IRD, the Tunisian Ministry of Agriculture, Water Resources and Fisheries, and the Tunisian Ministry of Higher Education and Scientific Research. The project also benefited from additional funding by IFREMER, by the MIO Action Sud and Transverse Axis programs (CONTAM Transverse Axis), by the IRD Ocean Department, and by the CONTAMPUMP project (ANR JCJC #19-CE34-0001-01). We are grateful to the captains and crew of the R/V *Antea* for their help and assistance during the

cruise. Various MIO platforms also provided valuable support: the Service Atmosphère-Mer (SAM), the Plateforme Analytique de Chimie des Environnements Marins (PACEM platform) and the Platforme Microscopie et Imagerie (MIM platform). We warmly thank J.-F. Rontani for his expertise on lipid biomarkers. Finally, we acknowledge two Reviewers for their relevant and helpful comments.

Supplementary information

Supplementary material related to this article is available online at: xxx

References

Adhikari, P.L., Maiti, K., Overton, E.B., 2015. Vertical fluxes of polycyclic aromatic hydrocarbons in the northern Gulf of Mexico. Marine Chemistry, 168, 60–68. https://doi.org/10.1016/j.marchem.2014.11.001

Alekseenko, E., Thouvenin, B., Tronczyński, J., Carlotti, F., Garreau, P., Tixier, C., Baklouti, M., 2018. Modeling of PCB trophic transfer in the Gulf of Lions; 3D coupled model application. Marine Pollution Bulletin, 128, 140–155. https://doi.org/10.1016/j.marpolbul.2018.01.008.

Arnot, J.A., Gobas, F.A.P.C., 2006. A Review of Bioconcentration Factor (BCF) and Bioaccumulation Factor (BAF) Assessments for Organic Chemicals in Aquatic Organisms. Environmental Reviews, 14, 257–297. https://doi.org/10.1139/A06-005

Ayata, S.D., Irisson, J.O., Aubert, A., Berline, L., Dutay, J.C., Mayot, N., Nieblas, A.E., D'Ortenzio, F., Palmieri, J., Reygondeau, G., Rossi, V., Guieu, C., 2018. Regionalisation of the Mediterranean basin, a MERMEX synthesis. Progress in Oceanography, 163, 7–20. https://doi.org/10.1016/j.pocean.2017.09.016

Balcıoğlu, E.B., 2016. Potential effects of polycyclic aromatic hydrocarbons (PAHs) in marine foods on human health: a critical review. Toxin Reviews, 35, 98–105. https://doi.org/10.1080/15569543.2016.1201513

Båmstedt, U., 1986. Chemical composition and energy content. In: Corner, E.D.S., O'Hara, S. C.M. (eds.), The biological chemistry of marine copepods. Oxford University Press, New York, pp. 1–58.

Bănaru, D., Diaz, F., Verley, P., Campbell, R., Navarro, J., Yohia, C., Oliveros-Ramos, R., Mellon-Duval, C., Shin, Y.-J., 2019. Implementation of an end-to-end model of the Gulf of Lions ecosystem (NW Mediterranean Sea). I. Parameterization, calibration and evaluation. Ecological Modelling, 401, 1–19. https://doi.org/10.1016/j.ecolmodel.2019.03.005

Baumard, P., Budzinski, H., Garrigues, P., 1998. Polycyclic aromatic hydrocarbons in sediments and mussels of the western Mediterranean Sea. Environmental Toxicology and Chemistry, 17, 765–776. https://doi.org/10.1002/etc.5620170501

Béjaoui, B., Ben Ismail, S., Othmani, A., Ben Abdallah-Ben Hadj Hamida, O., Chevalier, C., Feki-Sahnoun, W., Harzallah, A., Ben Hadj Hamida, N., Bouaziz, R., Dahech, S., Diaz, F., Tounsi, K., Sammari, C., Pagano, M., Bel Hassen, M., 2019. Synthesis review of the Gulf of Gabes (eastern Mediterranean Sea, Tunisia): morphological, climatic, physical oceanographic, biogeochemical and fisheries features. Estuarine, Coastal and Shelf Science, 219, 395–408. https://doi.org/10.1016/j.ecss.2019.01.006

Ben Othman, H., Pick, F.R., Sakka Hlaili, A., Leboulanger, C., 2023. Effects of polycyclic aromatic hydrocarbons on marine and freshwater microalgae – A review. Journal of Hazardous Materials, 441, 129869. https://doi.org/10.1016/j.jhazmat.2022.129869

Berrojalbiz, N., Dachs, J., Ojeda, M.J., Valle, M.C., Castro-Jimenez, J., Wollgast, J., Ghiani, M., Hanke, G., Zaldivar, J.M., 2011. Biogeochemical and physical controls on

concentrations of polycyclic aromatic hydrocarbons in water and plankton of the Mediterranean and Black Seas. Global Biogeochemical Cycles, 25, GB4003. https://doi.org/10.1029/2010GB003775

Berrojalbiz, N., S. Lacorte, A. Calbet, E. Saiz, C. Barata, J. Dachs, 2009. Accumulation and cycling of polycyclic aromatic hydrocarbons in zooplankton, Environmental Science and Technology, 43, 2295–2301. https://doi.org/10.1021/es8018226

Blumer, M., Guillard, R.R.L., Chase, T., 1971. Hydrocarbons of marine phytoplankton. Marine Biology, 8, 183. https://doi.org/10.1007/BF00355214

Blumer, M., Mullin, M.M., Thomas, D.W., 1963. Pristane in Zooplankton. Science, 140, 974–974. https://doi.org/10.1126/science.140.3570.974

Bosse, A., Testor, P., Coppola L., Bretel, P., Dausse, D., Durrieu de Madron, X., Houpert, L., Labaste, M., Legoff, H., Mortier, L., D'Ortenzio, F., 2022. LION observatory data. SEANOE. https://doi.org/10.17882/44411

Boudriga, I., Thyssen, M., Zouari, A., Garcia, N., Tedetti, M., Bel Hassen, M., 2022. Ultraphytoplankton community structure in subsurface waters along a North-South Mediterranean transect. Marine Pollution Bulletin, 182, 113977. https://doi.org/10.1016/j.marpolbul.2022.113977

Bouloubassi, I., Méjanelle, L., Pete, R., Fillaux, J., Lorre, A., Point, V., 2006. PAH transport by sinking particles in the open Mediterranean Sea: A 1 year sediment trap study. Marine Pollution Bulletin, 52, 560–571. https://doi.org/10.1016/j.marpolbul.2005.10.003

Bouloubassi, I., Saliot, A., 1993. Investigation of anthropogenic and natural organic inputs in estuarine sediments using hydrocarbon markers (NAH, LAB, PAH). Oceanologica Acta 16, 145–161.

Castro-Jiménez, J., Bănaru, D., Chen, C.-T., Jiménez, B., Muñoz-Arnanz, J., Deviller, G., Sempéré, R., 2021. Persistent organic pollutants burden, trophic magnification and risk in

a pelagic food web from coastal NW Mediterranean Sea. Environmental Science and Technology, 55, 9557–9568. https://doi.org/10.1021/acs.est.1c00904

Chen, C.-T., Carlotti, F., Harmelin-Vivien, M., Lebreton, B., Guillou, G., Vassallo, L., Le Bihan, M., Bănaru, D., 2022. Diet and trophic interactions of Mediterranean planktivorous fishes. Marine Biology, 169, 119. https://doi.org/10.1007/s00227-022-04103-1

Chifflet, S., Briant, N., Tesán-Onrubia, J.A., Zaaboub, N., Amri, S., Radakovitch, O., Bãnaru, D., Tedetti, M., 2023. Distribution and accumulation of metals and metalloids in planktonic food webs of the Mediterranean Sea (MERITE-HIPPOCAMPE campaign). Marine Pollution Bulletin, 186, 114384. https://doi.org/10.1016/j.marpolbul.2022.114384

Chouvelon, T., Strady, E., Harmelin-Vivien, M., Radakovitch, O., Brach-Papa, C., Crochet, S., Knoery, J., Rozuel, E., Thomas, B., Tronczynski, J., Chiffoleau, J.F., 2019. Patterns of trace metal bioaccumulation and trophic transfer in a phytoplankton-zooplankton-small pelagic fish marine food web, Marine Pollution Bulletin, 146, 1013–1030. https://doi.org/10.1016/j.marpolbul.2019.07.047

Dachs, J., Bayona, J.M., Raoux, C., Albaigés, J., 1997. Spatial, Vertical Distribution and Budget of Polycyclic Aromatic Hydrocarbons in the Western Mediterranean Seawater. Environmental Science and Technology, 31, 682–688. https://doi.org/10.1021/es960233j

Ding, Q., Gong, X., Jin, M., Yao, X., Zhang, L., Zhao, Z., 2021. The biological pump effects of phytoplankton on the occurrence and benthic bioaccumulation of hydrophobic organic contaminants (HOCs) in a hypereutrophic lake. Ecotoxicoly and Environmental Safety, 213, 112017. https://doi.org/10.1016/j.ecoenv.2021.112017

D'Ortenzio, F., d'Alcalà, M.R., 2009. On the trophic regimes of the Mediterranean Sea: a satellite analysis. Biogeosciences, 6, 139–148. https://doi.org/10.5194/bg-6-139-2009

Douglas, G., Eglinton, G., 1966. Distribution of Alkanes, in Comparative Phytochemistry. Academic Press, New York, 57–77.

Duran, R., Cravo-Laureau, C., 2016. Role of environmental factors and microorganisms in determining the fate of polycyclic aromatic hydrocarbons in the marine environment. FEMS Microbiological Reviews, 40, 814–830. https://doi.org/10.1093/femsre/fuw031

Elias, V.O., Simoneit, B.R.T., Cardoso, J.N., 1997. Even n-alkanes on the Amazon shelf and a northeast Pacific hydrothermal system. Naturwissenschaften, 84, 415. https://doi.org/10.1007/s001140050421

EU-Directive, 2013. Directive 2013/39/EU of the European Parliament and of the Council of 12 August 2013 amending directives 2000/60/EC and 2008/105/EC as regards priority substances in the field of water policy. Official Journal of the European Union 1–17.

Everaert, G., De Laender, F., Goethals, P.L.M., Janssen, C.R., 2015. Multidecadal field data support intimate links between phytoplankton dynamics and PCB concentrations in marine sediments and biota. Environmental Science and Technology, 49, 8704–8711. https://doi.org/10.1021/acs.est.5b01159

Fan, C.-W., Reinfelder, J.R., 2003. Phenanthrene Accumulation Kinetics in Marine Diatoms. Environmental Science and Technology, 37, 3405−3412. https://doi.org/10.1021/es026367g

Falk-Petersen, S., Gatten, R.R., Sargent, J.R., Hopkins, C.C.E., 1981. Ecological investigation on the zooplankton community in Balsfjorden, northern Norway: Seasonal changes in the lipid class composition of Meganyctiphanes norvegia (M. Sars), Thysanoessa raschii (M Sars), T. inermis (Krøyer). Journal of Experimental Marine Biology and Ecology, 54, 209–224.

Falk-Petersen, S., Sargent, J.R., Hopkins, C.C.E., Vaja, B., 1982. Ecological investigations on the zooplankton community of Balsfjorden, northern Norway: lipids in the euphausiids Thysanoessa raschii and T. inermis during the spring. Marine Biology, 68, 97–102.

Fierro-González, P., Pagano, M., Guilloux, L., Makhlouf Belkahia, N., Tedetti, M., Carlotti, F., 2023. Zooplankton biomass, size structure, and associated metabolic fluxes with focus on its roles at the chlorophyll maximum layer during the plankton-contaminant MERITE-HIPPOCAMPE cruise. Marine Pollution Bulletin, 193, 115056. https://doi.org/10.1016/j.marpolbul.2023.115056

Fourati, R., Tedetti, M., Guigue, C., Goutx, M., Garcia, N., Zaghden, H., Sayadi, S., Elleuch, B., 2018a. Sources and spatial distribution of dissolved aliphatic and polycyclic aromatic hydrocarbons in surface coastal waters from the Gulf of Gabès (Tunisia, Southern Mediterranean Sea). Progress in Oceanography, 163, 232–247. http://dx.doi.org/10.1016/j.pocean.2017.02.001

Fourati, R., Tedetti, M., Guigue, C., Goutx, M., Zaghden, H., Sayadi, S., Elleuch, B., 2018b. Natural and anthropogenic particulate-bound aliphatic and polycyclic aromatic hydrocarbons in surface waters of the Gulf of Gabès (Tunisia, Southern Mediterranean Sea). Environmental Science and Pollution Research, 25, 2476–2494. https://link.springer.com/article/10.1007/s11356-017-0641-7

Frouin, H., Dangerfield, N., Macdonald, R.W., Galbraith, M., Crewe, N., Shaw, P., Mackas, D., Ross, P.S., 2013. Partitioning and bioaccumulation of PCBs and PBDEs in marine plankton from the Strait of Georgia, British Columbia, Canada. Progress in Oceanography, 115, 65–75. http://dx.doi.org/10.1016/j.pocean.2013.05.023

Galeron, M.-A., Amiraux, R., Charriere, B., Radakovitch, O., Raimbault, P., Garcia, N., Lagadec, V., Vaultier, F., Rontani, J.-F., 2015. Seasonal survey of the composition and

degradation state of particulate organic matter in the Rhône River using lipid tracers. Biogeosciences, 12, 1431–1446. https://doi.org/10.5194/bg-12-1431-2015

González-Gaya, B., Martínez-Varela, A., Vila-Costa, M., Casal, P., Cerro-Gálvez, E., Berrojalbiz, N., Lundin, D., Vidal, M., Mompean, C., Bode, A., Jiménez, B., Dachs, J., 2019. Biodegradation as an important sink of aromatic hydrocarbons in the oceans. Nature Geosciences, 12, 119–125. https://doi.org/10.1038/s41561-018-0285-3

Goutx, M., Saliot, A., 1980. Relationship between dissolved and particulate fatty acids and hydrocarbons, chlorophyll-a and zooplankton biomass in Villefranche Bay, Mediterranean Sea. Marine Chemistry, 8, 299. http://doi.org/10.1016/0304-4203(80)90019-5

Graeve, M., 1993. Umsatz und Verteilung von Lipiden in arktischen marinen Organismen unter besonderer Berücksichtigung unterer trophischer Stufen. Reports on Polar Research, 124, 1–141.

Guigue, C., Tedetti, M., Dang, D.H., Mullot, J.-U., Garnier, C., Goutx, M., 2017. Remobilization of polycyclic aromatic hydrocarbons and organic matter in seawater during sediment resuspension experiments from a polluted coastal environment: insights from Toulon Bay (France). Environmental Pollution, 229, 627–638. https://doi.org/10.1016/j.envpol.2017.06.090

Guigue, C., Tedetti, M., Ferretto, N., Garcia, N., Méjanelle, L., Goutx, M., 2014. Spatial and seasonal variabilities of dissolved hydrocarbons in surface waters from the Northwestern Mediterranean Sea: Results from one-year intensive sampling. Science of the Total Environment, 466–467, 650–662. https://doi.org/10.1016/j.scitotenv.2013.07.082

Guigue, C., Tedetti, M., Giorgi, S., Goutx, M., 2011. Occurrence and distribution of hydrocarbons in the surface microlayer and subsurface water from the urban coastal

marine area off Marseilles, Northwestern Mediterranean Sea. Marine Pollution Bulletin, 62, 2741–2752. http://dx.doi.org/10.1016/j.marpolbul.2011.09.013

Guitart, C., García-Flor, N., Miquel, J. C., Fowler, S. W., Albaigés, J., 2010. Effect of the accumulation of polycyclic aromatic hydrocarbons in the sea surface microlayer on their coastal air-sea exchanges. Journal of Marine Systems, 79, 210–217. https://doi.org/10.1016/j.jmarsys.2009.09.003

Guyennon, A., Baklouti, M., Diaz, F., Palmieri, J., Beuvier, J., Lebaupin-Brossier, C., Arsouze, T., Béranger, K., Dutay, J.-C., and Moutin, T., 2015. New insights into the organic carbon export in the Mediterranean Sea from 3-D modeling. Biogeosciences, 12, 7025–7046. https://doi.org/10.5194/bg-12-7025-2015

Harrington, G.W., Beach, D.H., Dunham, J.E., Holz, G.G., 1970. The polyunsaturated fatty acids of dinoflagellates. Journal of Protozoology, 17, 213–219.

Heimbürger, L.E., Cossa, D., Marty, J.C., Migon, C., Averty, B., Dufour, A., Ras, J., 2010. Methylmercury distributions in relation to the presence of nano and picophytoplankton in an oceanic water column (Ligurian Sea, North-western Mediterranean). Geochimica Cosmochimica Acta, 74, 5549–5559. https://doi.org/10.1016/j.gca.2010.06.036

Honda, M., Suzuki, N., 2020. Toxicities of polycyclic aromatic hydrocarbons for aquatic animals. International Journal of Environmental Research and Public Health, 17, 1363. https://doi.org/10.3390%2Fijerph17041363

Hylland, K., 2006. Polycyclic Aromatic Hydrocarbon (PAH) ecotoxicology in marine ecosystems. Journal of Toxicology and Environmental Health Part A, 69, 109–123. https://doi.org/10.1080/15287390500259327.

Islam, Md. S., Tanaka, M., 2004. Impacts of pollution on coastal and marine ecosystems including coastal and marine fisheries and approach for management: a review and

synthesis. Marine Pollution Bulletin, 48, 624–649. https://doi.org/10.1016/j.marpolbul.2003.12.004

Jónasdóttir, S.H., 2019. Fatty Acid Profiles and Production in Marine Phytoplankton. Marine Drugs, 17, 151. https://doi.org/10.3390/md17030151

Kates, K., Volcani, B.E., 1966. Lipid components of diatoms. Biochemical and Biophysical Acta, 116, 264–278.

Lee, R.F., Hagen, W., Kattner, G., 2006. Lipid storage in marine zooplankton. Marine Ecology Progress Series, 307, 273–306. http://dx.doi.org/10.3354/meps307273

Li, H., Duan, D., Beckingham, B., Yang, Y., Ran, Y., Grathwohl, P., 2020. Impact of trophic levels on partitioning and bioaccumulation of polycyclic aromatic hydrocarbons in particulate organic matter and plankton. Marine Pollution Bulletin, 160, 111527. https://doi.org/10.1016/j.marpolbul.2020.111527

Li, Z., Chi, J., Wu, Z., Zhang, Y., Liu, Y., Huang, L., Lu, Y., Uddin, M., Zhang, W., Wand, X., Lin, Y., Tong, Y., 2021. Characteristics of plankton Hg bioaccumulations based on a global data set and the implications for aquatic systems with aggravating nutrient imbalance. Frontiers of Environmental Science & Engineering, 16, 37. https://doi.org/10.1007/s11783-021-1471-x

Lipiatou, E., Marty, J.-C., Saliot, A., 1993. Sediment trap fluxes of polycyclic aromatic hydrocarbons in the Mediterranean Sea. Marine Chemistry, 44, 43–54. https://doi.org/10.1016/0304-4203(93)90005-9

Lipiatou, E., Tolosa, I., Simó, R., Bouloubassi, I., Dachs, J., Marti, S., Sicre, M.A., Bayona, J.M., Grimalt, J.O., Saliot, A., Albaigés, J., 1997. Mass budget and dynamics of polycyclic aromatic hydrocarbons in the Mediterranean Sea. Deep-Sea Research II, 44, 881–905. https://doi.org/10.1016/S0967-0645(96)00093-8

Love, C.R., Arrington, E.C., Gosselin, K.M., Reddy, C.M., Van Mooy, B.A.S., Nelson, R.K., Valentine, D.L., 2021. Nature Microbiology, 6, 489–498. https://doi.org/10.1038/s41564-020-00859-8

Mackay, D., Fraser, A., 2000. Bioaccumulation of Persistent Organic Chemicals: Mechanisms and Models. Environmental Pollution, 110, 375-391. http://dx.doi.org/10.1016/S0269-7491(00)00162-7

Mandić, J., Tronczyński, J., Kušpilić, G., 2018. Polycyclic aromatic hydrocarbons in surface sediments of the mid-Adriatic and along the Croatian coast: Levels, distributions and sources. Environmental Pollution, 242, 519–527. https://doi.org/10.1016/J.ENVPOL.2018.06.095

Margirier, F., Testor, P., Heslop, E., Mallil, K., Bosse, A., Houpert, L., Mortier, L., Bouin, M.-N., Coppola, L., D'Ortenzio, F., Durrieu de Madron, X., Mourre, B., Prieur, L., Raimbault, P., Taillandier, V., 2020. Abrupt warming and salinification of intermediate waters interplays with decline of deep convection in the Northwestern Mediterranean Sea. Scientific Reports, 10, 20923. https://doi.org/10.1038/s41598-020-77859-5.

Martí, S., Bayona, J.M., Méjanelle, L., Saliot, A., Albaigés, J., 2001. Biogeochemical evolution of the outflow of the Mediterranean deep-lying particulate organic matter into the northeasterne Atlantic. Marine Chemistry, 76, 211–231. https://doi.org/10.1016/S0304-4203(01)00064-0

Martin, J.H., Knauer, G.A., 1973. The elemental composition of plankton. Geochimica Cosmochimica Acta, 37, 1639–1653. https://doi.org/10.1016/0016-7037(73)90154-3.

Mille, G., Asia, L., Guiliano, M., Malleret, L., Doumenq, P., 2007. Hydrocarbons in coastal sediments from the Mediterranean Sea (Gulf of Fos area, France). Marine Pollution Bulletin, 54, 566–575. https://doi.org/10.1016/j.marpolbul.2006.12.009

Morales, L., Dachs, J., Fernández-Pinos, M.C., Berrojalbiz, N., Mompean, C., González-Gaya, B., Jiménez, B., Bode, A., Abalos, M., Abad, E., 2015. Oceanic sink and biogeochemical controls on the accumulation of polychlorinated dibenzo-pdioxins, dibenzofurans, and biphenyls in plankton. Environmental Science and Technology, 49, 13853–13861. https://doi.org/10.1021/acs.est.5b01360

Mzoughi, N., Chouba, L., 2011. Distribution and partitioning of aliphatic hydrocarbons and polycyclic aromatic hydrocarbons between water, suspended particulate matter, and sediment in harbours of the West coastal of the Gulf of Tunis (Tunisia). Journal of Environmental Monitoring, 13, 689–698. https://doi.org/10.1039/C0EM00616E

Nizzetto, L., Gioia, R., Li, J., Borga, K., Pomati, F., Bettinetti, R., Dachs, J., Jones, K.C., 2012. Biological pump control of the fate and distribution of hydrophobic organic pollutants in water and plankton. Environmental Science and Technology, 46, 3204–3211. http://dx.doi.org/10.1021/es204176q

Nizzetto, L., Lohmann, R., Gioia, R., Jahnke, A., Temme, C., Dachs, J., Herckes, P., Di Guardo, A., Jones, K.C., 2008. PAHs in air and seawater along north-south Atlantic transect: trends, processes and possible sources. Environmental Science and Technology, 42, 1580. https://doi.org/10.1021/ES0717414

Pirsaheb, M., Irandost, M., Asadi, F., Fakhri, Y., Asadi, A., 2018. Evaluation of polycyclic aromatic hydrocarbons (PAHs) in fish: a review and meta-analysis. Toxin Reviews, 39, 205–213. https://doi.org/10.1080/15569543.2018.1522643

Raimbault, P., Pouvesle, W., Sempéré, R., 1999. Wet-oxidation and automated colorimetry for simultaneous determination of organic carbon, nitrogen and phosphorus dissolved in seawater. Marine Chemistry, 66, 161–169. https://doi.org/10.1016/S0304-4203%2899%2900038-9

Raimbault, P., Lantoine, F., Neveux, J., 2004. Dosage rapide de la chlorophylle a et des phéopigments a par fluorimétrie après extraction au méthanol. Comparaison avec la méthode classique d'extraction à l'acétone. Océanis, 30, 189–205.

Rocha, M.J., Rocha, E., 2021. Concentrations, sources and risks of PAHs in dissolved and suspended material particulate fractions from the Northwest Atlantic Coast of the Iberian Peninsula. Marine Pollution Bulletin, 165, 112–143. https://doi.org/10.1016/j.marpolbul.2021.112143

Romero, I.C., Sutton, T., Carr, B., Quintana-Rizzo, E., Ross, S.W., Hollander, D.J., Torres, J.J., 2018. Decadal Assessment of Polycyclic Aromatic Hydrocarbons in Mesopelagic Fishes from the Gulf of Mexico Reveals Exposure to Oil-Derived Sources. Environmental Science and Technology, 52, 10985–10996. https://doi.org/10.1021/acs.est.8b02243

Rontani, J.-F., Galeron, M.-A., Amiraux, R., Artigue, L., Belt, S.T., 2017. Identification of di- and triterpenoid lipid tracers confirms the significant role of autoxidation in the degradation of terrestrial vascular plant material in the Canadian Arctic. Organic Geochemistry, 108, 43–50. https://doi.org/10.1016/j.orggeochem.2017.03.011

Salas, N., Ortiz L., Gilcoto, M., Varela, M., Bayona J.M., Groom, S., Álvarez-Salgado, X.A., Albaigés J., 2006. Fingerprinting petroleum hydrocarbons in plankton and surface sediments during the spring and early summer blooms in the Galician coast (NW Spain) after the Prestige oil spill. Marine Environmental Research, 62, 388–413. https://doi.org/10.1016/j.marenvres.2006.06.004

Sargent, J.R., Falk-Petersen, S.F., 1981. Ecological investigations on the zooplankton community in Balsfjorden, northern Norway: Lipids and fatty acids in Meganyctiphanes norvegia, Thysanoessa raschi, and T. inermis during midwinter. Marine Biology, 62, 131–137.

Schäfer, S., Buchmeier, G., Claus, E., Duester, L., Heininger, P., Körner, A., Mayer, P., Paschke, A., Rauert, C., Reifferscheid, G., Rüdel, H., Schlechtriem, C., Schröter-Kermani, C., Schudoma, D., Smedes, F., Steffen, D., Vietoris, F., 2015. Bioaccumulation in aquatic systems: methodological approaches, monitoring and assessment. Environmental Sciences Europe, 27, 5. https://doi.org/10.1186%2Fs12302-014-0036-z

Serrazanetti, G.P., Conte, L.S., Carpené, E., Bergami, C., Fonda-Umani, S., 1991. DISTRIBUTION OF ALIPHATIC HYDROCARBONS IN PLANKTON OF ADRIATIC SEA OPEN WATERS. Chemosphere, 23, 925–938. https://doi.org/10.1016/0045-6535(91)90097-W

Serrazanetti, G.P., Conte, L.S., Cattani, O., 1989. ALIPHATIC HYDROCARBON AND STEROL CONTENT OF ZOOPLANKTON OF THE EMILIA-ROMAGNA COAST (NORTHERN ADRIATIC). Comparative Biochemistry and Physiology, 94B, 143–148. https://doi.org/10.1016/0305-0491(89)90025-4

Siegel, D.A., Buesseler, K.O., Doney, S.C., Sailley, S.F., Behrenfeld, M.J., Boyd, P.W., 2014. Global assessment of ocean carbon export by combining satellite observations and food-web models. Global Biogeochemical Cycles, 28, 181–196, doi:10.1002/2013GB004743.

Stogiannidis, E., Laane, R., 2015. Source characterization of polycyclic aromatic hydrocarbons by using their molecular indices: an overview of possibilities. Reviews of Environmental Contamination and Toxicology, 234, 49–133. https://doi.org/10.1007/978-3-319-10638-0_2

Stortini, A.M., Martellini, T., Del Bubba, M., Lepri, L., Capodaglio, G., Cincinelli, A., 2009. n-Alkanes, PAHs and surfactants in the sea surface microlayer and sea water samples of the Gerlache Inlet sea (Antartica). Microchemical Journal, 92, 37–43. https://doi.org/10.1016/j.microc.2008.11.005

Strady, E., Harmelin-Vivien, M., Chiffoleau, J.F., Veron, A., Tronczynski, J., Radakovitch, O., 2015. ^{210}Po and ^{210}Pb trophic transfer within the phytoplankton–zooplankton–anchovy/sardine food web: a case study from the Gulf of Lion (NW Mediterranean Sea. Journal of Environmental Radioactivity, 143, 141–151. http://dx.doi.org/10.1016/j.jenvrad.2015.02.019

Swackhamer, D.L., Skoglund, R.S., 1993. Bioaccumulation of PCBs by algae: kinetics versus equilibrium. Environmental Toxicology and Chemistry, 12, 831–838. https://doi.org/10.1002/etc.5620120506

Tao, Y., Xue, B., Lei, G., Liu, F., Wang, Z., 2017a. Effects of climate change on bioaccumulation and biomagnification of polycyclic aromatic hydrocarbons in the planktonic food web of a subtropical shallow eutrophic lake in China. Environmental Pollution, 223, 624–634. https://doi.org/10.1016/j.envpol.2017.01.068

Tao, Y., Yu, J., Liu, X., Xue, B., Wang, S., 2018. Factors affecting annual occurrence, bioaccumulation, and biomagnification of polycyclic aromatic hydrocarbons in plankton food webs of subtropical eutrophic lakes. Water Research, 132, 1–11. https://doi.org/10.1016/j.watres.2017.12.053

Tao, Y., Yu, J., Xue, B., Yao, S., Wang, S., 2017b. Precipitation and temperature drive seasonal variation in bioaccumulation of polycyclic aromatic hydrocarbons in the planktonic food webs of a subtropical shallow eutrophic lake in China. Science of the Total Environment, 583, 447–457. http://dx.doi.org/10.1016/j.scitotenv.2017.01.100

Tedetti, M., Tronczynski, J., 2019. HIPPOCAMPE cruise, RV Antea. https://doi.org/10.17600/18000900

Tedetti, M., Tronczynski, J., Carlotti, F., Pagano, M., Sammari, C., Bel Hassen, M., Ben Ismail, S., Desboeufs, K., Poindron, C., Chifflet, S., Abdennadher, M., Amri, S., Bănaru, D., Ben Abdallah, L., Bhairy, N., Boudriga, I., Bourin, A., Brach-Papa, C., Briant, N.,

Cabrol, L., Chevalier, C., Chouba, L., Coudray, S., Daly Yahia, M.N., de Garidel-Thoron, T., Dufour, A., Dutay, J.-C., Espinasse, B., Fierro-González, P., Fornier, M., Garcia, N., Giner, F., Guigue, C., Guilloux, L., Hamza, A., Heimbürger-Boavida, L.-E., Jacquet, S., Knoery, J., Lajnef, R., Makhlouf Belkahia, N., Malengros, D., Martinot, P.L., Bosse, A., Mazur, J.-C., Meddeb, M., Misson, B., Pringault, O., Quéméneur, M., Radakovitch, O., Raimbault, P., Ravel, C., Rossi, V., Rwawi, C., Sakka Hlaili, A., Tesán Onrubia, J.A., Thomas, B., Thyssen, M., Zaaboub, N., Zouari, A., Garnier, C., 2023. Contamination of planktonic food webs in the Mediterranean Sea: Setting the frame for the MERITE-HIPPOCAMPE oceanographic cruise (spring 2019). Marine Pollution Bulletin, 189, 114765. https://doi.org/10.1016/j.marpolbul.2023.114765

Tesán-Onrubia, J.A., Tedetti, M., Carlotti, F., Tenaille, M., Guilloux, L., Pagano, M., Lebreton, B., Guillou, G., Fierro-González, P., Guigue, C., Chifflet, S., Garcia, T., Boudriga, I., Belhassen, M., Bellaaj-Zouari, M., Bănaru, D., 2023. Spatial variations of biochemical content and stable isotope ratios of size-fractionated plankton in the Mediterranean Sea (MERITE-HIPPOCAMPE campaign). Marine Pollution Bulletin, 189, 114787. https://doi.org/10.1016/j.marpolbul.2023.114787

Tiano, M., Tronczyński, J., Harmelin-Vivien, M., Tixier, C., Carlotti, F., 2014. PCB concentrations in plankton size classes, a temporal study in Marseille Bay, Western Mediterranean Sea. Marine Pollution Bulletin, 89, 331–339. https://doi.org/10.1016/j.marpolbul.2014.09.040

Tolosa, I., J. de Mora, S., Fowler, S.W., Villeneuve, J.-P., Bartocci, J., Cattini, C., 2005. Aliphatic and aromatic hydrocarbons in marine biota and coastal sediments from the Gulf and the Gulf of Oman, Marine Pollution Bulletin, 50, 1619-1633. https://doi.org/10.1016/j.marpolbul.2005.06.029

Tolosa, I., Vescovalib, I., LeBlond, N., Marty, J.C., de Moraa, S., Prieur, L., 2004. Distribution of pigments and fatty acid biomarkers in particulate matter from the frontal structure of the Alboran Sea (SW Mediterranean Sea). Marine Chemistry, 88, 103– 125. https://doi.org/10.1016/j.marchem.2004.03.005

Tong, Y., Chen, L., Liu, Y., Wang, Y., Tian, S., 2019. Distribution, sources an ecological risk assessment of PAHs in surface seawater from coastal Bohai Bay, China. Marine Pollution Bulletin, 142, 520–524. https://doi.org/10.1016/j.marpolbul.2019.04.004

US-EPA, 2012. US Environmental Protection Agency. Appendix A to 40 CFR, Part 423–126, Priority Pollutants.

Volkman, J.K., Holdsworth, D.G., Neill, G.P., Bavor, H.J., 1992. Identification of natural, anthropogenic and petroleum hydrocarbons in aquatic sediments. Science of The Total Environment, 112, 203–219. https://doi.org/10.1016/0048-9697(92)90188-X

Wang, Z., Fingas, M., 1995. Differentiation of the source of spilled oil and monitoring of the oil weathering process using gas chromatography–mass spectrometry. Journal of Chromatography A, 712, 321–43. https://doi.org/10.1016/0021-9673(95)00546-Y

Wang, Z., Fingas, M., Landriault, M., Sigouin, L., Feng, Y., Mullin, J., 1997. Using systematic and comparative analytical data to identify the source of an unknown oil on contaminated birds. Journal of Chromatography A, 775, 251–265.

Wang, Z., Fingas, M., Page, D.S., 1999. Oil spill identification. Journal of Chromatography A, 843, 369–411. http://dx.doi.org/10.1016/S0021-9673(99)00120-X

Welschmeyer, N.A., 1994. Fluorometric analysis of chlorophyll a in the presence of chlorophyll b and pheopigments. Limnology and Oceanography, 39, 1985–1992. https://doi.org/10.4319/LO.1994.39.8.1985

Yunker, M.B., Macdonald, R.W., Vingarzan, R., Mitchell, R.H., Goyette, D., Sylvestre, S., 2002. PAHs in the Fraser River basin: A critical appraisal of PAH ratios as indicators of

PAH source and composition. Organic Geochemistry, 33, 489–515. https://doi.org/10.1016/S0146-6380(02)00002-5

Zaghden, H., Tedetti, M., Sayadi, S., Serbaji, M.M., Elleuch, B., Saliot, A., 2017. Origin and distribution of hydrocarbons and organic matter in the surficial sediments of the Sfax-Kerkennah channel (Tunisia, Southern Mediterranean Sea). Marine Pollution Bulletin, 117, 414–428. https://doi.org/10.1016/j.marpolbul.2017.02.007

Figure caption

Figure 1. a) Location of the ten stations (black circles) investigated during the MERITE-HIPPOCAMPE cruise (13 April-14 May 2019) along a North-South transect in the Mediterranean Sea on board the R/V *Antea*, and **b)** cruise track with the position of the stations. St2, St4, St3, St10 and St11 were sampled during leg 1 (13-28 April; from La Seyne-sur-Mer to Tunis), whereas St15, St17, St19, St9 and St1 were sampled during leg 2 (30 April-14 May; from Tunis to Gulf of Gabès, and then return to La Seyne-sur-Mer). See the detailed description of stations in Tedetti et al. (2023).

Figure 2. a) Concentrations of total chlorophyll *a* (TChl*a*, in µg L^{-1}), suspended particulate matter (SPM, in mg L^{-1}) and particulate organic carbon (POC, in mg L^{-1}) in the size fraction 0.7-60 µm, **b)** total biomass (in µg dw L^{-1}) (see Fierro-González et al., 2023, this cumulates phytoplankton, zooplankton and detritus biomasses), and **c)** concentration of POC (in mg g^{-1} dw) in the planktonic size fractions 60-200, 200-500 and 500-1000 µm, sampled at the deep chlorophyll maximum (DCM). All measurements are presented for the 10 stations. For POC, sample St17 500-1000 µm is not available.

Figure 3. Concentrations of total lipid biomarkers (in mg g^{-1} dw) in the planktonic size fractions 60-200, 200-500 and 500-1000 µm recovered from the deep chlorophyll maximum (DCM) at the 10 stations: **a)** Σ_{39}lipids (= Σ_{25}fatty acids + Σ_{8}fatty alcohols + Σ_{6}sterols), **b)** Σ_{25}fatty acids, **c)** Σ_{8}fatty alcohols and **d)** Σ_{6}sterols. Sample St17 500-1000 µm is not available.

Figure 4. Concentrations of total aliphatic hydrocarbons (Σ_{28}AHs, in µg g^{-1} dw) in the particulate/planktonic size fractions **a)** 0.7-60 µm and **c)** 60-200, 200-500 and 500-1000 µm, recovered from the deep chlorophyll maximum (DCM) at the 10 stations, and mean relative abundances of individual AHs (in %) for the 10 stations in the fractions **b)** 0.7-60 µm and **d)** 60-200, 200-500 and 500-1000 µm. Σ_{28}AHs = Σ *n*-C_{15}–*n*-C_{40}, Pr, Phy (28 compounds).

Figure 5. Concentrations of total polycyclic aromatic hydrocarbons (Σ_{27}PAHs, in ng g^{-1} dw) in the particulate/planktonic size fractions **a)** 0.7-60 µm and **c)** 60-200, 200-500 and 500-1000 µm, recovered from the deep chlorophyll maximum (DCM) at the 10 stations, and mean relative abundances of individual PAHs (in %) for the 10 stations in the fractions **b)** 0.7-60 µm and **d)** 60-200, 200-500 and 500-1000 µm. Σ_{27}PAHs = Σ Nap–BP (27 compounds).

Figure 6. Concentrations (in ng g^{-1} dw) of **a)** Σ_{7}PAHs (= Nap + Flu + Phe + Flt + Pyr + BaA + Chr), **b)** Σ_{6}PAHs (= Nap + Flu + Flt + Pyr + BaA + Chr), and **c)** Phe, for all 10 stations in the particulate/planktonic size fractions 0.7-60, 60-200, 200-500 and 500-1000 µm recovered from the deep chlorophyll maximum (DCM). Letters ***a)*** and ***b)*** indicate significant differences between the means of the distributions (t-test; $p < 0.05$).

Figure 7. Concentrations (in ng g^{-1} dw) of **a)** Σ_7PAHs (= Nap + Flu + Phe + Flt + Pyr + BaA + Chr), **b)** Σ_6PAHs (= Nap + Flu + Flt + Pyr + BaA + Chr), and **c)** Phe, with regard to the C and N isotopic ratios ($\delta^{13}C$ and $\delta^{15}N$, in ‰) for all 10 stations in the particulate/planktonic size fractions 0.7-60, 60-200, 200-500 and 500-1000 µm recovered from the deep chlorophyll maximum (DCM).

Figure 8. Distribution of **a)** Log K_{OC} and **b)** slope value (-m) in the particulate/planktonic size fractions 0.7-60, 60-200, 200-500 and 500-1000 µm recovered from the deep chlorophyll maximum (DCM). The letters ***a)***, ***b)*** and ***c)*** indicate significant differences between the means of the distributions (t-test; $p < 0.05$). Log K_{OC} and -m were determined in each fraction, at the 10 stations, for each of the 7 PAHs (Nap, Flu, Phe, Flt, Pyr, BaA, Chr). For each size fraction, the value m is the slope of the regression (power function) between the SPM/biomass concentration (in mg L^{-1} dw) and the concentration of the given PAH (in ng g^{-1} dw) for the 10 stations. Examples of SPM/biomass *versus* PAH power relationships and associated -m values are presented for Phe for each size fraction. The detailed regression parameters of the power functions for the 7 PAHs, including m values, are found in Table S10.

Table 1. Comparison of plankton PAH concentrations and biological pump fluxes of PAHs determined here for the Western Mediterranean Sea (over our ten stations) with those reported previously in the same and other oceanic areas. We present the data for total PAHs (sum of individual compounds) and individual phenanthrene.

		This study[a, b]	Berrojalbiz et al. (2011)[c, d]	González-Gaya et al. (2019)[d, e]				
		Western Med. Sea	**Western and Eastern Med. Sea**	**North Atlantic**	**South Atlantic**	**North Pacific**	**South Pacific**	**Indian Ocean**
Plankton total PAH concentration (ng g^{-1} dw)	Min	40	57	18	13	11	40	15
	Max	163	1903	790	1300	7700	360	440
	Median	102	*na*	180	88	37	110	45
	Mean ± SD	96 ± 41	*na*	250 ± 230	280 ± 350	590 ± 2000	140 ± 120	130 ± 130
Plankton Phe concentration (ng g^{-1} dw)	Min	12	9	2	1	1	5	2
	Max	39	235	120	120	1035	33	59
	Median	26	*na*	8	7	4	8	6
	Mean ± SD	25 ± 10	77 ± *na*	30 ± 39	18 ± 28	78 ± 280	11 ± 11	13 ± 15
POC vertical flux (mg C m^{-2} day^{-1})	Mean	27[f]	*na*	39[g]	37[g]	57[g]	58[g]	46[g]
Biological pump flux of total PAHs (ng m^{-2} day^{-1})	Min	5	*na*	*na*	*na*	*na*	*na*	*na*
	Max	39	*na*	*na*	*na*	*na*	*na*	*na*
	Median	15	*na*	*na*	*na*	*na*	*na*	*na*
	Mean ± SD	15 ± 10	*na*	172 ± *na*	91 ± *na*	55 ± *na*	14 ± *na*	22 ± *na*
Biological pump flux of Phe (ng m^{-2} day^{-1})	Min	1	*na*	*na*	*na*	*na*	*na*	*na*
	Max	7	*na*	*na*	*na*	*na*	*na*	*na*
	Median	4	*na*	*na*	*na*	*na*	*na*	*na*
	Mean ± SD	4 ± 2	*na*	23 ± *na*	6 ± *na*	7 ± *na*	1 ± *na*	2 ± *na*

na: not available; Phe: phenanthrene; POC: particulate organic carbon; [a] Total PAHs = sum of 27 compounds (Σ_{27}PAHs); [b] The plankton fraction corresponds to the size fraction 60-1000 µm; [c] Total PAHs = sum of 19 compounds (Σ_{19}PAHs); [d] The plankton fraction corresponds to the size fraction > 50 µm; [e] Total PAHs = sum of 64 compounds (Σ_{64}PAHs); [f] Vertical settling flux of POC below 100-m depth for the western Mediterranean Sea estimated by Guyennon et al. (2015), where POC is defined as being fueled by the natural mortality of the largest organisms (mesozooplankton, diatoms and ciliates) and by the excretion of fecal pellets and sloppy feeding by mesozooplankton; [g] Vertical settling flux of POC from the surface mixed layer due to phytoplankton and to zooplankton-associated pellets estimated from Siegel et al. (2014)'s global climatology.

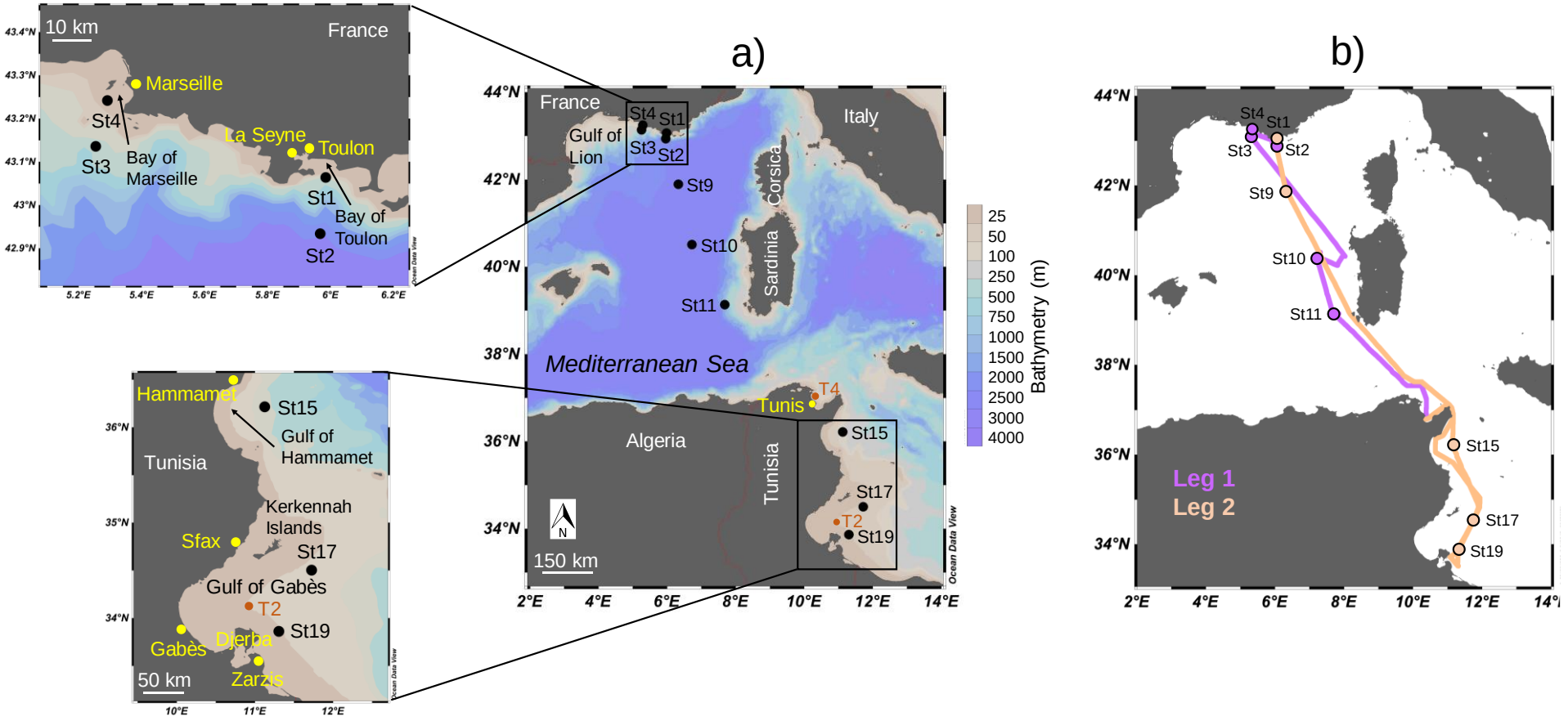
a)
b)
10 km
France
Marseille
St4
St3
Bay of Marseille
La Seyne
Toulon
St1
Bay of Toulon
St2
Hammamet
St15
Gulf of Hammamet
Tunisia
Kerkennah Islands
Sfax
St17
Gulf of Gabès
T2
St19
Gabès
Djerba
Zarzis
50 km
Gulf of Lion
Italy
St9
Corsica
St10
Sardinia
St11
Mediterranean Sea
T4
Tunis
Algeria
150 km
Bathymetry (m)
25
50
100
250
500
750
1000
1500
2000
2500
3000
4000
Leg 1
Leg 2

Figure 1

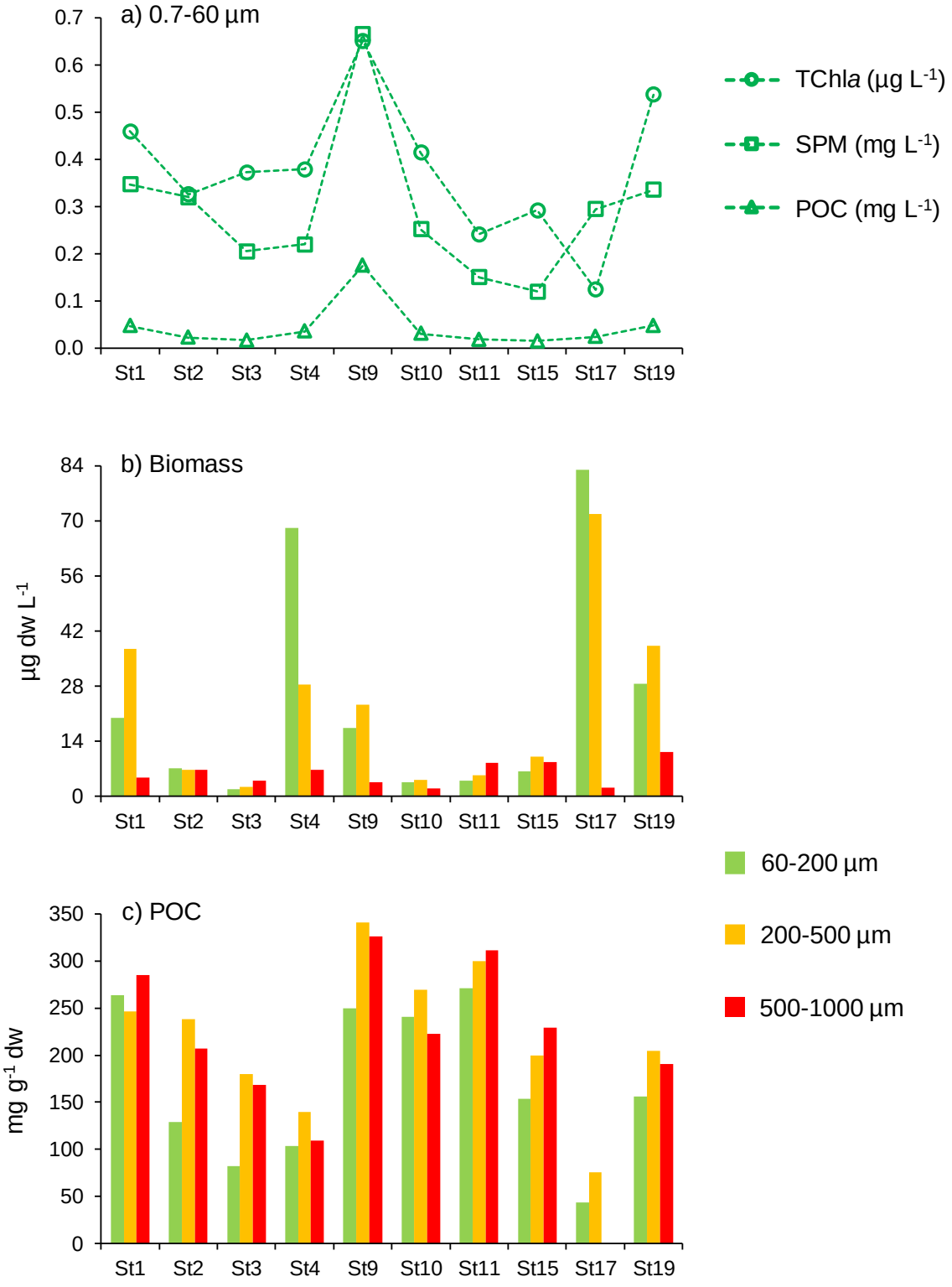
a) 0.7-60 µm
0.7
0.6
0.5
0.4
0.3
0.2
0.1
0.0
St1 St2 St3 St4 St9 St10 St11 St15 St17 St19
TChla (µg L-1)
SPM (mg L-1)
POC (mg L-1)
b) Biomass
µg dw L-1
84
70
56
42
28
14
0
St1 St2 St3 St4 St9 St10 St11 St15 St17 St19
60-200 µm
200-500 µm
500-1000 µm
c) POC
mg g-1 dw
350
300
250
200
150
100
50
0
St1 St2 St3 St4 St9 St10 St11 St15 St17 St19

Figure 2

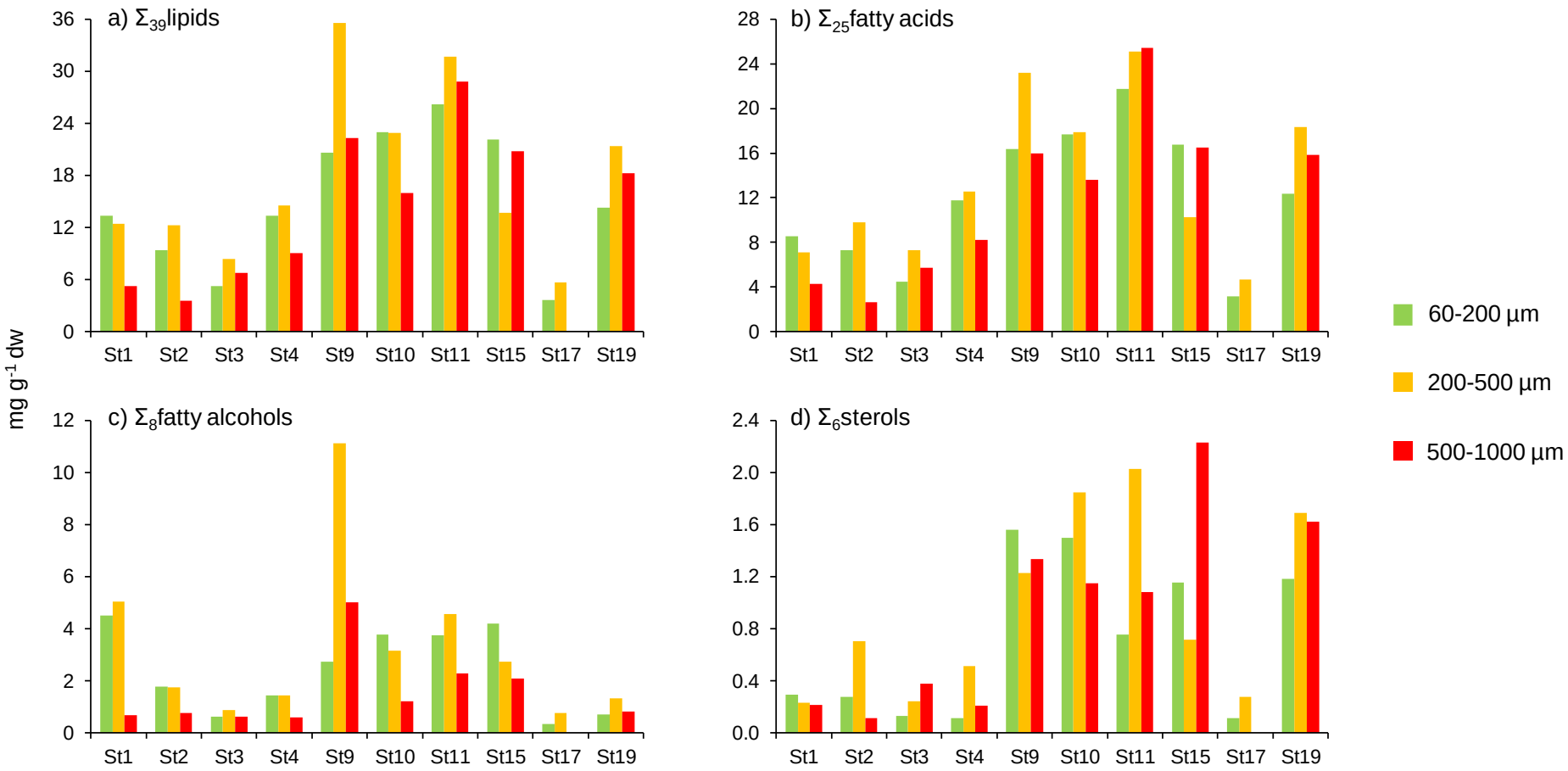
a) Σ39lipids
b) Σ25fatty acids
c) Σ8fatty alcohols
d) Σ6sterols
mg g-1 dw
St1
St2
St3
St4
St9
St10
St11
St15
St17
St19
60-200 µm
200-500 µm
500-1000 µm

Figure 3

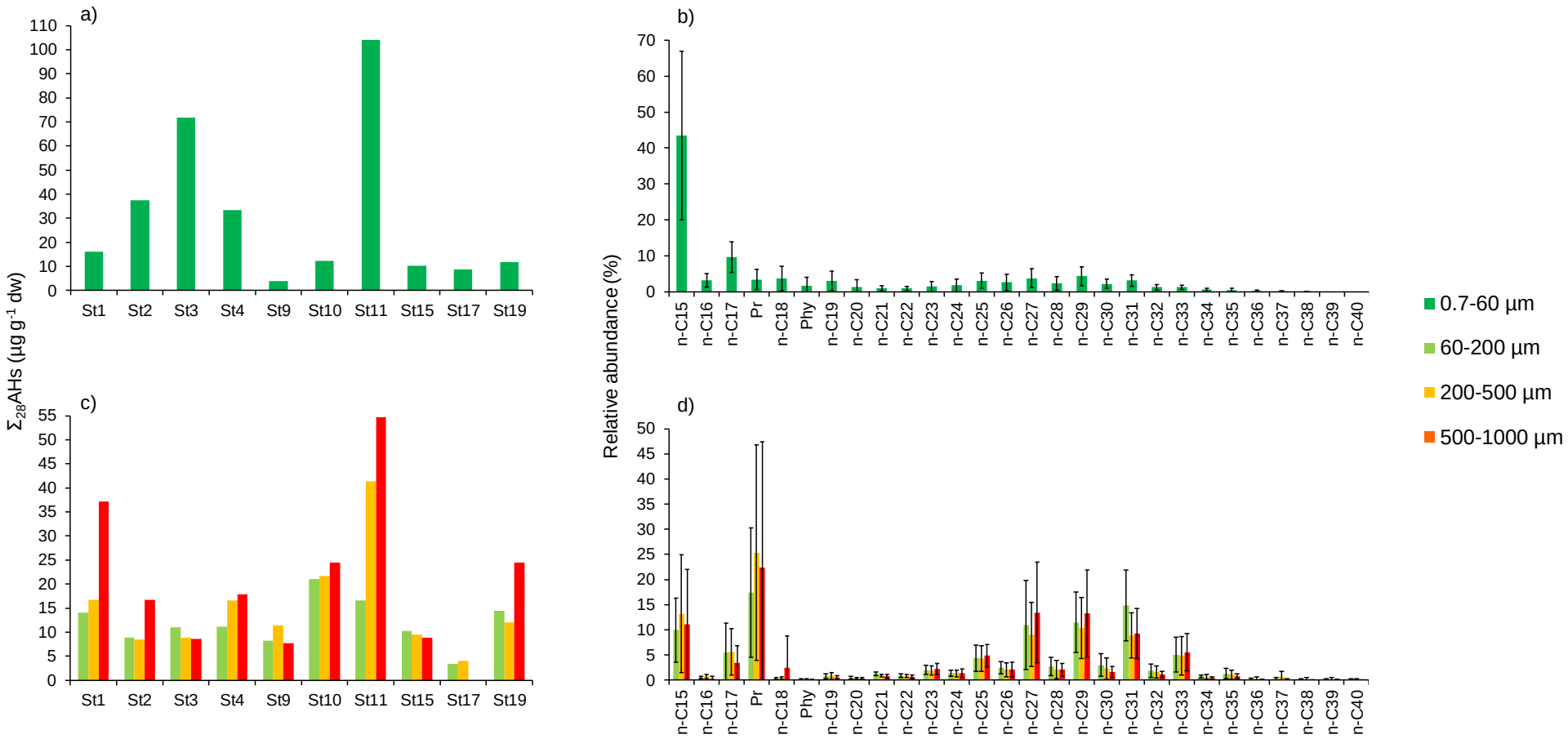
a)
b)
c)
d)
Σ_{28}AHs (µg g^{-1} dw)
Relative abundance (%)
St1
St2
St3
St4
St9
St10
St11
St15
St17
St19
n-C15
n-C16
n-C17
Pr
n-C18
Phy
n-C19
n-C20
n-C21
n-C22
n-C23
n-C24
n-C25
n-C26
n-C27
n-C28
n-C29
n-C30
n-C31
n-C32
n-C33
n-C34
n-C35
n-C36
n-C37
n-C38
n-C39
n-C40
0.7-60 µm
60-200 µm
200-500 µm
500-1000 µm

Figure 4

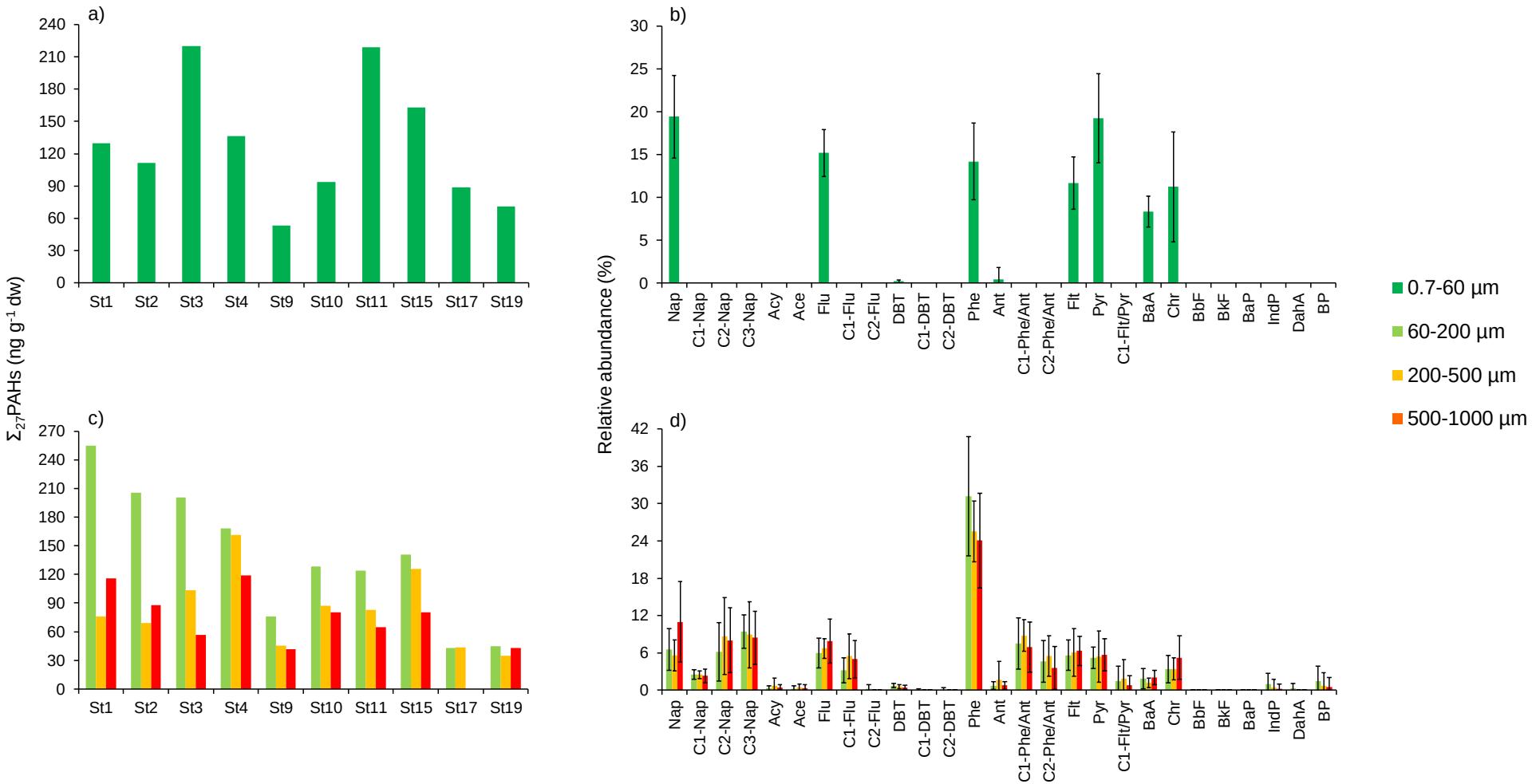
a)
b)
c)
d)
Σ27PAHs (ng g-1 dw)
Relative abundance (%)
St1
St2
St3
St4
St9
St10
St11
St15
St17
St19
Nap
C1-Nap
C2-Nap
C3-Nap
Acy
Ace
Flu
C1-Flu
C2-Flu
DBT
C1-DBT
C2-DBT
Phe
Ant
C1-Phe/Ant
C2-Phe/Ant
Flt
Pyr
C1-Flt/Pyr
BaA
Chr
BbF
BkF
BaP
IndP
DahA
BP
0.7-60 µm
60-200 µm
200-500 µm
500-1000 µm

Figure 5

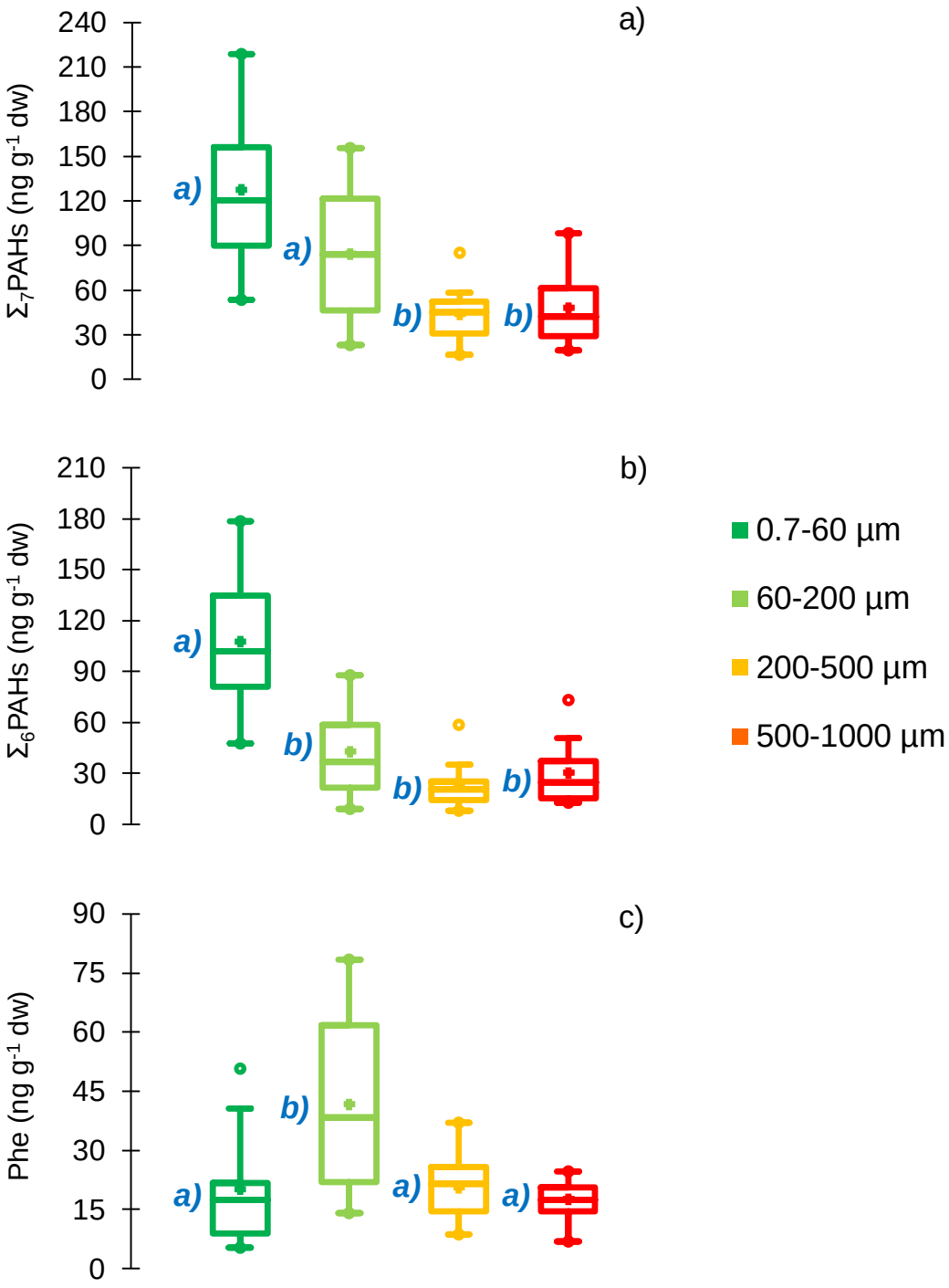
a)
240
210
180
150
120
90
60
30
0
Σ7PAHs (ng g-1 dw)
a)
a)
b)
b)
b)
210
180
150
120
90
60
30
0
Σ6PAHs (ng g-1 dw)
a)
b)
b)
b)
0.7-60 µm
60-200 µm
200-500 µm
500-1000 µm
c)
90
75
60
45
30
15
0
Phe (ng g-1 dw)
a)
b)
a)
a)

Figure 6

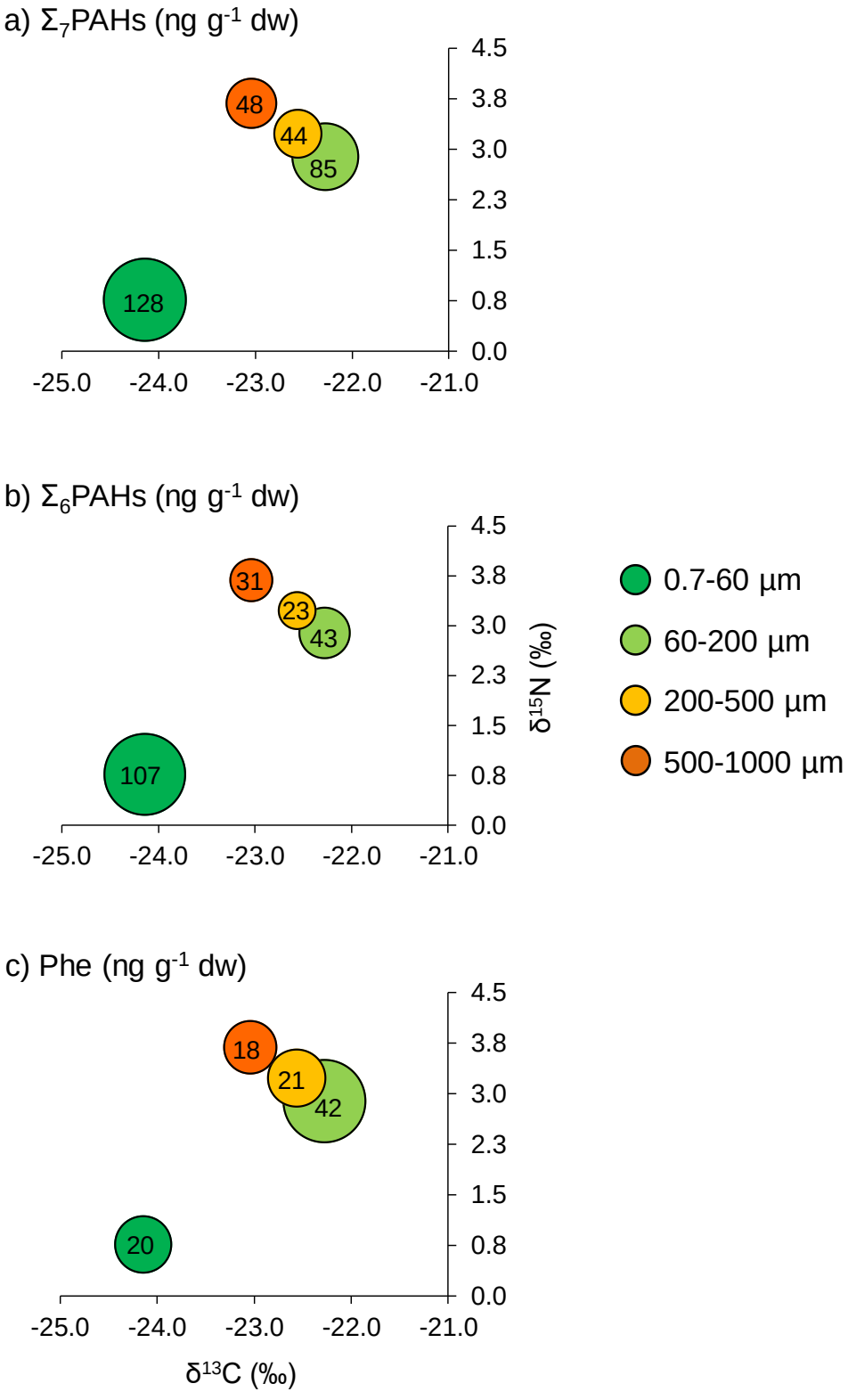
a) Σ7PAHs (ng g-1 dw)
48
44
85
128
4.5
3.8
3.0
2.3
1.5
0.8
0.0
-25.0
-24.0
-23.0
-22.0
-21.0
b) Σ6PAHs (ng g-1 dw)
31
23
43
107
δ15N (‰)
0.7-60 µm
60-200 µm
200-500 µm
500-1000 µm
c) Phe (ng g-1 dw)
18
21
42
20
δ13C (‰)

Figure 7

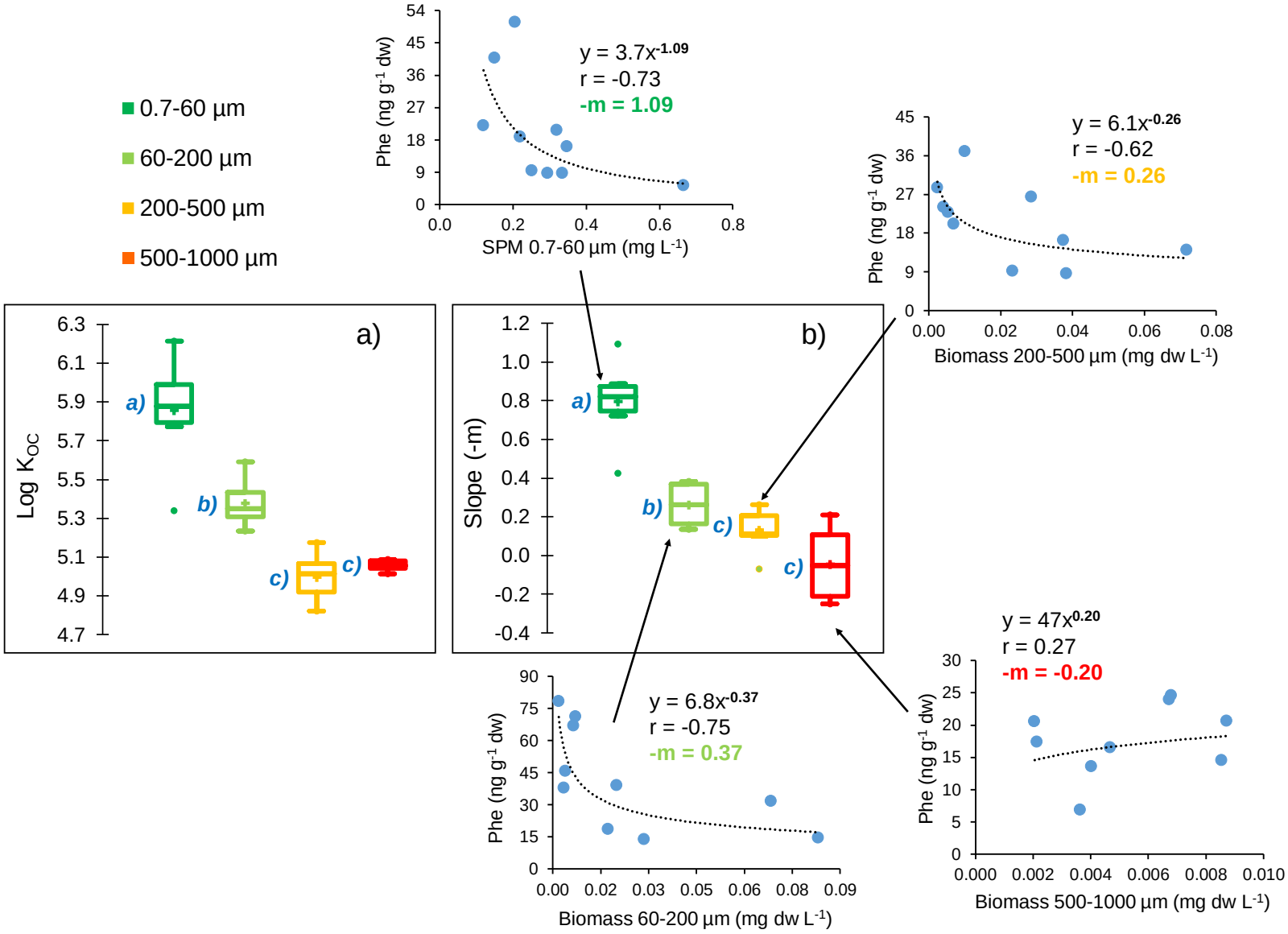
0.7-60 µm
60-200 µm
200-500 µm
500-1000 µm
Phe (ng g-1 dw)
y = 3.7x-1.09
r = -0.73
-m = 1.09
SPM 0.7-60 µm (mg L-1)
y = 6.1x-0.26
r = -0.62
-m = 0.26
Biomass 200-500 µm (mg dw L-1)
a)
Log KOC
b)
Slope (-m)
y = 6.8x-0.37
r = -0.75
-m = 0.37
Biomass 60-200 µm (mg dw L-1)
y = 47x0.20
r = 0.27
-m = -0.20
Biomass 500-1000 µm (mg dw L-1)

Figure 8

Supplementary Material

The supplementary material contains 26 pages, and includes 11 tables and 6 figures.

Table S1. Biogeochemical parameters measured in the different particulate/planktonic size fractions (0.7-60, 60-200, 200-500 and 500-1000 µm) recovered from the deep chlorophyll maximum (DCM) at the 10 stations.

			St1	**St2**	**St3**	**St4**	**St9**	**St10**	**St11**	**St15**	**St17**	**St19**
Sampling depth range in the DCM (m)			20-24	25-53	53-58	13-35	20	40-60	30-58	60-68	37-46	30-46
Parameter	Unit	Size fraction (µm)										
TChl*a*	µg L^{-1}	0.7-60	0.46	0.33	0.37	0.38	0.65	0.41	0.24	0.29	0.12	0.54
SPM	mg L^{-1}	0.7-60	0.35	0.32	0.21	0.22	0.67	0.25	0.15	0.12	0.29	0.34
Biomass	µg dw L^{-1}	60-200	20.0	7.1	1.9	68.3	17.3	3.5	3.9	6.4	83.1	28.5
		200-500	37.4	6.8	2.3	28.5	23.3	4.1	5.4	10.0	71.8	38.2
		500-1000	4.7	6.7	4.0	6.8	3.6	2.0	8.6	8.7	2.1	11.2
		Tot 60-1000	62.1	20.6	8.2	103.5	44.2	9.6	17.9	25.2	157.0	77.9
POC	mg L^{-1}	0.7-60	0.047	0.022	0.016	0.035	0.175	0.030	0.018	0.014	0.024	0.048
	mg g^{-1} dw	0.7-60	134.5	67.3	78.3	159.5	261.8	118.6	121.7	120.6	80.9	141.9
		60-200	263.4	129.4	81.9	103.5	249.8	240.3	271.5	153.7	43.5	156.0
		200-500	246.4	238.0	179.6	139.4	341.0	269.8	299.9	199.6	75.9	204.7
		500-1000	284.9	207.1	168.5	109.7	326.2	222.8	311.4	228.9	*na*	190.5
	%	0.7-60	13.5	6.7	7.8	15.9	26.2	11.9	12.2	12.1	8.1	14.2
		60-200	26.3	12.9	8.2	10.4	25.0	24.0	27.1	15.4	4.4	15.6
		200-500	24.6	23.8	18.0	13.9	34.1	27.0	30.0	20.0	7.6	20.5
		500-1000	28.5	20.7	16.9	11.0	32.6	22.3	31.1	22.9	*na*	19.1
$\delta^{13}C$	‰	0.7-60	-24.5	-24.8	-23.6	-23.2	-24.2	-24.6	-24.1	-25.1	-23.7	-23.6
		60-200	-22.8	-22.7	-21.7	-20.5	-22.7	-22.8	-22.9	-22.8	-21.8	-22.3
		200-500	-23.9	-23.9	-23.0	-21.5	-23.2	-23.7	-24.0	-23.4	-17.4	-21.8
		500-1000	-23.4	-23.8	-22.7	-22.2	-22.9	-23.3	-23.4	-22.7	*na*	-23.1
$\delta^{15}N$		0.7-60	1.8	0.9	0.1	2.1	-1.3	0.4	0.9	1.6	0.8	0.3
		60-200	3.2	3.1	2.9	3.6	2.0	3.6	3.5	3.6	1.9	1.5
		200-500	3.7	3.3	3.4	3.6	2.7	3.9	3.8	3.9	2.4	1.6
		500-1000	4.4	3.5	3.4	3.5	3.9	4.5	4.2	3.3	*na*	2.5

na: not available; TChl*a*: total chlorophyll *a*; SPM: suspended particulate matter; Biomass: total biomass including the biomasses of zooplankton, phytoplankton and detritus (see Fierro-González et al., 2023); POC: particulate organic carbon; $\delta^{13}C$ and $\delta^{15}N$: C and N stable isotopic ratios.

Table S2. Concentrations (in mg g^{-1} dw) of individual and total lipid biomarkers (fatty acids, fatty alcohols and sterols) in the planktonic size fractions 60-200, 200-500 and 500-1000 µm recovered from the DCM at the 10 stations.

	St1			**St2**			**St3**			**St4**			**St9**		
Size fraction (µm)	60-200	200-500	500-1000	60-200	200-500	500-1000	60-200	200-500	500-1000	60-200	200-500	500-1000	60-200	200-500	500-1000
Σ_{39}lipids (mg g^{-1} dw)	13.4	12.4	5.21	9.36	12.3	3.53	5.22	8.37	6.72	13.3	14.5	9.01	20.7	35.6	22.3
Σ_{25}fatty acids (mg g^{-1} dw)	8.58	7.13	4.30	7.32	9.80	2.65	4.46	7.27	5.74	11.8	12.6	8.21	16.4	23.2	16.0
14:0	1.61	1.12	0.76	1.07	1.08	0.51	0.58	0.86	0.81	4.28	3.73	2.24	1.99	1.86	1.58
i15:0	0.07	0.05	0.03	0.05	0.06	0.02	0.05	0.06	0.06	0.05	0.07	0.04	0.10	0.14	0.12
a15:0	0.04	0.03	0.02	0.03	0.04	0.01	0.02	0.03	0.03	0.03	0.04	0.03	0.06	0.07	0.05
15:0	0.16	0.14	0.12	0.15	0.21	0.07	0.11	0.17	0.16	0.18	0.21	0.15	0.26	0.31	0.35
16:0	4.53	3.60	2.23	3.95	4.92	1.31	2.15	3.83	3.03	3.50	4.46	2.90	8.21	10.2	8.18
16:1ω7	0.32	0.30	0.16	0.25	0.55	0.15	0.13	0.23	0.18	1.77	1.54	1.06	0.48	0.53	0.37
16:1ω11	0.08	0.07	0.03	0.05	0.05	0.02	0.02	0.03	0.02	0.09	0.09	0.06	0.17	0.14	0.08
br17:0	*nd*	*nd*	*nd*	*nd*	*nd*	*nd*	*nd*	*nd*	*nd*	*nd*	*nd*	*nd*	*nd*	*nd*	*nd*
i17:0	*nd*	*nd*	0.01	*nd*	0.02	*nd*	0.02	0.02	0.02	0.02	0.02	0.02	0.03	0.04	0.03
a17:0	*nd*	*nd*	*nd*	*nd*	0.03	*nd*	0.02	0.02	0.02	0.02	0.02	0.01	*nd*	0.06	*nd*
17:0	0.02	0.14	0.08	0.14	0.22	0.05	0.07	0.17	0.13	0.08	0.13	0.07	0.41	0.51	0.46
18:0	0.51	0.44	0.24	0.59	0.88	0.16	0.45	0.80	0.60	0.58	0.79	0.54	1.28	2.12	1.43
18:1ω9	0.90	0.95	0.41	0.75	1.19	0.23	0.59	0.64	0.35	0.54	0.71	0.42	1.67	5.31	2.04
18:1ω7	0.15	0.16	0.11	0.13	0.24	0.08	0.09	0.15	0.11	0.29	0.32	0.26	0.37	0.45	0.34
18:2	0.05	0.07	0.06	0.04	0.11	0.01	0.04	0.05	0.04	0.07	0.08	0.06	0.20	0.17	0.12
18:4	*nd*	*nd*	0.01	*nd*	*nd*	*nd*	0.00	0.00	*nd*	0.01	*nd*	*nd*	0.14	0.13	0.07
20:0	*nd*	*nd*	*nd*	0.01	0.04	*nd*	0.03	0.03	0.03	0.03	0.05	0.03	0.08	0.14	0.04
20:1	*nd*	*nd*	*nd*	0.02	0.04	*nd*	0.03	0.04	0.04	0.04	0.07	0.03	0.07	0.12	0.10
20:5	*nd*	*nd*	*nd*	*nd*	*nd*	*nd*	0.01	0.02	0.02	0.08	0.06	0.07	0.11	0.12	0.09
22:0	*nd*	*nd*	*nd*	*nd*	*nd*	*nd*	*nd*	0.01	0.01	0.03	0.05	0.02	0.05	0.07	0.03
22:1	*nd*	*nd*	*nd*	*nd*	*nd*	*nd*	*nd*	0.00	*nd*	*nd*	*nd*	*nd*	*nd*	*nd*	0.01
22:6	*nd*	*nd*	*nd*	*nd*	*nd*	*nd*	0.01	0.02	0.02	0.02	0.02	0.04	0.19	0.22	0.13
24:1	*nd*	*nd*	*nd*	*nd*	0.07	*nd*	*nd*	0.01	0.02	*nd*	0.02	0.01	0.13	0.28	0.22
Phytanic acid	0.13	0.07	0.03	0.08	0.06	0.02	0.04	0.06	0.05	0.07	0.11	0.08	0.23	0.12	0.08

Isomeric dihydroxy 16:0	*nd*	0.00	*nd*	*nd*	0.00	*nd*	*nd*	0.00	*nd*	*nd*	*nd*	0.05	0.14	0.10	0.03
$\Sigma_8$fatty alcohols (mg g^{-1} dw)	4.52	5.04	0.69	1.77	1.75	0.76	0.62	0.86	0.61	1.43	1.44	0.59	2.73	11.1	5.01
14:0	0.77	0.13	0.03	0.27	0.04	0.03	0.09	0.04	0.05	0.22	0.15	0.04	0.28	0.15	0.09
16:0	3.48	4.64	0.54	1.33	1.56	0.47	0.37	0.70	0.41	0.62	0.77	0.25	2.17	10.1	4.28
16:1	0.01	0.00	*nd*	*nd*	*nd*	*nd*	0.01	*nd*	0.01	0.02	0.03	0.01	*nd*	0.01	*nd*
18:0	0.21	0.19	0.04	0.10	0.08	0.03	0.05	0.06	0.03	0.11	0.12	0.07	0.16	0.63	0.28
18:1	0.01	0.08	0.02	0.05	0.05	0.04	0.03	0.03	0.03	0.04	0.05	0.03	0.08	0.24	0.13
20:1	*nd*	*nd*	0.02	*nd*	*nd*	0.09	0.03	0.00	0.03	*nd*	*nd*	*nd*	*nd*	*nd*	0.08
22:1	*nd*	*nd*	0.02	*nd*	*nd*	0.09	0.03	0.02	0.03	*nd*	0.04	0.01	nd	0.06	0.14
Phytol	0.03	0.01	0.01	0.02	0.01	0.01	0.02	0.01	0.02	0.41	0.28	0.18	0.04	*nd*	*nd*
$\Sigma_6$sterols (mg g^{-1} dw)	0.30	0.23	0.22	0.28	0.71	0.11	0.13	0.24	0.38	0.12	0.52	0.21	1.56	1.23	1.34
24-Norcholesta-5,22E-dien-3β-ol	0.01	*nd*	*nd*	0.02	0.03	*nd*	0.01	0.01	0.02	*nd*	0.02	0.01	0.06	0.05	0.03
5α-Cholestan-3β-ol	0.03	0.01	0.01	0.02	0.04	0.01	0.02	0.02	0.04	0.01	0.04	0.01	0.12	0.08	0.06
Cholesta-5,22E-dien-3β-ol	0.05	0.04	0.02	0.04	0.10	0.02	0.02	0.03	0.06	0.04	0.12	0.05	0.17	0.13	0.12
Cholest-5-en-3β-ol	0.18	0.16	0.16	0.17	0.45	0.08	0.07	0.15	0.21	0.06	0.29	0.13	0.99	0.82	1.01
Cholesta-5,24-dien-3β-ol	0.02	0.01	0.01	0.01	0.03	*nd*	*nd*	0.01	0.01	*nd*	0.02	0.01	0.17	0.12	0.09
24-Methylcholesta-5,22E-dien-3β-ol	0.01	0.01	0.01	0.01	0.05	0.01	0.01	0.02	0.04	*nd*	0.03	0.01	0.06	0.03	0.03
	St10			**St11**			**St15**			**St17**			**St19**		
Size fraction (µm)	60-200	200-500	500-1000	60-200	200-500	500-1000	60-200	200-500	500-1000	60-200	200-500	500-1000	60-200	200-500	500-1000
Σ_{39}lipids (mg g^{-1} dw)	23.0	22.9	16.0	26.2	31.7	28.8	22.1	13.7	20.8	3.60	5.69	*na*	14.3	21.4	18.3
Σ_{25}fatty acids (mg g^{-1} dw)	17.7	17.9	13.6	21.7	25.1	25.5	16.7	10.3	16.5	3.14	4.66	*na*	12.4	18.3	15.8
14:0	2.08	2.14	1.44	2.76	3.13	2.01	2.38	1.38	1.73	0.74	1.13	*na*	1.38	2.80	2.01
i15:0	0.16	0.17	0.12	0.20	0.20	0.16	0.14	0.08	0.10	0.02	0.04	*na*	0.16	0.20	0.16
a15:0	0.08	0.09	0.08	0.10	0.10	0.08	0.09	0.03	0.05	0.02	0.02	*na*	0.04	0.09	0.05
15:0	0.31	0.36	0.32	0.42	0.42	0.45	0.37	0.21	0.32	0.07	0.11	*na*	0.26	0.43	0.41
16:0	7.32	8.07	6.35	9.28	10.1	9.51	7.05	4.35	7.61	1.18	1.80	*na*	6.58	9.26	8.20
16:1ω7	0.59	0.59	0.59	0.77	0.77	0.88	1.19	0.61	1.09	0.47	0.55	*na*	0.47	0.60	0.57
16:1ω11	0.08	0.09	0.08	0.14	0.13	0.11	0.10	0.05	0.07	0.03	0.03	*na*	0.06	0.12	0.11
br17:0	0.02	0.04	0.02	0.04	0.04	0.05	0.03	0.03	0.04	0.00	*nd*	*na*	*nd*	*nd*	*nd*
i17:0	0.04	0.06	0.05	0.06	0.08	0.09	0.05	0.04	0.09	0.02	0.02	*na*	0.06	0.07	0.06
a17:0	0.07	0.07	0.06	0.06	0.07	0.05	0.05	0.04	0.05	0.01	0.01	*na*	0.04	0.05	0.04

17:0	0.38	0.47	0.31	0.45	0.48	0.51	0.32	0.22	0.37	0.05	0.08	*na*	0.35	0.06	0.44
18:0	1.37	1.77	1.18	1.65	1.91	1.75	1.07	0.79	1.25	0.22	0.35	*na*	1.48	2.61	1.98
18:1ω9	3.67	2.44	1.62	3.18	5.16	5.12	2.30	1.55	1.87	0.14	0.25	*na*	0.53	0.85	0.68
18:1ω7	0.33	0.40	0.30	0.42	0.46	0.47	0.47	0.30	0.60	0.07	0.08	*na*	0.25	0.28	0.27
18:2	0.14	0.13	0.09	0.36	0.31	0.51	0.19	0.08	0.18	0.03	0.03	*na*	0.11	0.10	0.10
18:4	0.10	0.10	0.07	0.16	0.13	0.13	0.09	0.05	0.09	*nd*	*nd*	*na*	0.05	0.06	0.05
20:0	0.11	0.11	0.07	0.10	0.12	0.20	0.08	0.07	0.10	*nd*	0.02	*na*	0.07	0.15	0.12
20:1	0.09	0.10	0.10	0.16	0.27	0.16	0.13	0.08	0.15	*nd*	0.02	*na*	0.06	0.09	0.05
20:5	0.07	0.10	0.07	0.29	0.17	0.73	0.09	0.05	0.21	0.01	0.02	*na*	0.03	0.08	0.05
22:0	0.05	0.04	0.07	0.08	0.09	0.12	0.05	0.03	0.08	0.02	0.02	*na*	0.05	0.11	0.06
22:1	*nd*	*nd*	0.08	0.09	0.13	0.66	0.11	0.05	0.09	*nd*	*nd*	*na*	*nd*	*nd*	*nd*
22:6	0.13	0.13	0.14	0.47	0.29	1.18	0.16	0.06	0.18	0.01	0.02	*na*	0.06	0.10	0.05
24:1	0.16	0.19	0.15	0.20	0.37	0.26	0.08	0.06	0.08	0.00	*nd*	*na*	0.07	0.12	0.11
Phytanic acid	0.12	0.11	0.08	0.19	0.15	0.15	0.11	0.06	0.10	0.04	0.04	*na*	0.05	0.07	0.06
Isomeric dihydroxy 16:0	0.24	0.12	0.16	0.10	0.06	0.11	0.05	*nd*	*nd*	*nd*	*nd*	*na*	0.14	0.04	0.20
$\Sigma_8$fatty alcohols (mg g^{-1} dw)	3.78	3.15	1.20	3.75	4.58	2.29	4.20	2.72	2.08	0.35	0.76	*na*	0.72	1.31	0.82
14:0	1.12	0.34	0.09	1.68	0.38	0.26	1.50	0.47	0.17	0.04	0.07	*na*	0.09	0.23	0.09
16:0	2.06	2.44	0.75	1.71	3.83	1.67	2.03	1.85	0.94	0.20	0.54	*na*	0.44	0.83	0.49
16:1	0.02	0.01	0.02	0.02	0.01	0.01	0.05	0.02	0.04	0.01	0.01	*na*	0.03	0.03	0.03
18:0	0.23	0.17	0.07	0.14	0.23	0.13	0.19	0.15	0.13	0.06	0.07	*na*	0.12	0.16	0.12
18:1	0.24	0.13	0.10	0.11	0.13	0.15	0.15	0.12	0.12	0.01	0.02	*na*	0.04	0.07	0.10
20:1	*nd*	*nd*	0.03	*nd*	*nd*	*nd*	*nd*	*nd*	0.17	*nd*	*nd*	*na*	*nd*	*nd*	*nd*
22:1	*nd*	*nd*	0.05	*nd*	*nd*	0.07	0.04	*nd*	0.39	*nd*	*nd*	*na*	*nd*	*nd*	*nd*
Phytol	0.12	0.06	0.10	0.09	*nd*	*nd*	0.23	0.12	0.12	0.03	0.03	*na*	*nd*	*nd*	*nd*
$\Sigma_6$sterols (mg g^{-1} dw)	1.50	1.85	1.15	0.75	2.03	1.08	1.16	0.72	2.23	0.11	0.28	*na*	1.18	1.69	1.62
24-Norcholesta-5,22E-dien-3β-ol	0.06	0.04	0.04	0.03	0.08	0.03	0.04	0.04	0.11	0.00	0.01	*na*	0.04	0.00	0.05
5α-Cholestan-3β-ol	0.14	0.11	0.10	0.09	0.16	0.08	0.09	0.05	0.07	0.02	0.04	*na*	0.09	0.10	0.07
Cholesta-5,22E-dien-3β-ol	0.20	0.22	0.16	0.10	0.25	0.13	0.18	0.11	0.21	0.02	0.04	*na*	0.12	0.15	0.14
Cholest-5-en-3β-ol	0.95	1.31	0.70	0.42	1.30	0.70	0.67	0.42	1.67	0.06	0.16	*na*	0.75	1.18	1.20
Cholesta-5,24-dien-3β-ol	0.06	0.08	0.04	0.07	0.11	0.07	0.08	0.03	0.06	0.01	0.01	*na*	0.07	0.11	0.06
24-Methylcholesta-5,22E-dien-3β-ol	0.09	0.09	0.10	0.03	0.13	0.07	0.10	0.07	0.11	0.01	0.02	*na*	0.12	0.15	0.10

na: not available; *nd*: not detected; Σ_{39}lipids = Σ_{25}fatty acids + $\Sigma_8$fatty alcohols + $\Sigma_6$sterols; Σ_{25}fatty acids = Σ 14:0–isomeric dihydroxy 16:0 (25 compounds); $\Sigma_8$fatty alcohols = Σ 14:0–phytol (8 compounds); $\Sigma_6$sterols = Σ 24-Norcholesta-5,22E-dien-3β-ol–24-Methylcholesta-5,22E-dien-3β-ol (6 compounds).

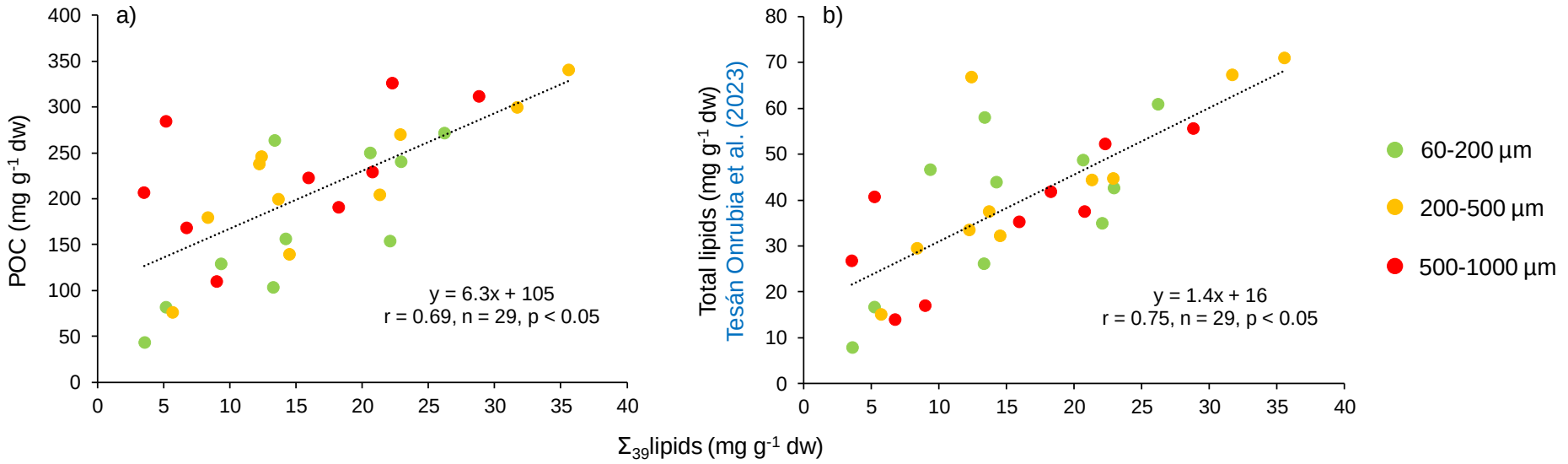

Figure S1. Relationships between the concentration of Σ_{39}lipids (= Σ_{25}fatty acids + Σ_{8}fatty alcohols + Σ_{6}sterols; in mg g^{-1} dw) measured in the present study (horizontal axis), and **a)** the concentration of POC (in mg g^{-1} dw) measured in the present study and **b)** the concentration of total lipids (in mg g^{-1} dw) determined by Tésan Onrubia et al. (2023) using a global method (vertical axes), on the same planktonic size fractions (60-200, 200-500 and 500-1000 µm) recovered from the DCM at the 10 stations.

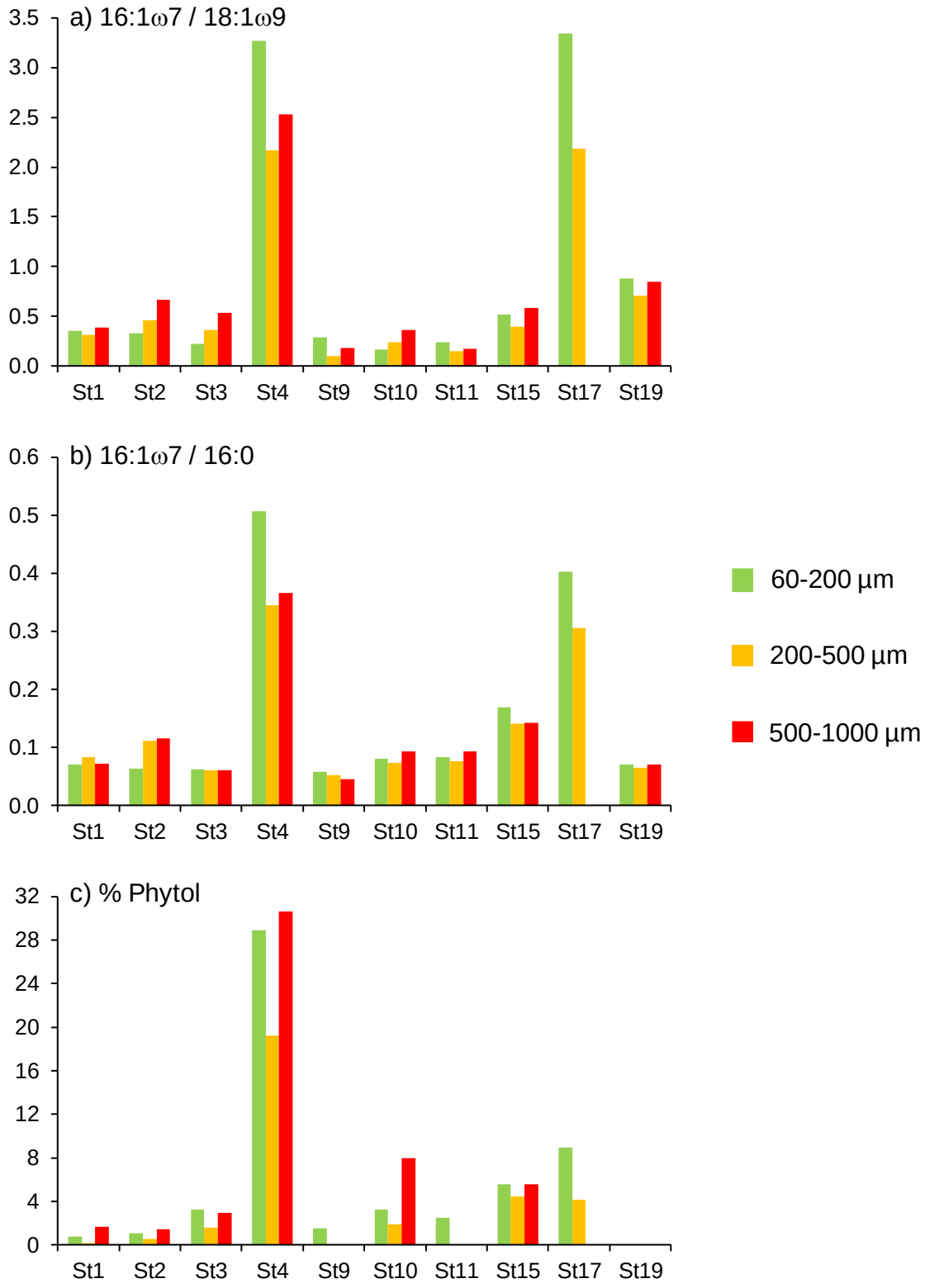

Figure S2. Phytoplankton biomarkers in the planktonic size fractions 60-200, 200-500 and 500-1000 µm, recovered from the DCM at the 10 stations: **a)** the ratio of fatty acids 16:1ω7/18:1ω9, **b)** the ratio of fatty acids 16:1ω7/16:0, and **c)** the relative abundance of phytol within fatty alcohols (in %).

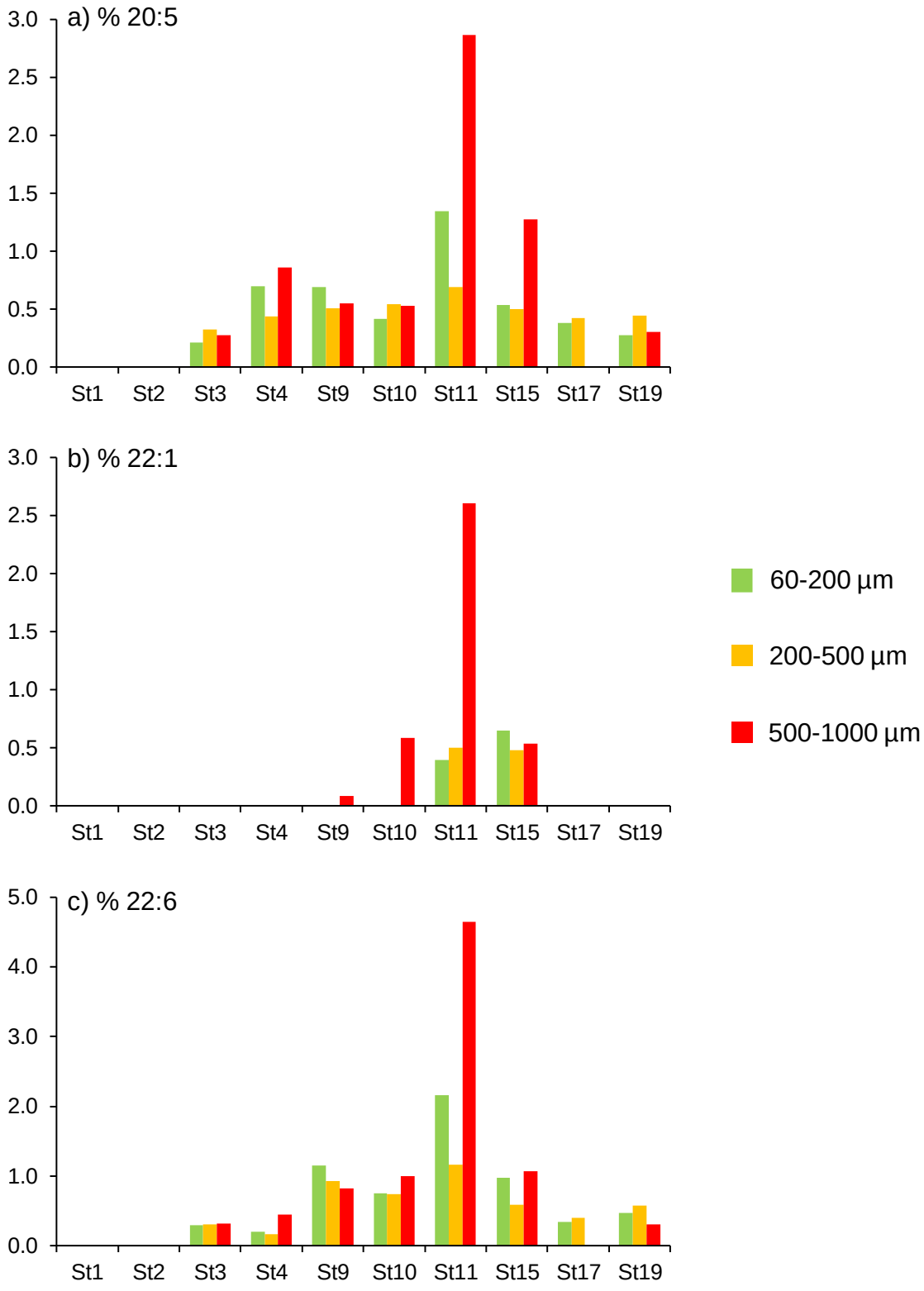

Figure S3. Zooplankton biomarkers in the planktonic size fractions 60-200, 200-500 and 500-1000 µm, recovered from the DCM at the 10 stations: relative abundances of **a)** 20:5, **b)** 22:1 and **c)** 22:6 within fatty acids (in %).

Table S3. Concentrations (in ng L^{-1}) of individual and total aliphatic hydrocarbons (AHs) in the dissolved phase (< 0.7 µm) of water collected at 5-20-m depth at the 10 stations.

	St1	**St2**	**St3**	**St4**	**St9**	**St10**	**St11**	**St15**	**St17**	**St19**
n-C_{15}	1.3	1.9	1.5	1.9	3.0	1.8	1.1	1.2	0.8	0.5
n-C_{16}	*nd*	6.2	4.5	8.3	*nd*	7.3	2.6	0.9	0.3	0.9
n-C_{17}	*nd*	0.2	0.1	1.4	0.3	0.4	*nd*	0.7	*nd*	0.1
Pr	*nd*	*nd*	0.5	0.9	*nd*	0.8	*nd*	0.7	*nd*	0.8
n-C_{18}	*nd*	1.3	1.3	2.6	*nd*	2.4	1.0	1.1	1.1	0.6
Phy	0.6	*nd*	0.8	0.9	*nd*	0.7	*nd*	0.6	*nd*	0.4
n-C_{19}	*nd*	0.2	*nd*	0.9	*nd*	0.4	*nd*	0.6	*nd*	0.1
n-C_{20}	*nd*	0.7	0.3	1.2	*nd*	0.9	0.4	0.9	0.1	0.5
n-C_{21}	1.0	1.0	0.2	0.6	*nd*	0.3	0.9	1.2	0.8	0.7
n-C_{22}	2.1	1.1	*nd*	*nd*	*nd*	0.2	1.1	1.6	1.3	0.9
n-C_{23}	7.6	0.6	*nd*	*nd*	0.5	*nd*	1.6	2.5	3.8	3.6
n-C_{24}	22	0.3	0.8	*nd*	5.0	*nd*	4.0	5.6	9.3	11
n-C_{25}	51	1.8	3.5	1.2	13	*nd*	9.7	11	22	23
n-C_{26}	73	2.8	6.7	1.4	19	*nd*	12	17	33	31
n-C_{27}	68	2.8	8.5	3.2	24	*nd*	15	22	31	40
n-C_{28}	67	4.0	9.2	2.5	24	*nd*	15	20	31	38
n-C_{29}	66	5.6	9.9	3.3	23	0.4	15	20	31	36
n-C_{30}	49	4.5	8.4	2.6	18	0.2	12	15	24	29
n-C_{31}	37	4.7	6.8	2.2	14	0.7	10	12	19	21
n-C_{32}	23	3.4	4.8	1.5	8.9	0.3	5.8	7.3	13	13
n-C_{33}	13	2.3	3.1	1.1	5.7	0.5	3.7	4.1	7.4	7.5
n-C_{34}	5.4	1.6	2.1	0.9	3.6	0.4	2.3	2.4	4.5	4.5
n-C_{35}	2.6	0.9	1.2	0.6	1.5	0.3	0.9	0.8	1.7	1.4
n-C_{36}	1.2	0.4	0.5	0.8	0.7	*nd*	0.4	0.3	0.8	0.6
n-C_{37}	*nd*	*nd*	*nd*	0.3	0.7	*nd*	*nd*	0.1	0.7	0.3
n-C_{38}	*nd*	*nd*	*nd*	0.6	0.5	*nd*	*nd*	*nd*	*nd*	0.3
n-C_{39}	*nd*	*nd*	*nd*	0.5	*nd*	*nd*	*nd*	*nd*	*nd*	*nd*
n-C_{40}	*nd*	*nd*	*nd*	0.4	*nd*	*nd*	*nd*	*nd*	*nd*	*nd*
Σ_{28}AHs	**489**	**48**	**75**	**42**	**165**	**18**	**113**	**150**	**235**	**267**

nd: not detected; Pr: pristane; Phy: phytane; Σ_{28}AHs = Σ *n*-C_{15}–*n*-C_{40}, Pr, Phy (28 compounds).

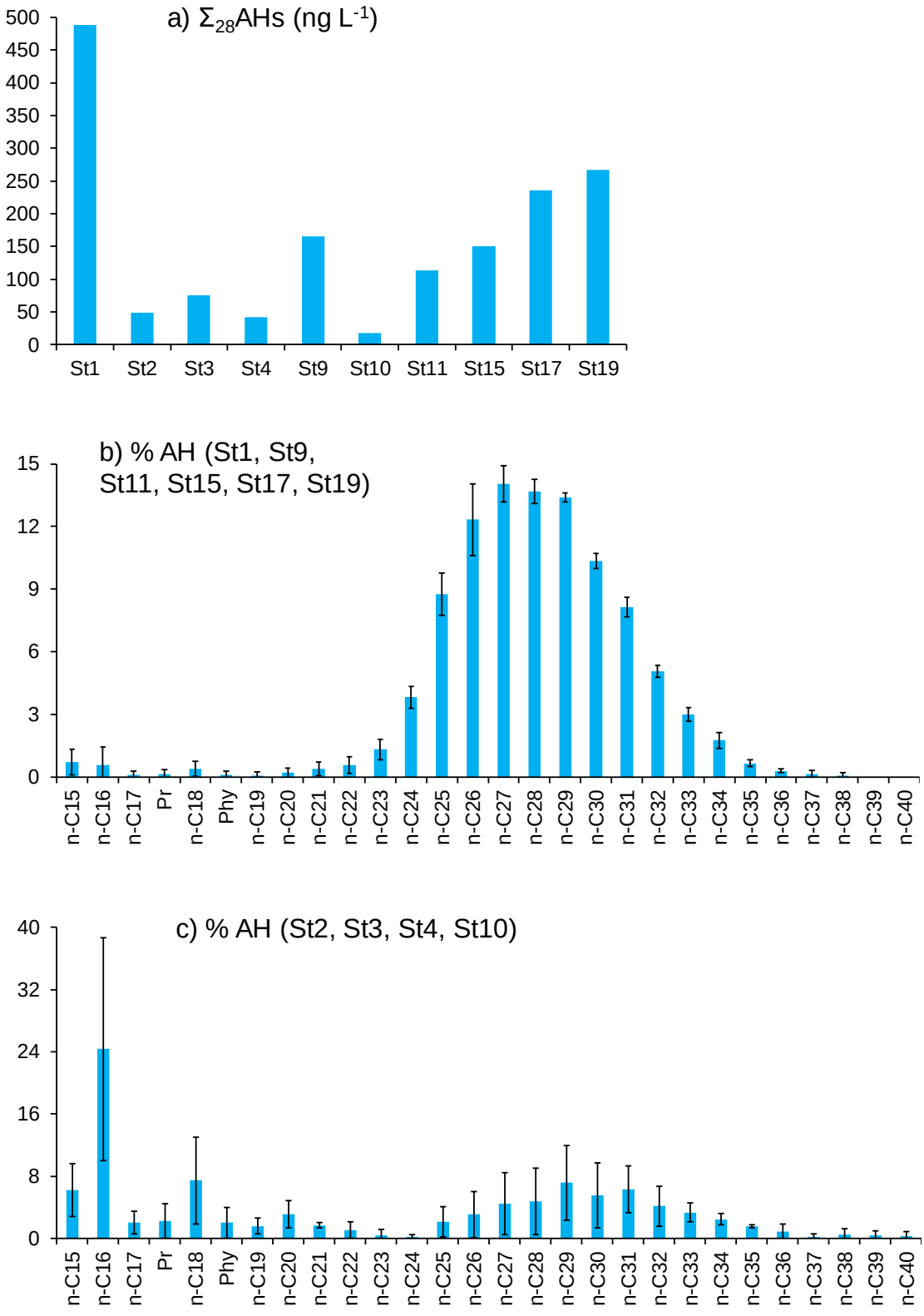

Figure S4. a) Concentrations of total aliphatic hydrocarbons (Σ_{28}AHs, in ng L^{-1}) at the 10 stations, and **b)** mean relative abundances of individual AHs (in %) for stations St1, St9, St11, St15, St17, St19 and **c)** stations St 2, St3, St4, St10, for the dissolved phase (< 0.7 µm) of water collected at 5-20-m depth. Σ_{28}AHs = Σ *n*-C_{15}–*n*-C_{40}, Pr, Phy (28 compounds).

Table S4. Concentrations (in µg g^{-1} dw) of individual and total aliphatic hydrocarbons (AHs) in the particulate/planktonic size fractions 0.7-60, 60-200, 200-500 and 500-1000 µm recovered from the DCM at the 10 stations.

	St1				**St2**				**St3**				**St4**				**St9**			
Size fraction (µm)	0.7-60	60-200	200-500	500-1000	0.7-60	60-200	200-500	500-1000	0.7-60	60-200	200-500	500-1000	0.7-60	60-200	200-500	500-1000	0.7-60	60-200	200-500	500-1000
n-C_{15}	11	0.7	1.8	1.2	16	1.9	3.2	5.4	9.2	1.5	1.9	1.8	5.0	0.3	0.5	0.8	2.1	0.5	0.2	0.1
n-C_{16}	0.5	0.1	0.1	0.1	1.2	0.0	0.1	0.2	1.7	0.1	0.1	0.0	0.4	*nd*	*nd*	*nd*	0.3	0.1	0.1	*nd*
n-C_{17}	1.4	0.4	0.4	0.4	4.6	0.4	0.3	0.7	7.2	0.4	0.5	0.1	2.2	0.3	0.3	0.1	0.3	0.2	0.1	0.1
Pr	0.2	0.9	2.5	2.0	1.6	3.7	2.6	3.1	6.9	2.1	1.5	0.4	1.1	1.3	1.5	1.0	*nd*	0.2	0.3	0.4
n-C_{18}	0.3	*nd*	*nd*	0.1	1.9	*nd*	*nd*	0.1	8.9	*nd*	*nd*	1.7	0.6	0.1	0.1	0.1	0.1	*nd*	*nd*	*nd*
Phy	*nd*	*nd*	*nd*	*nd*	1.1	*nd*	*nd*	*nd*	5.5	*nd*	*nd*	*nd*	0.4	*nd*	*nd*	*nd*	*nd*	*nd*	*nd*	*nd*
n-C_{19}	0.1	0.1	0.1	0.1	1.6	*nd*	*nd*	0.1	7.3	*nd*	0.1	*nd*	0.7	0.2	0.4	0.1	0.1	0.1	0.1	*nd*
n-C_{20}	*nd*	0.1	*nd*	0.1	1.1	0.1	*nd*	0.1	4.6	*nd*	*nd*	*nd*	0.2	0.1	0.1	0.1	*nd*	*nd*	*nd*	*nd*
n-C_{21}	0.1	0.2	0.2	0.2	0.6	0.1	0.1	0.1	1.8	0.1	0.1	0.1	0.4	0.1	0.2	0.2	*nd*	0.1	0.1	0.1
n-C_{22}	0.1	0.1	0.1	0.1	0.4	0.1	0.1	0.2	0.7	0.1	0.1	0.1	0.7	0.1	0.2	0.2	*nd*	0.1	0.1	*nd*
n-C_{23}	0.1	0.4	0.6	0.9	0.4	0.2	0.1	0.4	0.4	0.2	0.2	0.4	1.7	0.2	0.4	0.6	*nd*	0.3	0.4	0.2
n-C_{24}	0.1	*nd*	0.1	0.2	0.5	0.2	0.1	0.3	0.7	0.3	0.2	0.1	2.0	0.2	0.2	0.3	*nd*	0.2	0.2	0.1
n-C_{25}	0.3	0.8	1.4	2.6	0.7	0.2	0.2	0.6	1.4	0.5	0.4	0.4	2.4	0.5	0.8	1.3	0.1	0.9	1.0	0.6
n-C_{26}	0.1	0.3	*nd*	0.3	0.8	0.2	0.1	0.3	2.3	0.6	0.4	0.2	2.3	0.3	0.6	0.5	*nd*	0.2	0.2	0.1
n-C_{27}	0.3	2.8	2.5	10	0.8	0.5	0.5	1.5	2.5	1.0	0.9	0.8	2.4	1.6	2.5	4.4	0.1	2.6	2.4	2.0
n-C_{28}	0.1	0.3	*nd*	0.5	0.7	0.2	0.1	0.3	2.3	0.6	0.4	0.3	1.8	0.7	0.9	0.6	*nd*	0.1	0.2	0.1
n-C_{29}	0.4	3.1	2.6	10	0.9	0.4	0.3	1.0	2.3	1.0	0.7	0.9	2.2	1.5	2.2	2.3	0.4	0.3	2.5	1.8
n-C_{30}	0.2	0.2	0.2	0.2	0.5	0.1	0.1	0.3	1.7	0.7	0.4	0.2	1.6	0.8	1.2	0.6	0.1	0.2	0.1	0.1
n-C_{31}	0.3	1.9	1.6	4.2	0.7	0.4	0.2	0.8	1.6	0.9	0.5	0.6	2.1	1.2	1.8	1.9	0.1	1.7	1.6	0.9
n-C_{32}	0.1	0.0	0.3	0.2	0.4	0.1	0.0	0.3	1.1	0.4	0.3	0.1	1.0	0.5	0.6	0.3	*nd*	0.1	0.1	0.1
n-C_{33}	0.1	1.7	1.1	3.1	0.4	0.1	0.2	0.7	0.8	0.3	0.3	0.3	0.9	0.4	1.2	1.8	*nd*	0.1	1.6	0.9
n-C_{34}	*nd*	0.1	0.2	0.1	0.3	*nd*	0.1	0.1	0.5	0.1	*nd*	*nd*	0.5	0.2	0.2	0.1	*nd*	0.1	*nd*	*nd*
n-C_{35}	*nd*	*nd*	0.3	0.3	0.2	*nd*	*nd*	0.2	0.3	0.1	*nd*	*nd*	0.5	0.1	0.2	0.2	*nd*	0.2	0.2	0.1
n-C_{36}	*nd*	*nd*	0.2	*nd*	0.2	*nd*	*nd*	0.0	0.2	*nd*	*nd*	*nd*	0.2	0.1	0.1	*nd*	*nd*	*nd*	*nd*	*nd*
n-C_{37}	*nd*	*nd*	0.1	*nd*	*nd*	*nd*	*nd*	0.1	0.1	*nd*	*nd*	*nd*	*nd*	0.1	0.1	*nd*	*nd*	*nd*	*nd*	*nd*
n-C_{38}	*nd*	*nd*	0.1	*nd*	*nd*	*nd*	*nd*	*nd*	*nd*	*nd*	*nd*	*nd*	*nd*	*nd*	0.1	*nd*	*nd*	*nd*	*nd*	*nd*
n-C_{39}	*nd*	*nd*	0.1	*nd*	*nd*	*nd*	*nd*	*nd*	*nd*	*nd*	*nd*	*nd*	*nd*	*nd*	0.1	*nd*	*nd*	*nd*	*nd*	*nd*
n-C_{40}	*nd*	*nd*	0.1	*nd*	*nd*	*nd*	*nd*	*nd*	*nd*	*nd*	*nd*	*nd*	*nd*	*nd*	0.1	*nd*	*nd*	*nd*	*nd*	*nd*
Σ_{28}AHs	**16**	**14**	**17**	**37**	**38**	**8.9**	**8.5**	**17**	**72**	**11**	**8.9**	**8.6**	**33**	**11**	**17**	**18**	**3.9**	**8.2**	**11**	**7.7**

	St10				**St11**				**St15**				**St17**				**St19**			
Size fraction (µm)	0.7-60	60-200	200-500	500-1000	0.7-60	60-200	200-500	500-1000	0.7-60	60-200	200-500	500-1000	0.7-60	60-200	200-500	500-1000	0.7-60	60-200	200-500	500-1000
n-C_{15}	7.0	1.3	1.9	1.8	11.9	1.4	1.6	2.3	3.7	1.7	2.3	1.9	5.6	0.5	0.7	*na*	8.3	0.6	0.5	1.1
n-C_{16}	0.5	0.1	0.2	0.1	1.7	0.1	0.1	0.1	0.3	0.1	0.1	0.1	0.2	*nd*	*nd*	*na*	0.3	0.1	*nd*	*nd*
n-C_{17}	1.5	0.7	2.1	1.2	10.8	3.5	2.8	3.0	1.9	0.5	1.4	1.0	0.7	0.3	0.3	*na*	0.3	0.2	0.2	0.4
Pr	0.2	1.0	4.3	4.2	5.4	3.6	32.9	45	0.1	0.9	1.8	3.1	0.1	1.0	1.5	*na*	0.6	4.4	2.9	6.9
n-C_{18}	0.3	*nd*	0.1	0.1	6.0	0.1	*nd*	*nd*	0.2	*nd*	0.1	0.1	0.1	*nd*	*nd*	*na*	0.2	*nd*	0.1	*nd*
Phy	0.1	*nd*	*nd*	*nd*	3.5	*nd*	*nd*	*nd*	*nd*	*nd*	*nd*	*nd*	*nd*	*nd*	*nd*	*na*	0.1	*nd*	*nd*	*nd*
n-C_{19}	0.2	0.1	0.2	0.1	4.1	0.2	0.1	0.1	*nd*	*nd*	*nd*	*nd*	*nd*	*nd*	*nd*	*na*	0.2	0.1	0.1	0.1
n-C_{20}	0.0	0.1	0.1	0.0	2.2	0.1	*nd*	*nd*	0.0	0.1	0.0	0.1	nd	*nd*	*nd*	*na*	*nd*	*nd*	*nd*	*nd*
n-C_{21}	0.1	0.2	0.2	0.1	1.4	0.2	0.1	0.1	0.1	0.1	0.1	0.1	0.1	*nd*	*nd*	*na*	0.1	0.1	0.1	0.1
n-C_{22}	0.1	0.1	0.1	0.1	1.0	0.1	0.1	0.1	0.2	0.1	0.1	0.1	0.1	*nd*	*nd*	*na*	*nd*	0.1	0.1	0.1
n-C_{23}	0.1	0.4	0.4	0.4	2.3	0.2	0.1	0.1	0.2	0.2	0.1	0.2	0.1	*nd*	0.1	*na*	0.1	0.1	0.2	0.4
n-C_{24}	0.1	0.2	0.2	0.2	3.3	0.2	0.1	0.1	0.3	0.1	0.1	0.1	0.1	*nd*	0.1	*na*	0.1	0.2	0.3	0.8
n-C_{25}	0.1	0.8	0.8	1.0	6.9	0.4	0.3	0.3	0.4	0.4	0.3	0.3	0.3	0.1	0.1	*na*	0.1	0.3	0.6	1.3
n-C_{26}	0.1	0.4	0.3	0.4	6.7	0.3	0.2	0.3	0.3	0.2	0.1	0.2	0.1	0.1	0.1	*na*	0.1	0.2	0.5	1.3
n-C_{27}	0.2	2.0	1.8	2.8	10	0.7	0.4	0.5	0.4	0.7	0.4	0.3	0.3	0.1	0.1	*na*	0.1	0.6	0.8	1.9
n-C_{28}	0.1	0.4	0.3	0.5	5.8	0.2	0.1	0.2	0.3	0.3	0.1	0.1	0.1	0.1	0.1	*na*	0.1	0.2	0.4	1.0
n-C_{29}	0.3	4.0	3.0	4.8	7.3	1.5	0.8	0.9	0.4	1.4	0.7	0.5	0.3	0.2	0.2	*na*	0.3	2.0	1.3	2.9
n-C_{30}	0.2	0.6	0.3	0.4	3.7	0.2	0.2	0.1	0.3	0.2	0.1	0.1	0.1	0.1	0.1	*na*	0.1	0.3	0.3	0.7
n-C_{31}	0.2	5.1	3.0	4.2	5.3	2.3	1.0	1.0	0.5	2.2	0.7	0.4	0.3	0.3	0.3	*na*	0.3	3.2	1.8	3.5
n-C_{32}	0.2	0.5	0.3	0.3	1.7	0.2	0.0	0.1	0.2	0.1	0.1	0.1	0.1	0.0	0.0	*na*	0.1	0.3	0.3	0.5
n-C_{33}	0.2	1.8	1.0	1.2	1.6	0.8	0.3	0.3	0.1	0.5	0.2	0.1	0.1	0.1	0.1	*na*	0.1	1.1	0.7	1.1
n-C_{34}	0.1	0.2	0.1	0.1	0.6	0.1	*nd*	*nd*	*nd*	*nd*	*nd*	*nd*	*nd*	*nd*	*nd*	*na*	*nd*	0.1	0.1	0.2
n-C_{35}	0.1	0.8	0.7	0.2	0.4	0.2	0.1	0.1	*nd*	0.1	0.1	*nd*	*nd*	*nd*	*nd*	*na*	0.2	0.2	0.2	0.2
n-C_{36}	0.1	*nd*	*nd*	*nd*	0.2	*nd*	*nd*	*nd*	*nd*	*nd*	*nd*	*nd*	*nd*	*nd*	*nd*	*na*	*nd*	*nd*	0.1	0.1
n-C_{37}	0.1	0.1	0.3	nd	0.2	*nd*	*nd*	*nd*	*nd*	*nd*	*nd*	*nd*	*nd*	*nd*	*nd*	*na*	*nd*	*nd*	0.4	0.1
n-C_{38}	0.1	*nd*	0.1	nd	*nd*	*nd*	*nd*	*nd*	*nd*	*nd*	*nd*	*nd*	*nd*	*nd*	*nd*	*na*	*nd*	*nd*	*nd*	*nd*
n-C_{39}	*nd*	*nd*	*nd*	*nd*	*nd*	*nd*	*nd*	*nd*	*nd*	*nd*	*nd*	*nd*	*nd*	*nd*	*nd*	*na*	*nd*	*nd*	*nd*	*nd*
n-C_{40}	*nd*	*nd*	*nd*	*nd*	*nd*	*nd*	*nd*	*nd*	*nd*	*nd*	*nd*	*nd*	*nd*	*nd*	*nd*	*na*	*nd*	*nd*	*nd*	*nd*
Σ_{28}AHs	**12**	**21**	**22**	**24**	**104**	**17**	**41**	**55**	**10**	**10**	**9.4**	**8.8**	**8.8**	**3.4**	**4.0**	***na***	**12**	**14**	**12**	**25**

na: not available; *nd*: not detected; Pr: pristane; Phy: phytane; Σ_{28}AHs = Σ *n*-C_{15}–*n*-C_{40}, Pr, Phy (28 compounds).

Table S5. Concentrations (in ng L^{-1}) of individual and total polycyclic aromatic hydrocarbons (PAHs) in the dissolved phase (< 0.7 µm) of water collected at 5-20-m depth at the 10 stations.

	St1	**St2**	**St3**	**St4**	**St9**	**St10**	**St11**	**St15**	**St17**	**St19**
Nap	0.29	0.69	0.24	0.93	0.11	0.44	0.06	0.34	0.18	0.41
C1-Nap	*nd*	*nd*	*nd*	3.13	*nd*	*nd*	*nd*	*nd*	*nd*	*nd*
C2-Nap	*nd*	*nd*	*nd*	7.06	*nd*	*nd*	*nd*	*nd*	*nd*	*nd*
C3-Nap	*nd*	*nd*	*nd*	2.43	*nd*	*nd*	*nd*	*nd*	*nd*	*nd*
Acy	*0.01*	*nd*	*nd*	*nd*	*nd*	*nd*	*nd*	*nd*	0.01	0.01
Ace	0.08	0.10	0.12	0.12	0.08	0.09	0.04	0.06	0.06	0.06
Flu	0.27	0.26	0.21	0.40	0.14	0.23	0.09	0.16	0.15	0.19
DBT	0.01	0.07	0.03	0.18	0.03	0.02	0.02	0.01	0.01	0.01
Phe	0.43	1.06	0.91	1.14	3.52	0.46	0.33	0.34	0.28	0.32
Ant	0.03	*nd*	0.07	*nd*	*nd*	*nd*	*nd*	0.05	0.03	0.06
Flt	0.17	0.34	0.82	0.17	0.13	0.15	0.13	0.14	0.15	0.12
Pyr	0.10	0.29	0.65	0.12	0.10	0.13	0.09	0.12	0.12	0.12
BaA	0.05	0.04	0.13	0.05	0.04	0.03	0.04	0.05	0.05	0.05
Chr	0.10	0.13	0.62	0.06	0.09	0.11	0.08	0.12	0.18	0.11
Σ_{14}PAHs	**1.5**	**3.0**	**3.8**	**16**	**4.2**	**1.7**	**0.9**	**1.4**	**1.2**	**1.4**
Σ_{7}PAHs	**1.4**	**2.8**	**3.6**	**2.9**	**4.1**	**1.6**	**0.8**	**1.3**	**1.1**	**1.3**
LMW PAHs (%)	73	73	42	97	92	74	61	69	59	73
HMW PAHs (%)	27	27	58	3	8	26	39	31	41	27

nd: not detected; C1: methyl; C2: di-methyl; C3: tri-methyl; Σ_{14}PAHs = Σ Nap–Chr (14 compounds); Σ_{7}PAHs = Σ Nap, Flu, Phe, Flt, Pyr, BaA, Chr; LMW: low molecular weight, i.e., 2-3 rings; HMW: high molecular weight, i.e., 4-6 rings.

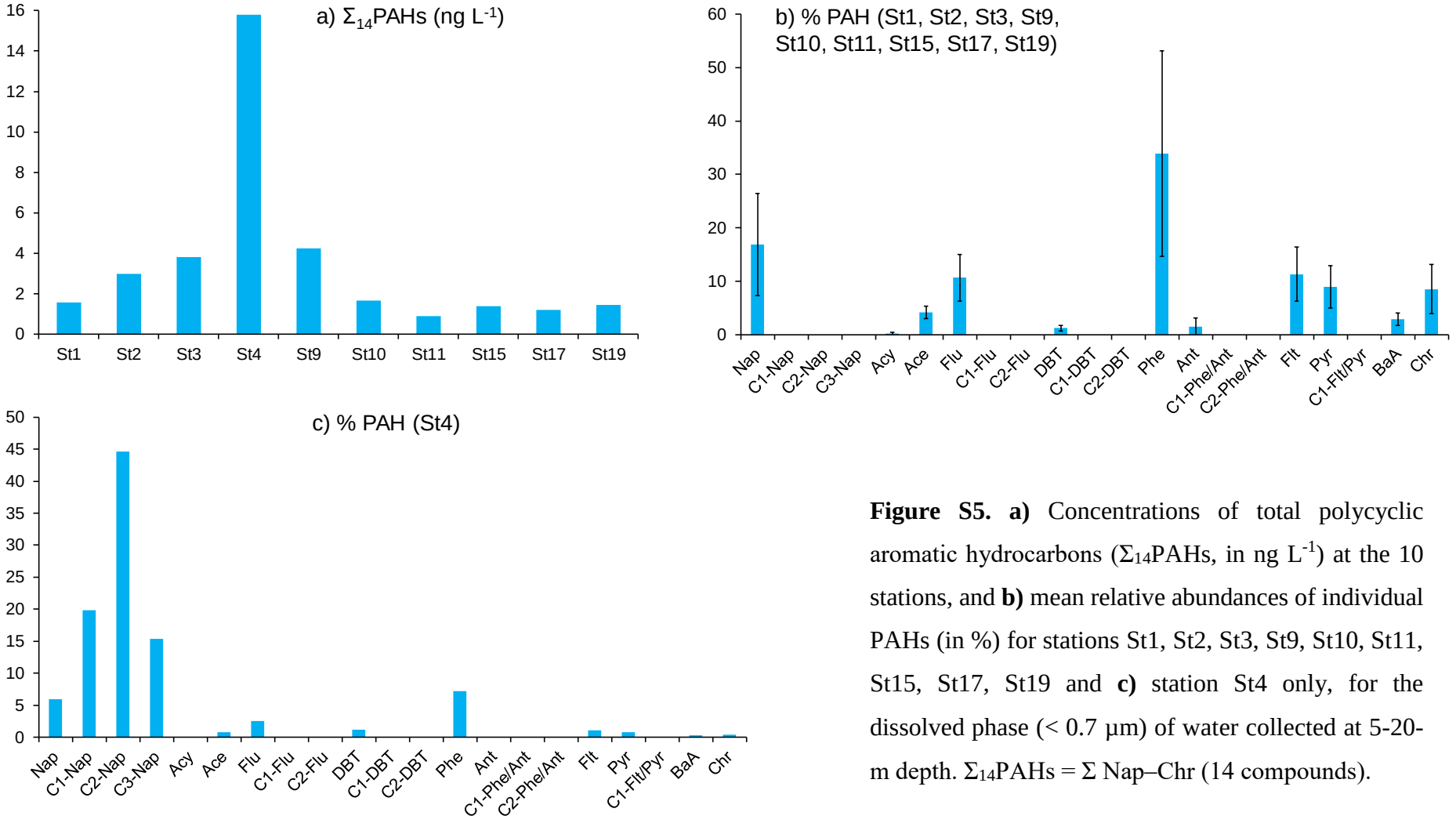

Figure S5. a) Concentrations of total polycyclic aromatic hydrocarbons (Σ_{14}PAHs, in ng L^{-1}) at the 10 stations, and **b)** mean relative abundances of individual PAHs (in %) for stations St1, St2, St3, St9, St10, St11, St15, St17, St19 and **c)** station St4 only, for the dissolved phase (< 0.7 µm) of water collected at 5-20-m depth. Σ_{14}PAHs = Σ Nap–Chr (14 compounds).

Table S6. Concentrations (in ng g^{-1} dw) of individual and total polycyclic aromatic hydrocarbons (PAHs) in the particulate/planktonic size fractions 0.7-60, 60-200, 200-500 and 500-1000 µm recovered from the DCM at the 10 stations.

	St1				**St2**				**St3**				**St4**				**St9**			
Size fraction (µm)	0.7-60	60-200	200-500	500-1000	0.7-60	60-200	200-500	500-1000	0.7-60	60-200	200-500	500-1000	0.7-60	60-200	200-500	500-1000	0.7-60	60-200	200-500	500-1000
Nap	18	8.0	2.9	13	25	31	7.0	7.0	36	14	5.6	3.6	20	6.2	7.8	18	11	3.9	2.1	5.2
C1-Nap	*nd*	4.5	1.3	2.9	*nd*	8.1	2.1	1.7	*nd*	5.0	2.4	1.2	*nd*	3.9	5.1	4.7	*nd*	1.5	0.9	1.5
C2-Nap	*nd*	16	4.4	8.1	*nd*	18	2.0	5.9	*nd*	18	14	7.8	*nd*	*nd*	*nd*	*nd*	*nd*	6.4	4.0	5.9
C3-Nap	*nd*	16	0.2	6.1	*nd*	17	5.4	5.9	*nd*	16	12.5	5.8	*nd*	10.3	14	10	*nd*	6.4	4.0	5.8
Acy	*nd*	1.8	3.1	1.4	*nd*	*nd*	*nd*	*nd*	*nd*	0.9	0.4	0.3	*nd*	*nd*	1.2	0.8	*nd*	0.5	0.2	*nd*
Ace	*nd*	*nd*	*nd*	*nd*	*nd*	*nd*	*nd*	*nd*	*nd*	*nd*	*nd*	*nd*	*nd*	*nd*	*nd*	*nd*	*nd*	0.5	0.4	*nd*
Flu	14	4.3	3.4	7.6	20	19	5.5	6.9	38	15	4.9	2.2	18	5.5	14	11	9.7	3.1	2.7	2.3
C1-Flu	*nd*	6.8	3.6	4.0	*nd*	7.5	4.5	4.5	*nd*	7.9	7.8	4.0	*nd*	4.9	4.4	3.0	*nd*	3.6	2.9	2.1
C2-Flu	*nd*	5.7	*nd*	*nd*	*nd*	*nd*	*nd*	*nd*	*nd*	*nd*	*nd*	*nd*	*nd*	*nd*	*nd*	*nd*	*nd*	*nd*	*nd*	*nd*
DBT	0.6	2.1	*nd*	0.5	*nd*	*nd*	*nd*	*nd*	*nd*	1.9	0.8	0.4	0.5	0.8	1.1	0.0	0.2	0.4	0.1	0.2
C1-DBT	*nd*	1.7	*nd*	*nd*	*nd*	*nd*	*nd*	*nd*	*nd*	*nd*	*nd*	*nd*	*nd*	*nd*	*nd*	*nd*	*nd*	*nd*	*nd*	*nd*
C2-DBT	*nd*	2.4	*nd*	*nd*	*nd*	*nd*	*nd*	*nd*	*nd*	*nd*	*nd*	*nd*	*nd*	*nd*	*nd*	*nd*	*nd*	*nd*	*nd*	*nd*
Phe	16	39	16	17	21	71	20	24	51	79	29	14	19	32	26	25	5.3	19	9.1	6.8
Ant	*nd*	1.7	*nd*	1.3	*nd*	*nd*	7.0	0.0	10	3.8	1.1	0.5	*nd*	2.1	1.9	2.4	*nd*	0.7	0.4	0.3
C1-Phe/Ant	*nd*	16	6.0	8.1	*nd*	*nd*	2.6	8.7	*nd*	9.1	6.9	4.7	*nd*	17	14	0.0	*nd*	6.9	5.1	4.0
C2-Phe/Ant	*nd*	12	nd	4.0	*nd*	*nd*	*nd*	*nd*	*nd*	5.7	5.1	2.9	*nd*	9.0	12	0.0	*nd*	4.8	2.8	1.4
Flt	23	24	12	9.3	7.0	14	4.3	8.3	22	10	5.1	3.4	17	16	13	12	6.6	3.4	3.4	2.1
Pyr	31	21	12	8.6	19	12	5.2	7.3	41	8.4	3.6	2.4	14	13	11	12	13	2.9	1.6	1.1
C1-Flt/Pyr	*nd*	17	6.1	4.7	*nd*	*nd*	*nd*	*nd*	*nd*	*nd*	*nd*	*nd*	*nd*	7.8	5.6	0.0	*nd*	2.2	3.0	1.2
BaA	9.0	14	0.3	3.6	8.2	2.9	1.1	1.6	11	2.5	1.3	0.6	14	5.9	4.9	4.7	4.4	2.3	0.4	0.7
Chr	19	17	4.8	8.2	12	5.1	2.6	6.1	12	3.9	3.0	3.5	35	13	8.9	16	3.5	3.0	2.4	1.2
BbF	*nd*	*nd*	*nd*	*nd*	*nd*	*nd*	*nd*	*nd*	*nd*	*nd*	*nd*	*nd*	*nd*	*nd*	*nd*	*nd*	*nd*	*nd*	*nd*	*nd*
BkF	*nd*	*nd*	*nd*	*nd*	*nd*	*nd*	*nd*	*nd*	*nd*	*nd*	*nd*	*nd*	*nd*	*nd*	*nd*	*nd*	*nd*	*nd*	*nd*	*nd*
BaP	*nd*	*nd*	*nd*	*nd*	*nd*	*nd*	*nd*	*nd*	*nd*	*nd*	*nd*	*nd*	*nd*	*nd*	*nd*	*nd*	*nd*	*nd*	*nd*	*nd*
IndP	*nd*	8.2	*nd*	2.5	*nd*	*nd*	*nd*	*nd*	*nd*	*nd*	*nd*	*nd*	*nd*	*nd*	7.3	6.9	*nd*	2.1	*nd*	*nd*
DahA	*nd*	6.1	*nd*	*nd*	*nd*	*nd*	*nd*	*nd*	*nd*	*nd*	*nd*	*nd*	*nd*	*nd*	1.7	*nd*	*nd*	*nd*	*nd*	*nd*
BP	*nd*	8.6	*nd*	5.2	*nd*	*nd*	*nd*	*nd*	*nd*	*nd*	*nd*	*nd*	*nd*	*nd*	11.5	11	nd	2.4	*nd*	*nd*
Σ_{27}PAHs	**130**	**255**	**76**	**116**	**111**	**206**	**69**	**88**	**220**	**201**	**104**	**57**	**136**	**168**	**162**	**119**	**53**	**76**	**45**	**42**
Σ_{7}PAHs	**129**	**127**	**51**	**67**	**111**	**155**	**46**	**61**	**211**	**133**	**52**	**29**	**136**	**91**	**85**	**98**	**53**	**37**	**22**	**19**
LMW PAHs	37	55	54	64	59	83	81	73	61	88	83	81	41	55	62	63	48	76	76	85
HMW PAHs	63	45	46	36	41	17	19	27	39	12	17	19	59	45	38	37	52	24	24	15

	St10				**St11**				**St15**				**St17**				**St19**			
Size fraction (µm)	0.7-60	60-200	200-500	500-1000	0.7-60	60-200	200-500	500-1000	0.7-60	60-200	200-500	500-1000	0.7-60	60-200	200-500	500-1000	0.7-60	60-200	200-500	500-1000
Nap	23	8.9	3.0	8.2	64	5.5	4.0	3.0	29	11	2.9	4.3	15	2.7	3.8	*na*	13	2.9	2.7	11
C1-Nap	*nd*	2.4	2.0	1.9	*nd*	2.2	1.6	1.4	*nd*	4.1	2.7	1.4	*nd*	1.5	1.6	*na*	*nd*	1.1	0.9	*nd*
C2-Nap	*nd*	8.4	14	6.7	*nd*	10	9.1	7.4	*nd*	0.0	17	8.8	*nd*	*nd*	*nd*	*na*	*nd*	6.2	5.5	*nd*
C3-Nap	*nd*	19	0.0	6.3	*nd*	12	13	8.5	*nd*	17	16	8.6	*nd*	5.1	4.2	*na*	*nd*	4.0	4.9	*nd*
Acy	*nd*	1.2	0.6	0.7	*nd*	0.5	0.2	0.2	*nd*	*nd*	0.6	0.2	*nd*	*nd*	*nd*	*na*	*nd*	*nd*	*nd*	*nd*
Ace	*nd*	*nd*	*nd*	*nd*	*nd*	*nd*	1.0	0.9	*nd*	*nd*	1.8	1.1	*nd*	*nd*	*nd*	*na*	*nd*	0.6	0.3	*nd*
Flu	14	7.7	5.6	7.1	41	6.8	4.8	4.5	20	12	8.5	4.8	13	3.1	4.2	*na*	11	2.9	2.5	6.9
C1-Flu	*nd*	6.3	9.3	4.9	*nd*	7.8	7.8	7.0	*nd*	4.1	8.2	3.9	*nd*	*nd*	*nd*	*na*	*nd*	*nd*	*nd*	*nd*
C2-Flu	*nd*	*nd*	*nd*	*nd*	*nd*	*nd*	*nd*	*nd*	*nd*	*nd*	*nd*	*nd*	*nd*	*nd*	*nd*	*na*	*nd*	*nd*	*nd*	*nd*
DBT	0.2	0.8	0.7	0.3	*nd*	1.1	0.5	0.3	0.6	1.9	1.0	0.5	*nd*	0.4	0.3	*na*	0.2	0.4	0.3	0.4
C1-DBT	*nd*	*nd*	*nd*	*nd*	*nd*	*nd*	*nd*	*nd*	*nd*	*nd*	*nd*	*nd*	*nd*	*nd*	*nd*	*na*	*nd*	*nd*	*nd*	*nd*
C2-DBT	*nd*	*nd*	*nd*	*nd*	*nd*	*nd*	*nd*	*nd*	*nd*	*nd*	*nd*	*nd*	*nd*	*nd*	*nd*	*na*	*nd*	*nd*	*nd*	*nd*
Phe	9.4	38	24	21	41	46	23	15	22	67	37	21	8.7	15	14	*na*	8.7	14	8.6	17
Ant	*nd*	1.2	1.1	0.6	*nd*	1.4	0.6	0.4	*nd*	*nd*	1.3	0.7	*nd*	*nd*	*nd*	*na*	*nd*	0.3	0.1	0.0
C1-Phe/Ant	*nd*	9.9	10	6.7	*nd*	5.4	7.2	6.8	*nd*	9.3	9.8	7.0	*nd*	6.0	5.4	*na*	*nd*	5.7	3.3	0.0
C2-Phe/Ant	*nd*	6.0	5.9	3.1	*nd*	4.5	3.6	3.6	*nd*	0.0	11	8.6	*nd*	4.8	4.0	*na*	*nd*	3.5	2.6	0.0
Flt	9.1	7.3	4.8	4.9	20	7.2	2.6	2.3	24	5.2	3.6	3.2	11	1.4	1.7	*na*	9.0	1.1	1.0	2.0
Pyr	21	5.9	3.1	4.4	24	4.8	1.6	1.4	31	8.3	2.6	4.0	19	2.1	3.1	*na*	18	1.4	1.0	2.7
C1-Flt/Pyr	*nd*	*nd*	*nd*	*nd*	*nd*	*nd*	*nd*	*nd*	*nd*	*nd*	*nd*	*nd*	*nd*	*nd*	*nd*	*na*	*nd*	*nd*	*nd*	*nd*
BaA	7.6	1.3	0.8	1.0	18	1.9	0.6	0.6	19	0.0	1.3	0.9	7.3	0.3	0.4	*na*	6.9	0.3	0.3	1.5
Chr	9.4	4.1	2.9	2.7	11	4.4	1.6	1.8	18	2.1	2.0	2.0	15	0.9	0.9	*na*	4.3	0.5	0.5	1.0
BbF	*nd*	*nd*	*nd*	*nd*	*nd*	*nd*	*nd*	*nd*	*nd*	*nd*	*nd*	*nd*	*nd*	*nd*	*nd*	*na*	*nd*	*nd*	*nd*	*nd*
BkF	*nd*	*nd*	*nd*	*nd*	*nd*	*nd*	*nd*	*nd*	*nd*	*nd*	*nd*	*nd*	*nd*	*nd*	*nd*	*na*	*nd*	*nd*	*nd*	*nd*
BaP	*nd*	*nd*	*nd*	*nd*	*nd*	*nd*	*nd*	*nd*	*nd*	*nd*	*nd*	*nd*	*nd*	*nd*	*nd*	*na*	*nd*	*nd*	*nd*	*nd*
IndP	*nd*	*nd*	*nd*	*nd*	*nd*	*nd*	*nd*	*nd*	*nd*	*nd*	*nd*	*nd*	*nd*	*nd*	*nd*	*na*	*nd*	*nd*	*nd*	*nd*
DahA	*nd*	*nd*	*nd*	*nd*	*nd*	*nd*	*nd*	*nd*	*nd*	*nd*	*nd*	*nd*	*nd*	*nd*	*nd*	*na*	*nd*	*nd*	*nd*	*nd*
BP	*nd*	*nd*	*nd*	*nd*	*nd*	2.0	*nd*	*nd*	*nd*	*nd*	*nd*	*nd*	*nd*	*nd*	*nd*	*na*	*nd*	*nd*	*nd*	*nd*
Σ_{27}PAHs	**94**	**128**	**87**	**80**	**219**	**124**	**83**	**65**	**163**	**141**	**126**	**81**	**89**	**43**	**44**	***na***	**71**	**45**	**35**	**43**
Σ_{7}PAHs	**94**	**73**	**44**	**49**	**219**	**76**	**38**	**28**	**163**	**105**	**58**	**40**	**89**	**25**	**28**	***na***	**71**	**23**	**17**	**42**
LMW PAHs	50	85	87	84	66	84	92	90	43	89	92	87	41	89	86	*na*	47	93	92	83
HMW PAHs	50	15	13	16	34	16	8	10	57	11	8	13	59	11	14	*na*	53	7	8	17

na: not available; *nd*: not detected; C1: methyl; C2: di-methyl; C3: tri-methyl; Σ_{27}PAHs = Σ Nap–BP (27 compounds); Σ_{7}PAHs = Σ Nap, Flu, Phe, Flt, Pyr, BaA, Chr; LMW: low molecular weight, i.e., 2-3 rings; HMW: high molecular weight, i.e., 4-6 rings.

Table S7. Summary of SPM, biomass, POC and individual PAH concentration data for the particulate/planktonic size fractions 0.7-60, 60-200, 200-500, 500-1000 µm, but also 60-1000 µm, recovered from the DCM at the 10 stations.

	Size fractions (µm)	**Biomass (mg dw L^{-1}) or SPM (mg L^{-1})**	**$f_{Biomass}$**	**POC (mg g^{-1} dw)**	**f_{OC}**	**ng L^{-1} for < 0.7 µm, ng g^{-1} dw for other fractions**						
						Nap	**Flu**	**Phe**	**Flt**	**Pyr**	**BaA**	**Chr**
St1	< 0.7	*na*	*na*	*na*	*na*	0.29	0.27	0.43	0.17	0.10	0.05	0.10
	0.7-60	0.347	*na*	134.5	0.135	18.0	13.6	16.1	22.8	31.2	9.0	18.7
	60-200	0.020	0.3	263.4	0.263	8.0	4.3	39.1	23.8	20.5	13.7	17.4
	200-500	0.037	0.6	246.4	0.246	2.9	3.4	16.3	12.0	11.9	0.3	4.8
	500-1000	0.005	0.1	284.9	0.285	13.3	7.6	16.5	9.3	8.6	3.6	8.2
	60-1000	0.062	1.0	254.8	0.255	5.3	4.0	23.6	15.6	14.4	4.8	9.1
St2	< 0.7	*na*	*na*	*na*	*na*	0.69	0.26	1.06	0.34	0.29	0.04	0.13
	0.7-60	0.320	*na*	67.3	0.067	25.3	19.6	20.7	7.0	18.5	8.2	12.2
	60-200	0.007	0.3	129.4	0.129	31.2	19.0	71.2	13.9	12.1	2.9	5.1
	200-500	0.007	0.3	238.0	0.238	7.0	5.5	20.1	4.3	5.2	1.1	2.6
	500-1000	0.007	0.3	207.1	0.207	7.0	6.9	23.9	8.3	7.3	1.6	6.1
	60-1000	0.021	1.0	190.7	0.191	15.3	10.6	38.9	8.9	8.3	1.9	4.6
St3	< 0.7	*na*	*na*	*na*	*na*	0.24	0.21	0.91	0.82	0.65	0.13	0.62
	0.7-60	0.210	*na*	78.3	0.078	36.3	38.1	50.8	22.2	40.6	11.2	11.6
	60-200	0.002	0.2	81.9	0.082	14.0	15.4	78.5	10.2	8.4	2.5	3.9
	200-500	0.002	0.3	179.6	0.180	5.6	4.9	28.5	5.1	3.6	1.3	3.0
	500-1000	0.004	0.5	168.5	0.169	3.6	2.2	13.5	3.4	2.4	0.6	3.5
	60-1000	0.008	1.0	152.0	0.152	6.5	5.9	32.5	5.4	4.1	1.2	3.4
St4	< 0.7	*na*	*na*	*na*	*na*	0.93	0.4	1.14	0.17	0.12	0.05	0.06
	0.7-60	0.220	*na*	159.5	0.159	19.7	17.5	18.8	16.5	14.4	14.0	34.9
	60-200	0.068	0.7	103.5	0.104	6.2	5.5	31.7	16.4	13.2	5.9	12.6
	200-500	0.028	0.3	139.4	0.139	7.8	13.5	26.4	12.5	10.9	4.9	8.9
	500-1000	0.007	0.1	109.7	0.110	18.2	11.4	24.6	12.0	11.6	4.7	15.5
	60-1000	0.104	1.0	113.8	0.114	7.4	8.1	29.8	15.0	12.5	5.5	11.8
St9	< 0.7	*na*	*na*	*na*	*na*	0.11	0.14	3.52	0.13	0.1	0.04	0.09
	0.7-60	0.670	*na*	261.8	0.262	10.5	9.7	5.3	6.6	13.2	4.4	3.5
	60-200	0.017	0.4	249.8	0.250	3.9	3.1	18.7	3.4	2.9	2.3	3.0
	200-500	0.023	0.5	341.0	0.341	2.1	2.7	9.1	3.4	1.6	0.4	2.4
	500-1000	0.004	0.1	326.2	0.326	5.2	2.3	6.8	2.1	1.1	0.7	1.2
	60-1000	0.044	1.0	304.2	0.304	3.1	2.8	12.7	3.3	2.1	1.2	2.6
St10	< 0.7	*na*	*na*	*na*	*na*	0.44	0.23	0.46	0.15	0.13	0.03	0.11
	0.7-60	0.250	*na*	118.6	0.119	23.1	14.3	9.4	9.1	20.5	7.6	9.4
	60-200	0.003	0.4	240.3	0.240	8.9	7.7	37.9	7.3	5.9	1.3	4.1
	200-500	0.004	0.4	269.8	0.270	3.0	5.6	24.0	4.8	3.1	0.8	2.9
	500-1000	0.002	0.2	222.8	0.223	8.2	7.1	20.5	4.9	4.4	1.0	2.7
	60-1000	0.010	1.0	249.1	0.249	6.3	6.7	28.3	5.7	4.4	1.0	3.3
St11	< 0.7	*na*	*na*	*na*	*na*	0.06	0.09	0.33	0.13	0.09	0.04	0.08
	0.7-60	0.150	*na*	121.7	0.122	64.2	40.5	40.7	20.4	24.3	17.6	11.3
	60-200	0.004	0.2	271.5	0.271	5.5	6.8	45.9	7.2	4.8	1.9	4.4
	200-500	0.005	0.3	299.9	0.300	4.0	4.8	22.8	2.6	1.6	0.6	1.6

	500-1000	0.009	0.5	311.4	0.311	3.0	4.5	14.5	2.3	1.4	0.6	1.8
	60-1000	0.018	1.0	299.1	0.299	3.9	5.1	23.9	3.5	2.2	0.9	2.4
St15	< 0.7	*na*	*na*	*na*	*na*	0.34	0.16	0.34	0.14	0.12	0.05	0.12
	0.7-60	0.120	*na*	120.6	0.121	28.6	19.7	22.0	24.0	31.0	18.8	18.4
	60-200	0.006	0.3	153.7	0.154	10.5	12.0	66.9	5.2	8.3	*na*	2.1
	200-500	0.010	0.4	199.6	0.200	2.9	8.5	37.0	3.6	2.6	1.3	2.0
	500-1000	0.009	0.3	228.9	0.229	4.3	4.8	20.6	3.2	4.0	0.9	2.0
	60-1000	0.025	1.0	198.1	0.198	5.3	8.1	38.9	3.9	4.5	0.8	2.0
St17	< 0.7	*na*	*na*	*na*	*na*	0.18	0.15	0.28	0.15	0.12	0.05	0.18
	0.7-60	0.290	*na*	80.9	0.081	15.0	13.1	8.7	10.7	18.9	7.3	15.1
	60-200	0.083	0.5	43.5	0.044	2.7	3.1	14.5	1.4	2.1	0.3	0.9
	200-500	0.072	0.5	75.9	0.076	3.8	4.2	14.0	1.7	3.1	0.4	0.9
	500-1000	0.002	0.0	*na*	0.000	*na*	*na*	*na*	*na*	*na*	*na*	*na*
	60-1000	0.157	1.0	57.7	0.058	3.2	3.6	14.1	1.5	2.6	0.4	0.9
St19	< 0.7	*na*	*na*	*na*	*na*	0.41	0.19	0.32	0.12	0.12	0.05	0.11
	0.7-60	0.340	*na*	141.9	0.142	13.4	10.7	8.7	9.0	17.6	6.9	4.3
	60-200	0.029	0.4	156.0	0.156	2.9	2.9	14.0	1.1	1.4	0.3	0.5
	200-500	0.038	0.5	204.7	0.205	2.7	2.5	8.6	1.0	1.0	0.3	0.5
	500-1000	0.011	0.1	190.5	0.191	10.8	6.9	17.3	2.0	2.7	1.5	1.0
	60-1000	0.078	1.0	184.9	0.185	3.9	3.3	11.8	1.2	1.4	0.5	0.6

na: not available.

$f_{Biomass}$: contribution of the biomass of a given size fraction to the total biomass of the fraction 60-1000 µm (i.e., $f_{Biomass}$ *x* = biomass fraction *x* / biomass 60-1000 µm), with biomass 60-1000 µm = biomass 60-200 µm + biomass 200-500 µm + biomass 500-1000 µm.

f_{OC}: contribution of the OC mass (in g) to the total matter mass (in g) for a given size fraction (i.e., f_{OC} = POC in mg g^{-1} dw / 1000).

Concentrations of POC and individual PAHs in the size fraction 60-1000 µm were calculated by summing the concentrations of POC/PAH in the fractions 60-200, 200-500 and 500-1000 µm, each of these concentrations being weighted (multiplied) by the corresponding $f_{Biomass}$ value.

Table S8. Partition coefficient between particulate matter and water (K_D in L kg^{-1}) and Log K_D for the 7 individual PAHs in each particulate/ planktonic size fraction (0.7-60, 60-200, 200-500, 500-1000 and 60-1000 µm) and station.

	Size fractions (µm)	K_D (L kg^{-1})							Log K_D						
		Nap	Flu	Phe	Flt	Pyr	BaA	Chr	Nap	Flu	Phe	Flt	Pyr	BaA	Chr
St1	0.7-60	61968	50402	37546	133838	311743	180191	186903	4.79	4.70	4.57	5.13	5.49	5.26	5.27
	60-200	27589	16089	90814	140275	205392	274689	173735	4.44	4.21	4.96	5.15	5.31	5.44	5.24
	200-500	9828	12537	37820	70311	118644	5214	48387	3.99	4.10	4.58	4.85	5.07	3.72	4.68
	500-1000	45902	28186	38282	54476	86145	71473	82200	4.66	4.45	4.58	4.74	4.94	4.85	4.91
	60-1000	18260	14858	54904	91627	144104	96901	91261	4.26	4.17	4.74	4.96	5.16	4.99	4.96
St2	0.7-60	36609	75278	19529	20684	63624	204506	93689	4.56	4.88	4.29	4.32	4.80	5.31	4.97
	60-200	45212	73198	67132	40743	41854	72886	39568	4.66	4.86	4.83	4.61	4.62	4.86	4.60
	200-500	10146	21025	18963	12569	17848	27888	19819	4.01	4.32	4.28	4.10	4.25	4.45	4.30
	500-1000	10112	26496	22549	24554	25330	39204	46882	4.00	4.42	4.35	4.39	4.40	4.59	4.67
	60-1000	22158	40704	36652	26149	28527	47018	35442	4.35	4.61	4.56	4.42	4.46	4.67	4.55
St3	0.7-60	151402	181259	55817	27024	62409	86410	18700	5.18	5.26	4.75	4.43	4.80	4.94	4.27
	60-200	58158	73373	86227	12394	12911	19161	6264	4.76	4.87	4.94	4.09	4.11	4.28	3.80
	200-500	23466	23460	31367	6262	5549	10291	4771	4.37	4.37	4.50	3.80	3.74	4.01	3.68
	500-1000	14877	10256	14874	4152	3625	4582	5674	4.17	4.01	4.17	3.62	3.56	3.66	3.75
	60-1000	27090	28257	35665	6611	6268	9488	5553	4.43	4.45	4.55	3.82	3.80	3.98	3.74
St4	0.7-60	21168	43669	16528	96979	120318	279300	582278	4.33	4.64	4.22	4.99	5.08	5.45	5.77
	60-200	6636	13871	27774	96459	109872	117408	210352	3.82	4.14	4.44	4.98	5.04	5.07	5.32
	200-500	8399	33723	23161	73713	90808	98657	148349	3.92	4.53	4.36	4.87	4.96	4.99	5.17
	500-1000	19537	28604	21574	70335	96549	94223	259076	4.29	4.46	4.33	4.85	4.98	4.97	5.41
	60-1000	7969	20296	26098	88489	103755	110729	196512	3.90	4.31	4.42	4.95	5.02	5.04	5.29
St9	0.7-60	95270	68960	1493	50734	132374	110649	39342	4.98	4.84	3.17	4.71	5.12	5.04	4.59
	60-200	35853	21900	5322	25968	28505	57125	33596	4.55	4.34	3.73	4.41	4.45	4.76	4.53
	200-500	19084	19166	2576	26267	16184	10828	26720	4.28	4.28	3.41	4.42	4.21	4.03	4.43
	500-1000	47133	16105	1925	16116	10509	17476	13828	4.67	4.21	3.28	4.21	4.02	4.24	4.14
	60-1000	27946	19982	3595	25313	20528	29460	28343	4.45	4.30	3.56	4.40	4.31	4.47	4.45

St10	0.7-60	52540	62279	20510	60652	157676	254108	85776	4.72	4.79	4.31	4.78	5.20	5.41	4.93
	60-200	20289	33631	82380	48585	45451	44561	37710	4.31	4.53	4.92	4.69	4.66	4.65	4.58
	200-500	6842	24396	52248	31807	23638	26642	26065	3.84	4.39	4.72	4.50	4.37	4.43	4.42
	500-1000	18656	30738	44642	32334	33982	32109	24520	4.27	4.49	4.65	4.51	4.53	4.51	4.39
	60-1000	14207	29077	61501	37973	33709	34270	29938	4.15	4.46	4.79	4.58	4.53	4.53	4.48
St11	0.7-60	1069630	450076	123387	157163	269475	438959	141026	6.03	5.65	5.09	5.20	5.43	5.64	5.15
	60-200	92396	75597	138982	55169	52831	46976	55423	4.97	4.88	5.14	4.74	4.72	4.67	4.74
	200-500	66860	53573	69056	19705	17609	14275	20606	4.83	4.73	4.84	4.29	4.25	4.15	4.31
	500-1000	49587	49642	44022	17633	15897	14987	22986	4.70	4.70	4.64	4.25	4.20	4.18	4.36
	60-1000	64228	56554	72511	26545	24568	21838	29436	4.81	4.75	4.86	4.42	4.39	4.34	4.47
St15	0.7-60	84002	123336	64712	171305	258611	376558	153414	4.92	5.09	4.81	5.23	5.41	5.58	5.19
	60-200	30812	74703	196819	37477	68844	*na*	17260	4.49	4.87	5.29	4.57	4.84	*na*	4.24
	200-500	8393	53192	108873	25889	21841	25581	16829	3.92	4.73	5.04	4.41	4.34	4.41	4.23
	500-1000	12633	29775	60603	23024	33464	17750	16592	4.10	4.47	4.78	4.36	4.52	4.25	4.22
	60-1000	15576	50540	114513	27846	37849	16346	16856	4.19	4.70	5.06	4.44	4.58	4.21	4.23
St17	0.7-60	83560	87018	31093	71024	157840	146655	83961	4.92	4.94	4.49	4.85	5.20	5.17	4.92
	60-200	14794	20698	51923	9088	17663	6351	4730	4.17	4.32	4.72	3.96	4.25	3.80	3.67
	200-500	21283	27846	49855	11467	26234	8756	5032	4.33	4.44	4.70	4.06	4.42	3.94	3.70
	500-1000	*na*	*na*	*na*	*na*	*na*	*na*	*na*	*na*	*na*	*na*	*na*	*na*	*na*	*na*
	60-1000	17559	23683	50268	10051	21340	7364	4804	4.24	4.37	4.70	4.00	4.33	3.87	3.68
St19	0.7-60	32747	56337	27095	75145	146679	138735	39072	4.52	4.75	4.43	4.88	5.17	5.14	4.59
	60-200	7098	15390	43658	9115	11776	6363	4416	3.85	4.19	4.64	3.96	4.07	3.80	3.65
	200-500	6464	13385	26780	8743	8199	6837	4486	3.81	4.13	4.43	3.94	3.91	3.83	3.65
	500-1000	26428	36095	54197	17081	22413	29267	8729	4.42	4.56	4.73	4.23	4.35	4.47	3.94
	60-1000	9560	17377	36894	10076	11548	9881	5069	3.98	4.24	4.57	4.00	4.06	3.99	3.70

na: not available.

K_D in a given size fraction (in L kg^{-1}) was calculated as (C_P / C_W) × 1000 where C_P is the concentration in the given size fraction (0.7-60, 60-200, 200-500, 500-1000 or 60-1000 µm) in ng g^{-1} dw, and C_w is the concentration in the dissolved phase (size fraction < 0.7 µm) in ng L^{-1} (see concentration values in Table S7).

Table S9. Partition coefficient between particulate organic carbon and water (K_{OC} in L kg^{-1}) and Log K_{oc} for the 7 individual PAHs in each particulate/planktonic size fraction (0.7-60, 60-200, 200-500, 500-1000 and 60-1000 µm) and station.

	Size fractions (µm)	**K_{OC} (L kg^{-1})**							**Log K_{OC}**						
		Nap	**Flu**	**Phe**	**Flt**	**Pyr**	**BaA**	**Chr**	**Nap**	**Flu**	**Phe**	**Flt**	**Pyr**	**BaA**	**Chr**
St1	0.7-60	460668	374689	279118	994947	2317478	1339528	1389425	5.66	5.57	5.45	6.00	6.37	6.13	6.14
	60-200	104753	61088	344818	532618	779864	1042985	659666	5.02	4.79	5.54	5.73	5.89	6.02	5.82
	200-500	39882	50870	153465	285307	481430	21158	196344	4.60	4.71	5.19	5.46	5.68	4.33	5.29
	500-1000	161111	98931	134364	191204	302359	250863	288511	5.21	5.00	5.13	5.28	5.48	5.40	5.46
	60-1000	71668	58317	215492	359625	565591	380325	358190	4.86	4.77	5.33	5.56	5.75	5.58	5.55
St2	0.7-60	544172	1118977	290285	307460	945751	3039907	1392659	5.74	6.05	5.46	5.49	5.98	6.48	6.14
	60-200	349441	565739	518858	314903	323486	563330	305815	5.54	5.75	5.72	5.50	5.51	5.75	5.49
	200-500	42629	88340	79678	52811	74993	117177	83274	4.63	4.95	4.90	4.72	4.88	5.07	4.92
	500-1000	48817	127917	108860	118539	122289	189270	226335	4.69	5.11	5.04	5.07	5.09	5.28	5.35
	60-1000	116218	213486	192237	137151	149619	246607	185889	5.07	5.33	5.28	5.14	5.17	5.39	5.27
St3	0.7-60	1932978	2314155	712623	345014	796789	1103212	238747	6.29	6.36	5.85	5.54	5.90	6.04	5.38
	60-200	710302	896119	1053109	151376	157686	234022	76500	5.85	5.95	6.02	5.18	5.20	5.37	4.88
	200-500	130691	130660	174696	34874	30906	57318	26572	5.12	5.12	5.24	4.54	4.49	4.76	4.42
	500-1000	88273	60852	88254	24633	21508	27187	33664	4.95	4.78	4.95	4.39	4.33	4.43	4.53
	60-1000	178195	185871	234598	43486	41231	62414	36528	5.25	5.27	5.37	4.64	4.62	4.80	4.56
St4	0.7-60	132741	273843	103643	608138	754497	1751447	3651377	5.12	5.44	5.02	5.78	5.88	6.24	6.56
	60-200	64104	133993	268299	931804	1061367	1134174	2032019	4.81	5.13	5.43	5.97	6.03	6.05	6.31
	200-500	60238	241861	166114	528673	651276	707567	1063960	4.78	5.38	5.22	5.72	5.81	5.85	6.03
	500-1000	178166	260857	196749	641429	880487	859272	2362657	5.25	5.42	5.29	5.81	5.94	5.93	6.37
	60-1000	70029	178362	229349	777627	911784	973070	1726916	4.85	5.25	5.36	5.89	5.96	5.99	6.24
St9	0.7-60	363924	263421	5701	193802	505661	422670	150284	5.56	5.42	3.76	5.29	5.70	5.63	5.18
	60-200	143511	87660	21304	103943	114097	228659	134477	5.16	4.94	4.33	5.02	5.06	5.36	5.13
	200-500	55964	56205	7553	77028	47460	31755	78358	4.75	4.75	3.88	4.89	4.68	4.50	4.89
	500-1000	144472	49366	5900	49400	32212	53567	42386	5.16	4.69	3.77	4.69	4.51	4.73	4.63
	60-1000	91876	65691	11818	83219	67489	96851	93180	4.96	4.82	4.07	4.92	4.83	4.99	4.97

St10	0.7-60	443056	525175	172952	511461	1329629	2142808	723320	5.65	5.72	5.24	5.71	6.12	6.33	5.86
	60-200	84431	139949	342812	202181	189140	185436	156926	4.93	5.15	5.54	5.31	5.28	5.27	5.20
	200-500	25363	90433	193676	117905	87623	98759	96619	4.40	4.96	5.29	5.07	4.94	4.99	4.99
	500-1000	83737	137966	200373	145130	152524	144120	110055	4.92	5.14	5.30	5.16	5.18	5.16	5.04
	60-1000	57025	116708	246848	152412	135298	137552	120162	4.76	5.07	5.39	5.18	5.13	5.14	5.08
St11	0.7-60	8790529	3698855	1014031	1291613	2214626	3607490	1158992	6.94	6.57	6.01	6.11	6.35	6.56	6.06
	60-200	340341	278463	511941	203214	194604	173037	204152	5.53	5.44	5.71	5.31	5.29	5.24	5.31
	200-500	222956	178647	230279	65711	58719	47601	68714	5.35	5.25	5.36	4.82	4.77	4.68	4.84
	500-1000	159212	159389	141344	56615	51042	48120	73804	5.20	5.20	5.15	4.75	4.71	4.68	4.87
	60-1000	214702	189051	242391	88736	82127	73001	98398	5.33	5.28	5.38	4.95	4.91	4.86	4.99
St15	0.7-60	696518	1022653	536565	1420401	2144309	3122278	1272055	5.84	6.01	5.73	6.15	6.33	6.49	6.10
	60-200	200476	486051	1280589	243839	447930	*na*	112302	5.30	5.69	6.11	5.39	5.65	*na*	5.05
	200-500	42054	266527	545532	129722	109436	128180	84325	4.62	5.43	5.74	5.11	5.04	5.11	4.93
	500-1000	55199	130105	264806	100604	146222	77560	72498	4.74	5.11	5.42	5.00	5.17	4.89	4.86
	60-1000	78642	255181	578188	140595	191104	82533	85109	4.90	5.41	5.76	5.15	5.28	4.92	4.93
St17	0.7-60	1032441	1075161	384173	877555	1950225	1812018	1037395	6.01	6.03	5.58	5.94	6.29	6.26	6.02
	60-200	339793	475388	1192589	208734	405686	145862	108647	5.53	5.68	6.08	5.32	5.61	5.16	5.04
	200-500	280379	366838	656778	151058	345594	115350	66296	5.45	5.56	5.82	5.18	5.54	5.06	4.82
	500-1000	*na*	*na*	*na*	*na*	*na*	*na*	*na*	*na*	*na*	*na*	*na*	*na*	*na*	*na*
	60-1000	304082	410144	870539	174068	369568	127522	83192	5.48	5.61	5.94	5.24	5.57	5.11	4.92
St19	0.7-60	230824	397097	190980	529667	1033887	977889	275405	5.36	5.60	5.28	5.72	6.01	5.99	5.44
	60-200	45495	98644	279833	58425	75483	40786	28306	4.66	4.99	5.45	4.77	4.88	4.61	4.45
	200-500	31570	65375	130801	42704	40044	33392	21910	4.50	4.82	5.12	4.63	4.60	4.52	4.34
	500-1000	138704	189442	284452	89649	117631	153609	45814	5.14	5.28	5.45	4.95	5.07	5.19	4.66
	60-1000	51715	94001	199576	54504	62468	53453	27421	4.71	4.97	5.30	4.74	4.80	4.73	4.44

na: not available.

K_{OC} in a given size fraction (in L kg^{-1}) was calculated as K_D / f_{OC} in the corresponding fraction (0.7-60, 60-200, 200-500, 500-1000 or 60-1000 µm) (see values of K_D in Table S8 and values of f_{OC} in Table S7).

Table S10. Nonlinear regression parameters (power function) between SPM (in mg L^{-1}) or biomass (in mg dw L^{-1}; horizontal axis) and PAH concentration (C_p in ng g^{-1} dw; vertical axis) for each particulate/planktonic size fraction (0.7-60, 60-200, 200-500, 500-1000 and 60-1000 µm) and individual PAH; The power functions are of the form: $y = ax^{-m}$ (i.e., $C_p = aSPM^{-m}$ or $aBiomass^{-m}$). The number of samples n correspond to the stations. Power functions for Phe are shown Fig. 8.

	Size fractions (µm)	Constant (a)	Slope (-m)	Coefficient of correlation (r)	Number of samples (n)	Probability (p)
Nap	0.7-60	6.98	0.863	- 0.79	10	< 0.05
	60-200	1.44	0.362	- 0.62	10	< 0.05
	200-500	2.42	0.106	- 0.27	10	> 0.05
	500-1000	6.61	0.008	- 0.01	9	> 0.05
	60-1000	2.91	0.181	- 0.38	10	> 0.05
Flu	0.7-60	6.65	0.723	- 0.72	10	< 0.05
	60-200	1.18	0.384	- 0.72	10	< 0.05
	200-500	3.05	0.111	- 0.25	10	> 0.05
	500-1000	19.10	- 0.249	0.24	9	> 0.05
	60-1000	2.77	0.195	- 0.44	10	> 0.05
Phe	0.7-60	3.70	1.091	- 0.73	10	< 0.05
	60-200	6.81	0.373	- 0.75	10	< 0.05
	200-500	6.11	0.261	- 0.62	10	< 0.05
	500-1000	46.86	- 0.200	0.27	9	> 0.05
	60-1000	9.75	0.260	- 0.58	10	< 0.05
Flt	0.7-60	4.72	0.769	- 0.72	10	< 0.05
	60-200	1.93	0.262	- 0.33	10	> 0.05
	200-500	2.56	0.100	- 0.15	10	> 0.05
	500-1000	1.50	0.202	- 0.16	9	> 0.05
	60-1000	2.74	0.160	- 0.19	10	> 0.05
Pyr	0.7-60	12.29	0.423	- 0.57	10	< 0.05
	60-200	2.85	0.166	- 0.25	10	> 0.05
	200-500	4.48	- 0.071	0.10	10	> 0.05
	500-1000	4.86	- 0.054	0.23	9	> 0.05
	60-1000	4.46	- 0.014	0.12	10	> 0.05
BaA	0.7-60	2.92	0.886	- 0.94	10	< 0.05
	60-200	0.97	0.157	- 0.17	9	> 0.05
	200-500	0.26	0.254	- 0.33	10	> 0.05
	500-1000	4.09	- 0.226	0.16	9	> 0.05
	60-1000	1.37	- 0.026	0.03	10	> 0.05
Chr	0.7-60	3.84	0.821	- 0.58	10	< 0.05
	60-200	1.88	0.134	- 0.16	10	> 0.05
	200-500	1.17	0.154	- 0.22	10	> 0.05
	500-1000	1.07	0.209	- 0.12	9	> 0.05
	60-1000	1.69	0.153	- 0.16	10	> 0.05

Table S11. Mean values of Log K_D and Log K_{OC}, and slope (-m) of the power function between SPM or biomass and PAH concentration for each particulate/planktonic size fraction (0.7-60, 60-200, 200-500, 500-1000 and 60-1000 µm) and individual PAHs. Mean Log K_D and Log K_{OC} were determined over the 10 stations from Log K_D and Log K_{OC} values reported in Tables S8 and S9, respectively. Slope values are also reported Table S10.

	Size fractions (µm)	**Mean Log K_D**	**Mean Log K_{OC}**	**Slope (-m)**
Nap	0.7-60	4.895	5.818	0.863
	60-200	4.402	5.233	0.362
	200-500	4.130	4.820	0.106
	500-1000	4.366	5.029	0.008
	60-1000	4.277	5.016	0.181
Flu	0.7-60	4.955	5.877	0.723
	60-200	4.520	5.351	0.384
	200-500	4.402	5.092	0.111
	500-1000	4.418	5.081	- 0.249
	60-1000	4.437	5.177	0.195
Phe	0.7-60	4.414	5.337	1.091
	60-200	4.760	5.591	0.373
	200-500	4.485	5.175	0.261
	500-1000	4.393	5.056	- 0.200
	60-1000	4.580	5.320	0.260
Flt	0.7-60	4.851	5.773	0.769
	60-200	4.517	5.348	0.262
	200-500	4.324	5.014	0.100
	500-1000	4.350	5.013	0.202
	60-1000	4.400	5.140	0.160
Pyr	0.7-60	5.170	6.093	0.423
	60-200	4.608	5.439	0.166
	200-500	4.353	5.043	- 0.071
	500-1000	4.390	5.053	- 0.054
	60-1000	4.463	5.202	- 0.014
BaA	0.7-60	5.292	6.215	0.886
	60-200	4.593	5.426	0.157
	200-500	4.197	4.887	0.254
	500-1000	4.414	5.077	- 0.226
	60-1000	4.410	5.149	- 0.026
Chr	0.7-60	4.966	5.889	0.821
	60-200	4.436	5.267	0.134
	200-500	4.257	4.947	0.154
	500-1000	4.423	5.086	0.209
	60-1000	4.356	5.095	0.153

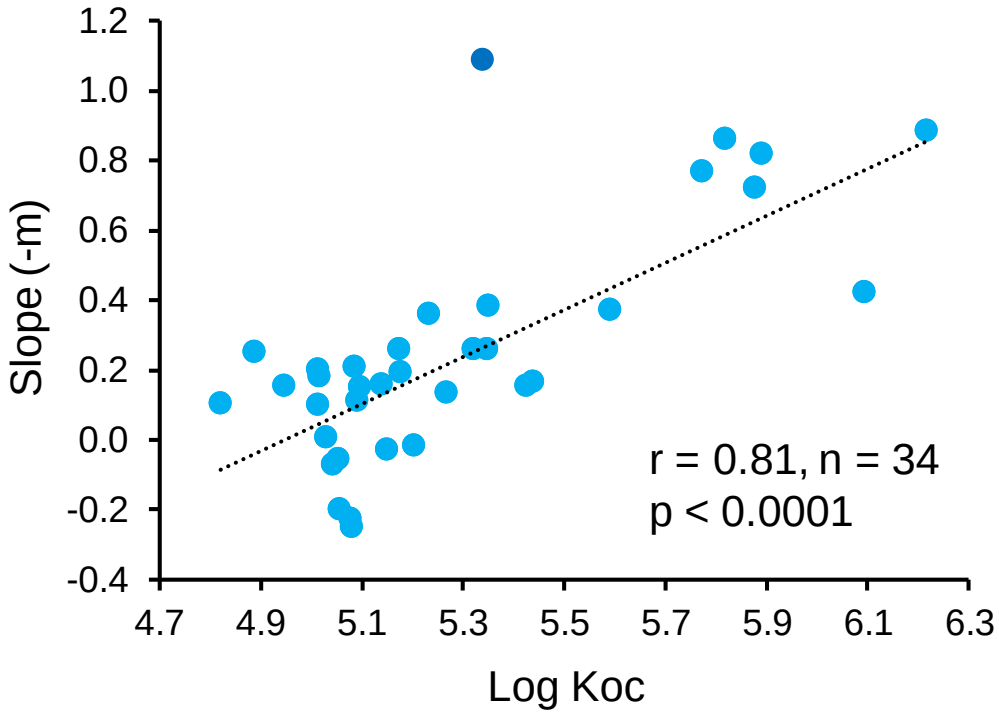

Figure S6. Linear relationship between the mean Log K_{OC} and slope (-m) values (reported in Table S11) for all the particulate/planktonic size fractions, i.e., 0.7-60, 60-200, 200-500, 500-1000 and 60-1000 µm, and the 7 PAHs (Nap, Flu, Phe, Flt, Pyr, BaA, Chr). The darker blue dot is not taken into account in the linear regression.

References cited

Fierro-González, P., Pagano, M., Guilloux, L., Makhlouf Belkahia, N., Tedetti, M., Carlotti, F., 2023. Zooplankton biomass, size structure, and associated metabolic fluxes with focus on its roles at the chlorophyll maximum layer during the plankton-contaminant MERITE-HIPPOCAMPE cruise. Marine Pollution Bulletin, 193, 115056. doi: 10.1016/j.marpolbul.2023.115056.

González-Gaya, B., Martínez-Varela, A., Vila-Costa, M., Casal, P., Cerro-Gálvez, E., Berrojalbiz, N., Lundin, D., Vidal, M., Mompean, C., Bode, A., Jiménez, B., Dachs, J., 2019. Biodegradation as an important sink of aromatic hydrocarbons in the oceans. Nature Geosciences, 12, 119–125. doi: 10.1038/s41561-018-0285-3

Tesán-Onrubia, J.A., Tedetti, M., Carlotti, F., Tenaille, M., Guilloux, L., Pagano, M., Lebreton, B., Guillou, G., Fierro-González, P., Guigue, C., Chifflet, S., Garcia, T., Boudriga, I., Belhassen, M., Bellaaj-Zouari, M., Bănaru, D., 2023a. Spatial variations of biochemical content and stable isotope ratios of size-fractionated plankton in the Mediterranean Sea (MERITE-HIPPOCAMPE campaign). Marine Pollution Bulletin, 189, 114787. doi: 10.1016/j.marpolbul.2023.114787